D-2

AEC-tr-3875

TRANSLATION SERIES

PRESSURE LOSS AND HEAT TRANSFER FOR TURBULENT FLOW

By
Rudolph Koch

TRANSLATED FROM VDI-FORSCHUNGSHEFT,
SERIES B, 24, NO. 469, 1-44(1958).

September 1960
[OTI Extension Issuance Date]

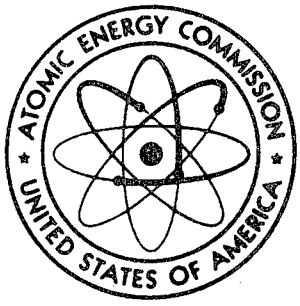

UNITED STATES ATOMIC ENERGY COMMISSION
Office of Technical Information

A translation of: Druckverlust und Warmeubergang bei Verwirbelter Strömung. Rudolph Koch. VDI-Forschungsheft, Series B, 24, No. 469, 1-44(1958).

Translated for Oak Ridge National Laboratory by the Technical Library Research Service under purchase order number 34B-54153, letter release number X-19.

Translated and published by permission of VDI-Verlag GmbH, Düsseldorf.

In the interest of expeditious dissemination this publication has been reproduced directly from copy prepared by the translating firm.

Printed in USA. Price $2.50. Available from the Office of Technical Services, Department of Commerce, Washington 25, D. C.

Issuance Date: September 1960.

USAEC Office of Technical Information Extension, Oak Ridge, Tennessee

CONTENTS

1. Problem and Denotations[1]

The mathematical interrelationships for pressure loss and heat transfer in smooth tubes can be considered as having been clarified with sufficient accuracy. While the pressure loss of rough tubes traversed by flow has been known for some time, it has recently been possible to treat pressure loss and heat transfer in a uniform manner during air flow through rough tubes and even to derive a theoretical heat transfer equation for rough tubes. [1] The most remarkable result of this investigation consists of the fact that the heat transfer depends only on the resistance coefficient of the tube and that it does not depend additionally on the type and arrangement of the roughness elements. In this connection, W. Nunner [1]

---

1) Dissertation by permission of the Technical College in Hannover, in 1957. At this point the author wishes to thank Prof. Dr. (Eng.) H. Glaser for instigating this study and for his valuable advice as well as the German Research Association [Deutsche Forschungsgemeinschaft] for making the financial means available for this investigation. The experimental results were reported in outline form at the meetings of the VDI auxiliary for heat exchangers and condensers on April 25, 1955 in Bad Homburg and on April 13, 1956 in Bingen.

already referred to the difference existing between roughnesses and turbulence incorporations, which was not taken into sufficient consideration previously because it is hardly possible to separate both concepts sharply from each other from the start.

The internal heat transfer coefficient in a tube traversed by flow can be artificially increased by means of turbulence promoters. But this is only suitable if the coefficient of heat transmission of a heat transmitter is mainly determined by the internal heat transfer coefficient. This will be true, for example, if the external heat transfer coefficient is large (such as during condensation or fluid flow), if only a small temperature drop occurs in the tube wall, and if relatively unfavorable conditions for heat transfer prevail inside the tube (for example, during gas flow).

The influence of turbulence promoters (wire helices, helically twisted metal sheets, propeller-shaped baffles, fin-like insertions, various packing materials) on heat transfer has been investigated several times already. Usually water served as the flow medium. Depending on the form and arrangement of the turbulence promoters as well as on the average flow rate in the tube, results were more or less favorable. However, generally valid theories are not yet available. For this reason, further experiments on the basis of uniform points of reference seemed desirable, especially for the purpose of clarifying the relation between the transmitted heat and the pressure loss in the presence of artificially turbulent flow.

Heat transfer and pressure loss had to be determined for each system of turbulence producers, since this is the only way in which an unobjectionable evaluation can be attempted. In addition, velocity and temperature ranges were determined

for a few systems of turbulence producers, resulting in a better insight into the mechanics of heat transfer.

One must differentiate between active and passive turbulence promoters [2]. Active turbulence promoters participate themselves in the heat transfer to a considerable extent; therefore they represent a part of the heat-transmitting area. Passive turbulence inserts only influence the heat transmission by causing the flow to be turbulent. Such inserts have been in use almost exclusively until now and have also been utilized in the experiments described below, because in this manner a large number of different forms and arrangements can be investigated with a small amount of effort. If certain passive turbulence promoters have been recognized as especially suitable, then the heat transfer can be improved for certain heat transmitters in practical use (perhaps even subsequently).

The denotations utilized most frequently are as follows:

$a = \lambda/\varrho\, c_p$	thermal conductivity coefficient
A_τ	magnitude of turbulent exchange of the impulse
A_q	magnitude of turbulent exchange of the heat
c_p	specific heat at constant pressure
d	internal diameter of the tube
d_B	width of a metal sheet
d_S	diameter of a disc
f	free flow cross section
f'	free flow cross section referred to the weight rate of flow
F	internal tube surface
G	mass weight rate of flow
h	amplitude for helical baffles
H	required heat surface
K	height of orifice and ring, respectively

l	distance of an insert in the direction of flow
l_E	hydrodynamic distance of intake
L	length of experimental tube
L'	distance between two turbulence promoters
m	exponent
m^*	aperture ratio
N	delivery efficiency of a blower
$Nu = \alpha d/\lambda$	Nusselt coefficient
p, $\triangle p$	static pressure and pressure drop, respectively, in the tube
$Pe = RePr$	Péclet coefficient
Pr	Prandtl coefficient
q	heat flux density
Q	heat flow
r	tube radius
R	gas constant
$Re = w\ d/\nu$	Reynolds number
Re_{kr}	critical Reynolds number
t	temperature in C
T	absolute temperature
$u^+=\sqrt{\tau_w/\varrho}$	rate of shear stress
w	average rate of flow
x	moisture content
y	distance from wall
$y^+=u^+y/\nu$	dimensionless wall distance
α, α'	average and local heat transfer coefficient, respectively
ε, ε_1	performance figures
ε_L	relative space volume of a packed tube
η	dynamic viscosity
ϑ	derived over-temperature
λ	coefficient of thermal conductivity

ν	kinematic viscosity'
ϱ	density
τ	shear stress
ψ	coefficient of resistance

2. Fundamentals

2.1 Pressure Loss and Intake Distance

In a fully formed, isothermal and incompressible flow through horizontal tubes the pressure loss Δp over tube length L is only caused by wall friction. According to definition, the following is true for the coefficient of resistance ψ:

$$\psi = \frac{\Delta p}{\frac{1}{2}\varrho w^2} \frac{d}{L} \qquad (1)$$

where w is the average rate of flow, ϱ the density of the flowing medium and d is the diameter of the tube. More generally, the definition equation for the coefficient of resistance of gases, neglecting static pressures in the tubing, is as follows:

$$\psi = \left[\frac{\Delta p}{\frac{1}{2}\varrho w^2} - 2 \ln \left(\frac{p_1 T_2}{p_2 T_1}\right)\right] \frac{d}{L} \qquad (2)$$

with T as the absolute temperature, p the static pressure, m as the index of an average value over the total flow path L, and with indices 1 and 2 as values at the start and at the end of the tube distance. Equations (1) and (2) are used not only for smooth tubes and channels, but also for those with roughnesses and turbulence inserts, the body resistance of which also causes pressure loss in addition to wall friction.

Furthermore, Δp also contains an accelerating component for profile formation in the intake distance l_E, which is necessary for the formation of the complete velocity distribution.

According to measurements of J. Nikuradse [3,4], the following is valid in turbulent flow independently of the Reynolds number Re--for smooth tubes:

$$l_E \approx 50\ d \tag{3}$$

and for rough tubes

$$l_E \approx 40\ d \tag{4}$$

For laminar flow, the value

$$l_E \approx 0.065\ d\ Re \tag{5}$$

is most valid for smooth as well as rough walls according to J. Boussinesq [5].

2.2 Laws of Resistance

With $Re = w\ d/\nu$ for the Reynolds number of the tube, in which ν denotes the kinematic viscosity, the following laws of resistance are valid:

$$\psi = 64/Re \tag{6}$$

for fully developed laminar flow in a smooth tube of cross section,

$$\psi = (100\ Re)^{-1/4} \tag{7}$$

for the fully developed turbulent flow according to H. Blasius [6] in the range $Re < 10^5$ as well as

$$\frac{1}{\sqrt{\psi}} = 2\ lg\ (Re\ \sqrt{\psi}) - 0.8 \tag{8}$$

according to Prandtl [7] for $Re > 5 \cdot 10^3$ in the smooth tube (an equation by R. Hermann [8] is also used frequently for smooth tubes and $Re > 10^5$).

Nothing further will be said about the laws of resistance

for non-isothermal and/or non-developed flow as well as for rough tubes, since these have only recently been compiled by W. Nunner [1].

2.3 Heat Transfer Laws

The heat flow Q transmitted with a fluid or gaseous flow results from:

$$dQ = \alpha'(t'_w - t_{F1})\, dF \tag{9}$$

with α' as the local heat transfer coefficient, F the heat-transmitting surface, t'_w the local wall temperature and t_{F1} as the fluid temperature determined at the point under consideration over cross sectional plane f. If density ϱ and the specific heat c_p of the flowing medium is assumed constant over cross section f with constant pressure p, then we have

$$t_{F1} = \int_t t\, w\, d\, f / \int_t w\, df \tag{10}$$

with t as the local fluid temperature in the cross sectional component df.

In order to obtain the total transmitted heat Q and an average heat transfer coefficient α, respectively, only the average fluid temperature t_m along the heat-transmitting portion of the tube needs to be utilized with constant wall temperature t_w, instead of t_{F1}. The following is valid:

$$t_m = t_w - \frac{t_2 - t_1}{\ln\left(\frac{t_w - t_1}{t_w - t_2}\right)} \tag{11}$$

where t_1 and t_2 are the average fluid temperatures at the start and at the end of the heat-transmitting tube portion, as well as

$$Q = \alpha(t_w - t_m)F \tag{12}$$

The similarity principle results in

$$Nu = \alpha d/\lambda = f(Re, Pr, L/d)$$

for the average Nusselt figure Nu in smooth tubings, where λ is the coefficient of thermal conductivity of the flowing medium, $Pr = \nu/a$ is the Prandtl coefficient, $\nu = \eta/\varrho$ is the kinematic viscosity, $a = \lambda/\varrho\, c_p$ is the thermal conductivity and η is the dynamic viscosity.

With the assumption t_w = const. W. Nusselt [9] found the fixed value Nu = 3.65 for the case of hydrodynamically and thermally developed laminar flow. For a thermally non-developed flow, the experimental results are well reproduced by the equation

$$Nu = 3.65 + \frac{0.0668\ Pe\ d/L}{1+0.045(Pe\ d/L)^{2/3}}\ (\eta_{F1}/\eta_w)^{0.14} \tag{13}$$

according to H. Hausen [10], in which $Pe = RePr$ denotes the Péclet number and in which the substance magnitudes in Nu and Pe are to be referred to the average fluid temperature t_m. The viscosities η_{F1} and η_w are to be substituted for the average fluid and wall temperatures.

The empirical formula by W. Nusselt [11]

$$Nu = 0.0326\ Re^{0.786} Pr^{0.45} (d/L)^{0.054} \tag{14}$$

is frequently used in the case of turbulent gas flow, in which the substance magnitudes are to be referred to the average boundary layer temperature $t_g = 1/2(t_w + t_m)$. The equation

$$Nu = 0.116[1 + (d/L)^{2/3}](Re^{2/3} - 125)Pr^m(\eta_{Fl}/\eta_w)^{0.14} \quad (15)$$

according to H. Hausen [10] with the exponent m = 0.33 for fluids and m = 0.45 for gases, is still quite accurate even for small Reynolds numbers down to Re $\approx$ 3000.

W. Nunner [1] generalized the known Prandtl equation [12] to the extent that it is valid for smooth and rough tubes. He found

$$Nu = \frac{\frac{1}{8}\Psi RePr}{1 + \frac{w'}{w}(Pr\frac{\Psi}{\Psi_o} - 1)} \quad (16)$$

In Equation (16), Ψ denotes the coefficient of resistance of the rough tube, Ψ_o the coefficient of resistance of the smooth tube with equal Reynolds number, and w' is the velocity at the imagined boundary of laminar wall layer and turbulent main flow. W. Nunner was well able to reproduce his experimental results with Equation (16) if he utilized an expression given by E. Hofmann [13] for the ratio w'/w.

In the range of the thermal intake distance l_{th}, the heat transfer coefficient is greater than in the case of fully developed velocity and temperature distribution, in which range it becomes independent of the length of the tube. The thermal intake distance l_{th} of tube flows has been calculated in various ways (compare e.g. [1, 14-16]). The values according to the equation of K. Elser [15] are obviously too low, while the other equations [1, 14, 16] produce values which agree well within the limits of the experiments which are still to be discussed. According to H. Latzko [14], l_{th}

depends on Re and α; according to V. J. Berry [16] it depends on Re and Pr. According to the equation of W. Nunner [1], l_{th} varies proportionally with Re and Pr as well as inversely proportionally with Nu. With respect to further details on thermal intake processes, the reader is referred to [1].

3. Experimental Equipment and Performance

3.1 Experimental Apparatus

The test stand which has already been described in detail by W. Nunner [1] was utilized for the experimental investigation of the influence of turbulence promoters on heat transfer and pressure loss. A radial blower presses the aspirated open air into an air reservoir which is first of all connected to a tube with electric heating (in order to adjust the temperature of the introduced air to a desired value), a sliding valve (for flow adjustment), and an orifice measuring section with two experimental chambers (for the flow measurement). The air then flows through a tube divergence filled with aluminum chips (in order to equalize velocity and temperature), over a straight intake section of 50 mm diameter and 2.5 m length into the experimental tube proper of 50 mm internal diameter and 980 mm length, and finally returns to the open air over a short outlet run.[2] The experimental tube proper was externally heated with steam at atmospheric pressure. In order to control the amount of heat which was absorbed by the air in the experimental tube and which was determined by a measurement of its temperature increase, the amount of condensed steam could be continuously weighed with a scale. The experimental tube section was wrapped with glass wool beginning at the tube divergence for the purpose of heat conservation.

2) Compare in this respect [1]; especially Fig. 2 on p. 20.

3.2 Measurement Arrangement

The experimental tube proper, i.e. the measuring section, consisted of brass with absolutely smooth inside walls and was externally wrapped with a double steam jacket each of which was provided with its own condensation runoff.[3] The heat radiated in the internal steam jacket was almost entirely absorbed by the air; the heat liberated in the external jacket generally overlapped with the heat losses to the outside. Narrow air gaps of 1 mm width at the entrance and outlet of the measuring section served to thermally insulate the latter from the entrance and outlet sections. Intermediate flange couplings of Turbax and a cooling chamber traversed by water in the front flange of the tube prevented a further undesirable heat conduction.

For the purpose of flow measurement, a valve and four orifices of varying widths were provided which made possible an approximately uniform measuring accuracy over the range of the adjustable weight rates of flow. The effective pressure of the orifices was measured by means of a micromanometer according to A. Betz, and the pressure in front of the orifice was measured with a U-tube. The measuring accuracy amounted to ± 1%.

The difference of static pressure before and behind the measuring section represented its pressure loss. The static pressures were obtained from annular chambers into which the mentioned air gaps opened at the two ends of the experimental tube. A micromanometer according to A. Betz also served for the measurement of the pressure loss, while a lever manometer was used for values below 1 mm water column which permitted the recording of pressure differences of 10^{-3} mm water column. In the case of pressure differences

---

3) Compare [1]; especially Figs. 6 a and b on p. 26

above 400 mm water column, U-tubes filled with water or mercury were utilized.

The transmitted heat could be most accurately measured from the temperature increase of the air, while the amount of heat calculated from the amount of condensation only served for purposes of control. The air temperature directly before the entrance section was measured with a mercury thermometer. Thus the velocity distribution could develop without interference up to the experimental tube. The latter was provided with ten external thermocouples at various axial distances from each other. These thermocouples were located in small grooves running around the tube. Since the wall thickness of the tube amounted to only 2.5 mm and since, thus, the temperature drop through the tube wall remained negligibly small, the thermocouples practically registered the internal temperature of the tube wall. Preliminary experiments demonstrated that the tube wall temperatures (aside from the first 20-30 mm of heated measuring section) was entirely constant. Therefore it was subsequently determined only with three thermocouples. Two filter thermocouples of different size at the outlet section served for the measurement of the average temperature of the heated air. In order to prevent heat losses in this outlet section, the air at the end of the tube was diverted by 180° and returned along the outside of the tube. The comparison terminals of the thermocouples were located in the tube divergence before the inlet section, so that the temperature differences required for the calculation could be determined directly. The thermoelectric voltage of the individual thermocouples was determined by means of a Steinwehr compensator and a reflecting galvanometer for a zero reading instrument.

A sliding instrument was available for a measurement of the velocity and temperature distribution which made possible an exploration of the tube cross section shortly before the end of the measuring section, after the outlet section was removed. The velocity distributions were measured with a Pitot tube of 1 mm external diameter, however only with isothermal flow. The temperature distributions were scanned with a copper-constantan thermocouple of 0.1 mm wire diameter. Due to the small wire diameter, a radiation protection could be dispensed with. The counter terminal of this thermocouple, just as all other counter terminals, was located in front of the inlet section in the air flow.

By the use of different basic forms of passive turbulence promoters (orifice- and disc-shaped inserts, propeller-shaped baffles, helically twisted metal sheets and various packing materials such as Raschig rings and spheres) a fairly good survey of the effect of turbulence promoters should result. The inserts--with the exception of the packing materials--were produced in such a manner that they could be easily introduced and withdrawn from the smooth experimental tube. In addition to the experimental tube proper, the inlet and outlet section also contained such inserts over a distance of 8 to 10, respectively, of 3 tube diameters. The air gaps for taking of the pressures were located in the middle between two turbulence promoter components. In this manner it was possible to determine the pressure loss without falsification.

In the case of pressure loss determinations for isothermal flow, the filter thermocouples and the air return at the end of the outlet section were removed, since these falsified the static pressure at the end of the experimental tube to some extent.

Before beginning a heat transfer determination, the state of equilibrium was waited for. This could be recognized from the fact that steam emerged from the condensation nozzles in addition to the condensate, and that the temperature of the filter thermocouples no longer varied. In addition, the water flow through the cooling chamber of the flange at the end of the inlet section has been adjusted in such a manner that the air temperature at this point exhibits the same value as at the start of the inlet section. If all of these assumptions occurred, then consecutive measurements were taken of the effective orifice pressure, the static pressure before the orifice, the temperatures of the tube wall, of the entering and heated air, as well as the amount of condensation (which was determined at least three times during each experimental series).

The experimental range was limited toward the top by the blower efficiency, and toward the bottom by technological measuring difficulties during the determinations of flow, pressure loss and heat transfer. In a smooth tube this corresponded to a range of Reynolds numbers Re between 500 and 80,000. Depending on the magnitude of the pressure loss, the two limit values of the tubes with turbulence promoters shifted to smaller values. Heat transfer measurements below $Re \approx 500$ were no longer carried out.

3.3 Evaluation Method

The density of the air ϱ was determined with the aid of the gas equation

$$\varrho = p/RT \qquad (17)$$

from the static pressure p, the absolute temperature T and the gas constant R = 29.3 kp m/kg°. The influence of atmospheric moisture on ϱ remained negligibly small.

The tabulated data according to [17] were utilized for the dynamic viscosity η and the coefficient of heat conductivity λ of the air. Compared to this, the influence of air humidity could amount up to 1% with a specific heat c_p. For humid air, c_p resulted from

$$c_p = \frac{0.240 + 0.46\ x}{1 + x} \tag{18}$$

in kcal/kg°, where x is the moisture content of air in kg per kg of dry air.

Since the pressure loss $\Delta p = p_1 - p_2$ over a measuring section L (with p_1 and p_2 as the static pressure at the start and at the end, respectively, of the measuring section) was only determined during isothermal flow, the following is valid for the coefficient of resistance from Equation (2):

$$\psi = 2\frac{d}{L}\left[\frac{(p_1-p_2)}{\varrho_m w^2} - \ln\left(\frac{p_1}{p_2}\right)\right] \tag{19}$$

Since the logarithmic member in comparison to the first member remained negligibly small even for the largest Δp-values which occurred, the following was valid with sufficient accuracy for the practical evaluation:

$$\psi = \frac{\Delta p}{\frac{1}{2}\varrho_m w^2}\frac{d}{L} = \frac{\pi^2 \Delta p\ \varrho_m d^5}{8\ G^2\ L} \tag{20}$$

with G as the weight rate of flow of mass and ϱ_m as the average density of the air in the experimental tube (derived as the arithmetic mean from the initial and terminal state). The diameter of the smooth tube was always used for the diameter of reference d; the former had to be determined with

great accuracy, since it enters in Equation (20) with a power of five. As will be shown later in section 4.111, it is of no advantage to utilize other values for d, whether for the individual turbulence promoter tubes or for the turbulent and laminar range of flow.

The heat flow Q absorbed by the air in the experimental tube amounts to:

$$Q = G\, c_p (t_2 - t_1) \tag{21}$$

where t_1 and t_2 are the average air temperatures at the beginning and at the end of the heating zone. At constant wall temperature t_w, the following is valid for the average heat transfer coefficient:

$$\alpha = \frac{G\, c_p}{\pi\, dL} \ln \left(\frac{t_w - t_1}{t_w - t_2}\right) \tag{22}$$

and for the average Nusselt number, respectively:

$$Nu = \frac{\alpha\, d}{\lambda} = \frac{G\, c_p}{\pi L \lambda} \ln \left(\frac{t_w - t_1}{t_w - t_2}\right) \tag{23}$$

The measuring results were evaluated by means of Equation (23) with the internal surface of the smooth tube as the heat transfer plane. In the absence of more accurate and suitable magnitudes of reference, this proved to be best.

The thermal intake length l_{tho} of the smooth tube was determined according to the data of V. J. Berry [16]. This l_{tho} value coincides almost entirely with the result according to H. Latzko [14] or according to W. Nunner [1]. According to W. Nunner, the thermal intake section varies inversely proportional to the Nusselt number. If this function is assumed to be also valid for tubes with turbulence inserts and if the corresponding equation by W. Nunner is introduced,

with which he approximates the values of H. Latzko, then the following relation results for the heat transfer coefficient α_∞ of the thermally developed flow:

$$\alpha_\infty = \frac{\alpha}{1 + 0.1 \frac{l_{tho}}{L} \frac{Nu_o}{Nu}} \tag{24}$$

where α is the average coefficient of heat transfer over the tube length L, Nu_o is the average Nusselt number of the smooth tube and Nu is the average Nusselt number of the tube with inserts. With an equal reference temperature of the mass magnitudes, the Nusselt number Nu_∞ for the thermally and hydrodynamically formed flow thus results as:

$$Nu_\infty \approx \frac{Nu}{1 + 0.1 \frac{l_{tho}}{L} \frac{Nu_o}{Nu}} \tag{25}$$

With the aid of Equation (25), the Nu values in some cases have been recalculated to Nu_∞ according to Equation (23).

In order to calculate the Reynolds number

$$Re = \frac{wd\varrho}{\eta} = \frac{4G}{\pi \eta d} \tag{26}$$

of the heated tube, the average boundary layer temperature $t_g = 1/2(t_w + t_m)$ served as the reference temperature.

4. Experimental Results

4.1 Disc-shaped Turbulence Inserts

Disc-shaped inserts were intended to represent a continuation of the investigation of W. Nunner [1] who, among other things, also used disc-shaped tube inserts to produce tube roughnesses, and were also to extend the range of investigated roughnesses to extremely high values. Table 1 gives a summary of the arrangements utilized.

The disc-shaped inserts had orifice heights (roughness heights) K = 2.5, 10 and 12.5 mm. Piston rings of 2 mm width and 2 mm height served as the smallest inserts which were individually pushed into the tube and which fitted well to the tube wall. The larger discs consisting of 1 mm thick brass sheets were under-dimensioned by a maximum of 0.3 mm in comparison to the experimental tube. so that they could be easily introduced. These discs were threaded onto three brass rods of 2 mm diameter and soldered on at certain distances, Fig. 1. It can be assumed that the influence of the bracing rods on

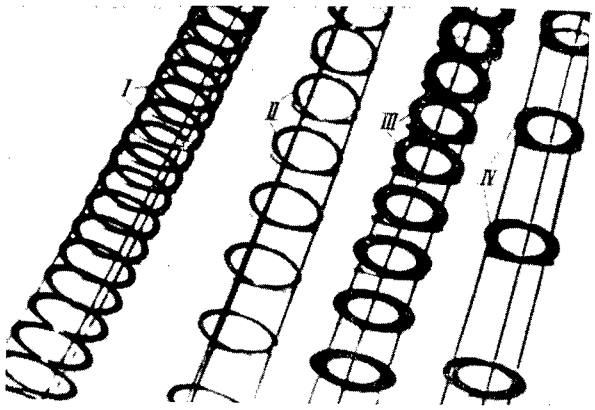

Fig. 1.--Examples for disc-shaped Turbulence Inserts. I to IV correspond to arrangements e, f, i and k in Table 1.

the pressure loss and the heat transfer remained negligibly small. The supporting rods proved to be too weak at disc distances of over 350 mm. In such cases, the individual discs were clamped tight with two lower piston rings each.

Care was always taken that the air gaps for the static pressure recording was located in the middle between two inserts. In this manner the numerical values recorded in Table 1 resulted for the ratio L'/K with L' as the distance between the center planes of two neighboring discs.

Table 1

Data of the Disc-Shaped Inserts

Disc Height° K mm	Orifice Ratio°° m* —	Referred Ring Distance°°° L'/K —	Denotation of Arrangement —
2	0.845	9.8	a
		19.6	b
		78.4	c
		156.8	d
5	0.64	3.92	e
		9.8	f
		65	g
		196	h
10	0.36	3.92	i
		9.8	k
		32.7	l
		98	m
12.5	0.25	26	n
		78.4	o

°Difference between external and internal diameter of the aperture disc.

°°$m^* = (d_B/d)^2$ with d_B as the internal diameter of the aperture disc and d as the tube diameter.

°°°The ring distance L' is measured from center to center of two neighboring rings.

4.11 Pressure Loss

4.111 Influence of the Reynolds Number:--Figs. 2 and 3 show the results of pressure loss determinations during isothermal air flow for the smooth tube and for tubes filled with disc-shaped inserts, plotted as the coefficient of resistance according to Equation (20) as a function of the Reynolds number Re. The straight line I corresponding to $\Psi = 64/Re$ in the laminar range and the Blasius curve II according to Equation (7) in the turbulent range have been plotted for comparison purposes.

The measuring values for the smooth tube are well located on the two comparison curves I and II. The change-over from the laminar to the turbulent state of flow occurs at Re = 2900.

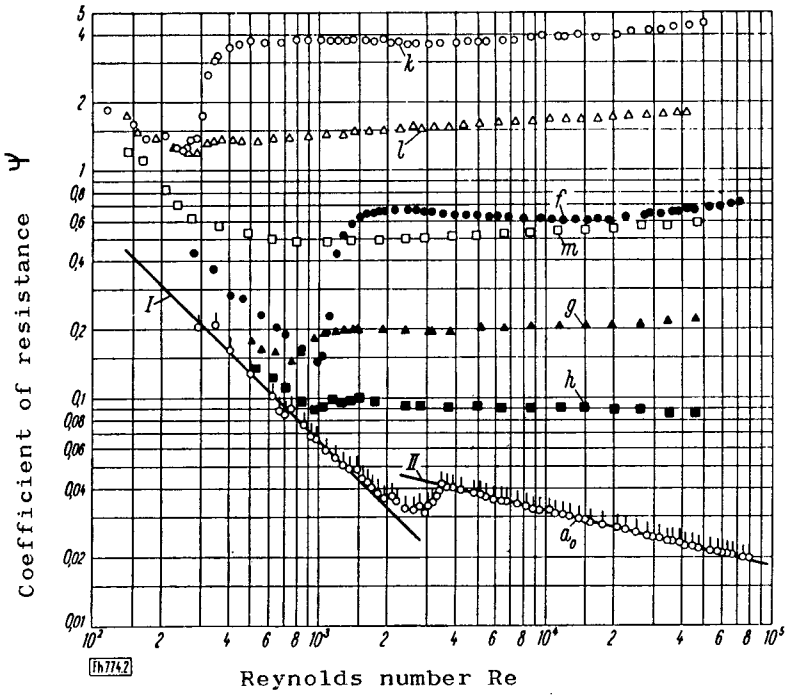

Fig. 2.--Path of ψ for average and large referred ring distances L'/K.

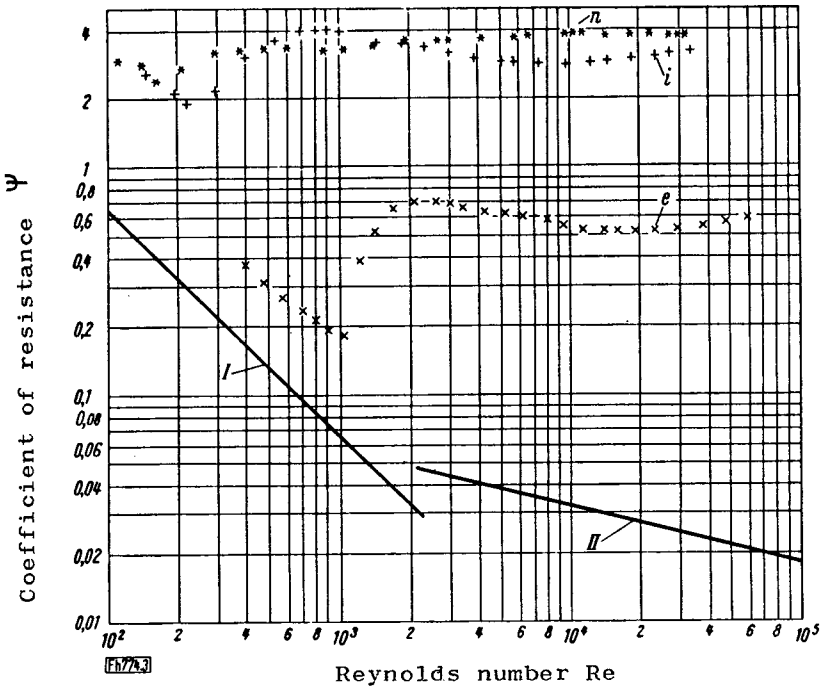

Fig. 3.--Path of ψ for small referred ring distances L'/K.

Figs. 2 and 3.--The Coefficient of resistance ψ in the tube with disc-shaped turbulence inserts as a function of the Reynolds number Re. I and II = comparison curve according to Equations (6) and (7), respectively, for the smooth tube without inserts; a_o = measuring values for the smooth tube; the other letters are valid for the corresponding arrangements in Table 1.

In the laminar range the measuring points deviate a little more from the theoretical curve I. This can be explained by the insufficient length of the inlet section of 50 d which, according to Equation (5), only suffices for Re < 800, as well as by technological measuring difficulties.

In the turbulent range, Ψ depends only little on Re for tubes with inserts and considerably exceeds the coefficient of resistance of the smooth tube. The curves for tubes with a small referred ring distance ($L'/K \approx 4$ and $L'/K \approx 10$) have a weakly defined minimum, which is most distinctly evident for the smallest L'/K values. This strange behavior has already been observed by L. Schiller [18], H. Möbius [19] and W. Nunner [1]. H. Möbius also utilized disc-shaped inserts with $K \leq 5$ mm in a tube of 50 mm internal diameter and found for most of his tubes that the minimums of the Ψ, Re curves occurred at a certain characteristic value of Re. H. Möbius formulated the Reynolds number with K and with the velocity which prevailed between the discs at the distance K from the wall. But even with discs of K = 5 mm it is no longer possible to determine this velocity accurately, since it changes considerably between a pair of discs and the measurement itself is very inaccurate. Possibly these Ψ, Re curves in Figs. 2 and 3 would again be almost horizontal in their course at higher Reynolds numbers, similar to the case of H. Möbius. Curve h for K = 5 mm with the largest L'/K value is the only one which has a slight downward slope throughout towards the right. (Compare Fig. 2). This might be attributable to the participation of wall friction in the total pressure loss.

The transition areas from laminar to turbulent flow, which extend only over a very small Re-range, are especially

distinct for disc arrangements with small L'/K values. In this instance the point of change-over is depressed to very small values of the Reynolds number (to Re ≈ 170, compare curve n in Fig. 3). In arrangements with large L'/K values the transition area is no longer distinctly recognizable. It is for this reason that little can be said about to what extent the change-over depends on L'/K. Nevertheless, it can be concluded on the basis of the course of the Ψ, Re curves that L'/K in these types of discs carries no particular weight and that only the orifice ratio m* of the discs has a considerable influence. If, in addition, a resistance curve for sharp-edged discs (K = 2 mm, L'/K ≈ 20) according to W. Nunner [1] is taken into account, then a relation results as below:

$$Re_{kr} = 2900\ m^{*2,2} \qquad (27)$$

which is between the critical Reynolds number Re_{kr} and m* for the case of sharp-edged discs as inserts.

In the case of a small Re, all curves have a course parallel to the straight line $\Psi = 64/Re$. This is an indication that the flow exhibits a laminar character. The differential parallel displacement of Ψ, Re curves in this case is due to the arbitrary selection of the tube diameter as a reference magnitude in Re. Within the area of one type of disc it can be said without doubt that the really effective diameter, which corresponds to the lateral extension of the main flow, decreases with decreasing L'/K. However, a determination of a suitable reference diameter with the aid of the measuring values was dispensed with; for every definition of the decisive tube dimension which deviates from the tube diameter d is, among other things, accompanied by the disadvantage that the processes during the transition from laminar to turbulent state

of flow are difficult to overlook, since the different reference diameters of both states would somehow have to pass from one into the other.

The question should still be considered whether the coefficients of resistance calculated from the measuring values contain any differential intake effects. It can be imagined that the flow in the case of very small disc distances ($L'/K \rightarrow 0$) behaves similar as in the case of a rough tube with correspondingly smaller diameter. With increasing L'/K the state of flow first still changes a little from disc to disc. Only when the flow has passed through a minimum number of discs, does the same course of flow always repeat itself between the subsequent disc pairs so that from now on one could speak of a "fully developed" flow,[4] since then every section of the tube between two inserts contributes the same amount to the total pressure loss. Evidently, the number of insert components necessary for the intake section increases with decreasing values of L' and K, which however does not mean that the absolute length of the intake section increases to the same extent. It follows from the measurements of H. Möbius [19] on the dependence of the intake effect on the dimensions of the disc inserts that the intake section and the number of installed inserts provided for the experiments described here, can be considered as sufficient. Only in the

---

4) The type of flow through tubes with inserts does not correspond to the state which is ordinarily designated as fully developed, even with a sufficiently dimensioned intake section. The difference in processes also affect the position and form of the change-over zone from the laminar to the turbulent type of flow.

case of the smallest discs (K = 2 mm and $L'/K \approx 10$) it has to be taken into consideration along with H. Möbius that on the basis of intake effects ψ is at too high a point by 3%. Up to this order of magnitude, errors hardly have significance for subsequent considerations.

4.112 Influence of the referred ring distance L'/K:-- Fig. 4 shows the course of ψ as a function of L'/K for the aperture ratios m* under investigation and for two different Reynolds numbers. As could already be seen previously from the course of the ψ, Re curves, the influence of Re is not great. The largest coefficient of resistance for a certain aperture ratio is found at $L'/K \approx 10$ in agreement with the results of H. Möbius and W. Nunner. In the range of very large L'/K values, all ψ, L'/K curves must asymptotically strive towards that ψ-value which is valid for smooth tubes. In the case of very small L'/K values, the coefficient of resistance of a smooth tube is reached, the diameter of which is equal to the internal disc diameter. With decreasing m* the ψ, L'/K curves have an increasingly steeper inclination up to their maximum.

4.113 Influence of the Aperture Ratio m*:--Fig. 5 contains the average values ψ_m of ψ formed from Figs. 2 and 3 on the turbulent range as a function of the aperture ratio m* for various L'/K values (in part the ψ_m values were interpolated from Fig. 4). Since ψ_m must become infinite at $m^* = 0$, the curves in Fig. 5 in the case of very small aperture ratios ($m^* < 0.25$) might have a considerably steeper inclination than would correspond to the course of the straight line. However, such small aperture ratios are hardly of practical significance. In the case of large m* values

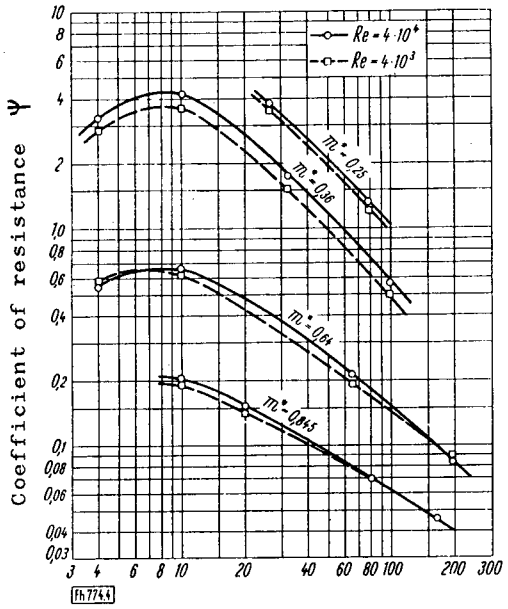

Fig. 4.--The coefficient of resistance ψ in the tube with disc-shaped turbulence inserts as a function of the reference ring distance L'/K for different values of the aperture ratio m* and the Reynolds number Re.

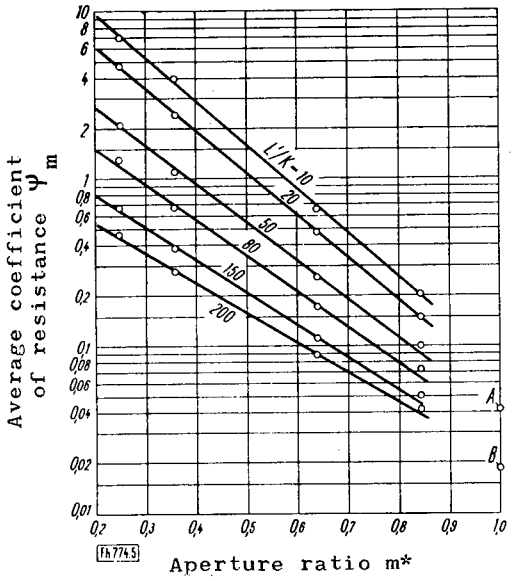

Fig. 5 .--The average coefficient of resistance ψ_m in the turbulent range as a function of the aperture ratio m* at various referred ring distances L'/K in the tube with disc-shaped turbulence inserts. A and B are points for the coefficient of resistance ψ of the smooth tube at a Reynolds number Re = 1500 and 80,000 respectively.

($m^* > 0.85$), the Reynolds number has a more extensive effect. This is also evident from the position of the points for the smooth tube ($m^* = 1.0$), which are in the range of $\Psi = 0.0427$ and 0.0187 for $1500 < Re < 80{,}000$. In the range of $1.5 \cdot 10^3 \leq Re \leq 8 \cdot 10^4$, $0.25 \leq m^* \leq 0.85$ and $10 \leq L'/K \leq 200$, the measuring points for L'/K in Fig. 5 can be approximated by straight lines which correspond to the exponential law:

$$\Psi_m = 17{,}500\ [(L'/K) + 25]^{-1.77} e^{-m^*[6-0.01(L'/K)]} \qquad (28)$$

Fig. 6 demonstrates the good agreement of the measured Ψ_m-values and those which were calculated according to Equation (28).

The given coefficients of resistance strictly speaking can only be transposed to other arrangements of the same type if the discs are geometrically similar. However it can be assumed that the width of the sharp-edged discs influences the total pressure loss only inconsiderably in the case of tube dimensions which are not excessively small.

4.114 Pressure Loss of an Individual Disc in the Total System:--Reference has already been made to the fact that after the first few preliminary discs, every individual disc in the subsequent tube section contributes to the pressure loss to the same extent. Thus, the individual resistance of a disc in a total system can be calculated from the coefficient of resistance Ψ of the tube flow with inserts and from the number of discs in the experimental tube; this factor shall be denoted by Ψ_E. Now it shall be assumed that in the case of the largest disc distances under investigation (L'/K = 157, 196, 98), the resistance of a disc in the unit is equal to the resistance of a single disc in a tube, the coefficient of resistance of which is denoted by Ψ_{E1}. In the determina-

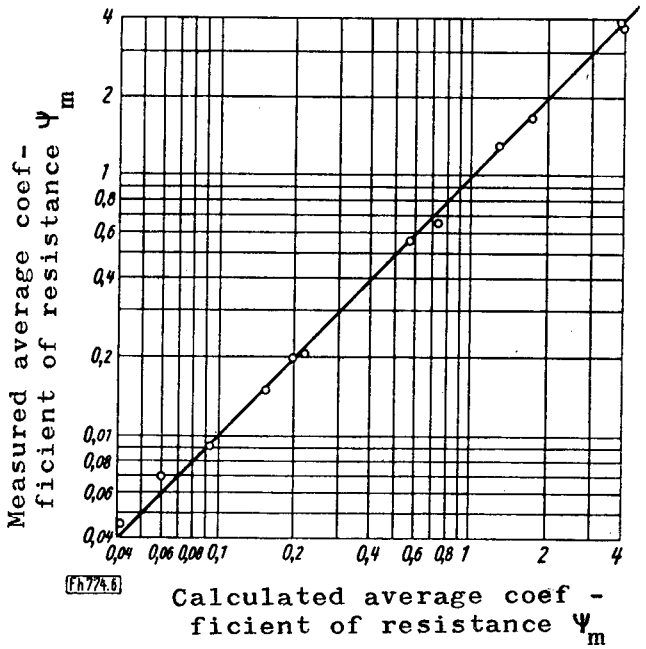

Fig. 6.--Comparison of the average coefficients of resistance ψ_m as measured and as calculated according to Equation (28) for the turbulent range of flow in the tube with disc-shaped turbulence promoters.

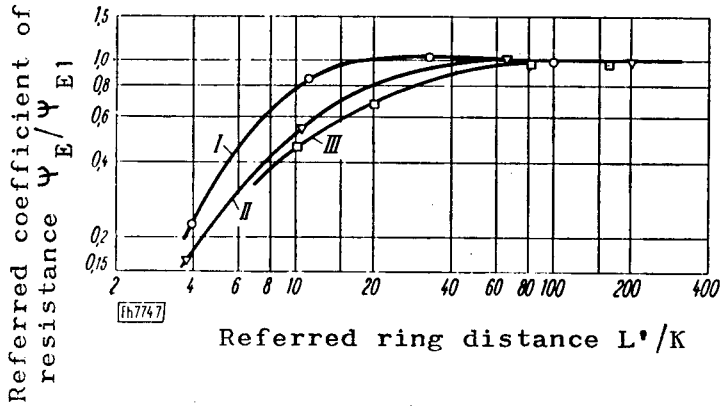

Fig. 7.--The referred coefficient of resistance ψ_E/ψ_{E1} of an individual disc in the total system as a function of the referred ring distance L'/K at different aperture ratios m*. I to III = course of m* = 0.36, 0.64 and 0.845, respectively.

tion of these new factors Ψ_E and Ψ_{E1} the pressure loss of the smooth tube (at Re = 40,000) was subtracted from the measured pressure loss and the result was divided by the number of discs. In the case of large disc heights K and small L'/K ratios, the true tube friction resistance will admittedly differ somewhat from that of the smooth tube; the possible error due to this factor however remained out of consideration.

Fig. 7 shows the course of Ψ_E/Ψ_{E1} as a function of L'/K for the three largest aperture ratios m*. This representation demonstrates the effect of the reciprocal masking of the inserts. Beginning with L'/K 50, we practically have $\Psi_E/\Psi_{E1} = 1$, i.e. every disc in the unit acts in the manner of a single disc in a tube. Ψ_E/Ψ_{E1} decreases with decreasing L'/K, and this occurs more readily with large m*-values than with small ones. It is evident from Fig. 7 that the individual resistances of the discs increase less than linearly with L'/K in the range L'/K > 10. On the basis of this it follows that the total resistance must decrease with increasing L'/K values (at L'/K > 10), since L'/K is almost exactly inversely proportional to the number of individual resistances. On the other hand, in the range of L'/K < 10, the individual resistance shows a more rapid decrease than the increase of the number of individual resistances, so that the total resistance in this range must also decrease in spite of the increasing number of individual resistances. The drop of the curves in Fig. 4 on both sides of the maximum at L'/K $\approx$ 10 thus can be plainly interpreted. E. Hübner [20] obtained similar results with tubes containing rod-shaped inserts.

4.12 Heat Transfer

4.121 Influence of the Reynolds Number:--In Figs. 8 and 9 the course of the average Nusselt numbers Nu calculated from the measuring values are reproduced as a function of the Reynolds number. The measurements include the thermal intake effect. Lines I and II represent the comparison curves for the laminar and turbulent ranges, respectively, in a smooth tube according to Equations (13) and (14). While the measuring points of the turbulent range in the smooth tube fall very well onto line II, greater deviations are noticeable at Re < 4000, which are caused by the influence of free convection. The fact that the measuring points fall considerably above line I is also due to this influence. An empirical equation by A. P. Colburn compiles these relations on the basis of their order of magnitude.[5]

The Nu values attained in the turbulent range of tubes with turbulence promoters are up to four times as large as in the smooth tube; the slope of the curves over a large range agrees altogether with that of the smooth tubes. In a comparison of the ψ, Re curves in Figs. 2 and 3 with the Nu,Re curves in Figs. 8 and 9, similar properties are evident: a small change of direction of the ψ, Re curves coincides with the same behavior of the Nu,Re curves. The sequence of curves admittedly has changed partly in Figs. 8 and 9 in comparison to Figs. 2 and 3, which can be attributed to the strong influence of L'/K and m^* on Nu.

In the laminar range in Figs. 8 and 9, all curves with decreasing Re approach each other more and more, i.e. the

5) Compare in this respect [1]; especially Equation (21) on p. 16

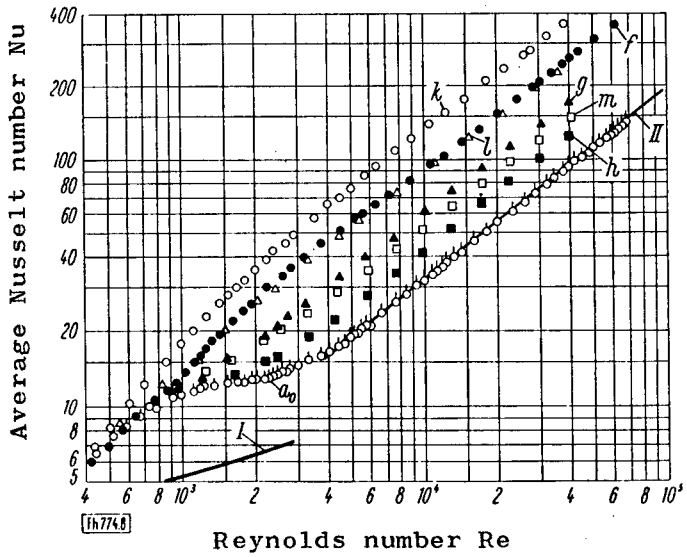

Fig. 8.--Path of Nu for average and large referred ring distances L'/K.

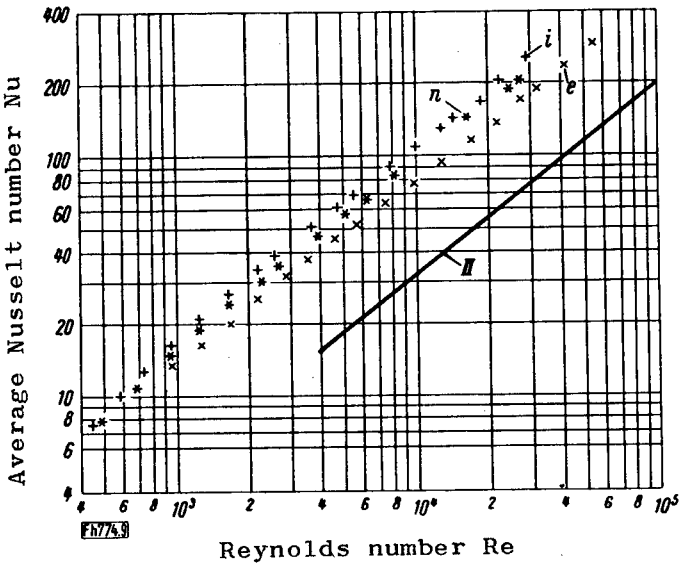

Fig. 9.--Path of Nu for small referred ring distances L'/K.

Figs. 8 and 9.--The average Nusselt number Nu as a function of the Reynolds number Re for the tube with disc-shaped turbulence promoters. I and II are comparison curves according to Equations (13) and (14), respectively, for the smooth tube without inserts; a_o = test values for the smooth tube; the remaining letters designate the corresponding arrangement according to Table 1.

influence of K and L' decreases continually until it disappears almost entirely at Re $\approx$600. In the range of Re > 600, the influence of the free convection continues to decrease not only with increasing Re but also with decreasing values of m* and L'/K.

It should still be noted that the disc inserts cover 5% of the heating area in the most unfavorable case; since they were slightly underdimensioned, however, and therefore adhered only little to the tube wall, the effective heating area could hardly be decreased by these inserts. The same is true for all other turbulence promoters under investigation.

4.122 Influence of the Referred Ring Distance L'/K:-- In the turbulent range Nu depends on L'/K in a similar manner as the resistance coefficient and also attains the highest value for the different types of discs (m* = const) at L'/K $\approx$ 10.

4.123 Influence of the Aperture Ratio m*:--For subsequent considerations it seemed suitable to eliminate the influence of the intake effect.[6] The representation in Fig. 10 in which the average Nusselt number Nu of the tube with inserts divided by the average Nusselt number Nu_o of the smooth

---

6) For this purpose the Nusselt numbers Nu were recalculated to Nu_∞ according to Equation (25) and designated as Nu (i.e. the index ∞ was omitted). In the experimental values for other turbulence inserts, which are still to be reported on in the following sections, only the Nu,Re curves contain the particular intake effect, while the Nusselt numbers in all other representations have been recalculated to values of fully developed flow in the same manner and have been denoted by Nu.

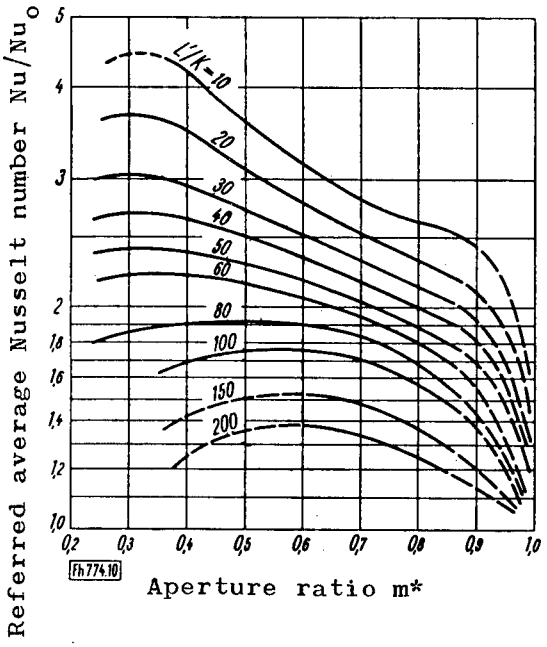

Fig. 10.--The referred average Nusselt number Nu/Nu_o as a function of the aperture ratio m* at different referred ring distances L'/K for tube with disc-shaped inserts.

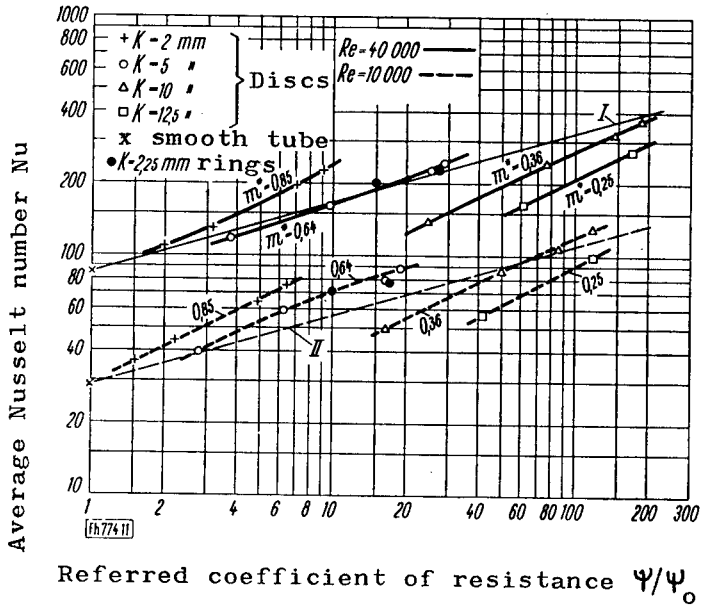

Fig. 11.--The average Nusselt number Nu as a function of the referred coefficient of resistance Ψ/Ψ_o for tubes with disc-shaped and ring-shaped inserts for different values of the ring height K, the aperture ratio m* and the Reynolds number Re. I and II is the course of Nu for the smooth tube with a velocity increase corresponding to the increase of the coefficient of resistance from Ψ_o to Ψ.

tube, is plotted for different L'/K values as a function of m^*, gives a good view of the manner in which the heat transfer in tubes can be increased by means of sharp-edged, disc-shaped inserts. The curves correspond to average values for the range of $10{,}000 < Re < 40{,}000$; the individual values deviate by $\pm$ 3% at the most. If the validity range is expanded to $4000 < Re < 80{,}000$, the individual values for different Reynolds numbers deviate by a maximum of $\pm$10% from these average curves. The greatest deviations in this case occasionally occur for the average aperture ratios ($m^* \approx 0.5$).

The curves for the values $L'/K < 10$ which still are present for a limited range have not been plotted in Fig. 10. They are again lower than the curve for $L'/K = 10$. While the curve for $L'/K = 8$ still nearly coincides with the one for $L'/K = 10$, the curves for $L'/K = 4$ and $L'/K = 20$ practically do coincide.

Mainly it is worthy of note that the Nusselt number can attain 4.5 times as large values for the maximum case than in the smooth tube. This is true for $m^* \approx 0.3$ and $L'/K \approx 10$. But for smaller m^* values the curves drop again. However this range of m^* hardly has significance, since the pressure loss in this area increases considerably.

Approximately half of the possible increase of Nu already results from the transition of $m^* = 1$ to $m^* \approx 0.85$, i.e. in a range which is barely touched by the new experiments. The results of W. Nunner [1] fill this gap. It is true that the coefficient of resistance also increases considerably more in the range $1 \geq m^* \geq 0.85$ than in the range $0.85 \geq m^* \geq 0.25$ (compare Fig. 5).

4.124 Relation between Heat Transfer and Resistance:--

In order to provide a better view of the relationship between the pressure loss and heat transfer, the average Nusselt number Nu was plotted as a function of the ratio ψ/ψ_o, which is the ratio of the resistance coefficients ψ and ψ_o of the tube with and without inserts, respectively, at equal Reynolds number. Since at Re = const and ϱ = const the weight rate of flow of mass was also constant, it is possible to introduce the ratio N/N_o of the delivery efficiency N and N_o of the blower with and without inserts, respectively, in place of ψ/ψ_o.

In Fig. 11 the Nu, ψ/ψ_o curves are valid for different values of m* = const. The straight lines I and II connecting the points obtained for the smooth tube at $\psi/\psi_o = 1$ show how the Nusselt number would increase in a smooth tube for the two Reynolds numbers under investigation if the velocity were increased from an initial value w_o to a value w in such a manner that the coefficient of resistance would increase from ψ_o to ψ. The energy input N_w for conveying the air through the smooth tube with velocity w then is exactly as great as the energy input N which is required to convey the air through a tube with inserts at velocity w_o.

Since the external tube dimensions remain the same, it is possible to determine with the aid of Fig. 11 and by neglecting differential heating area expenditures whether it is advantageous to improve the heat transfer by increasing the rate of flow in the smooth tube or by means of turbulence promoters. Thus, for example, at Re = 40,000 the values of the discs with K = 2 mm (m* = 0.85) and in part of the discs with K = 5 mm (m* = 0.64) are found above curve I; therefore from the energy-economy point of view these inserts are superior to the smooth tube. The reference ring distance L'/K = 10 has

the most favorable effect for all m* values. Small m* values on the other hand, are unfavorable, since the Nusselt number decreases with m* at Ψ/Ψ_o = const (and N/N_o = const or N_w/N_o = const, respectively).

Similar relationships exist also for the smaller Re values, only with the difference that the influence of turbulence promoters has even a somewhat more favorable effect. Above $m^* \approx 0.7$ all disc arrangements are superior to the smooth tube from the economic point of view.

4.2 Rings as Turbulence Promoters

In contrast to the disc-shaped inserts described in Section 4.1, which adhered relatively closely to the tube wall, similar inserts were studied in which an open gap of 2.7 mm width remained between the external circumference of the insert and the tubewall. In this manner it was to be demonstrated how such gaps influence the flow processes and the heat transfer. These arrangements shall be denoted as ring-shaped turbulence promoters.

Two types of rings were utilized. The external diameter of the rings generally amounted to 44.5 mm, the internal diameter to 40 and 37 mm, respectively, and the thickness to 1 mm. Thus the rings had a height of K = 2.25 mm and 3.75mm respectively. Three sheet-brass rods of 1 mm thickness which were externally soldered onto the rings kept the arrangement together. The optimum value of $L'/K \approx 10$ was selected for the reference ring distance, as had been found previously. The height of the brass rods was kept at such measurements that the entire ring system could be unobjectionably introduced into the experimental tube and that the rings were in concentric position to the tube axis. The greatest projec-

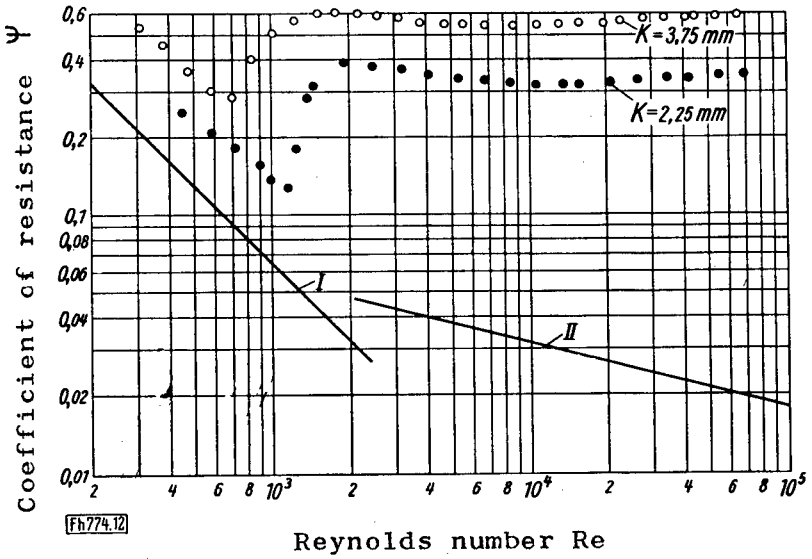

Fig. 12.--The coefficient of resistance ψ in the tube with ring-shaped turbulence inserts as a function of the Reynolds number Re. K = ring height; I and II = comparison curve according to Equations (6) and (7) for the smooth tube without inserts.

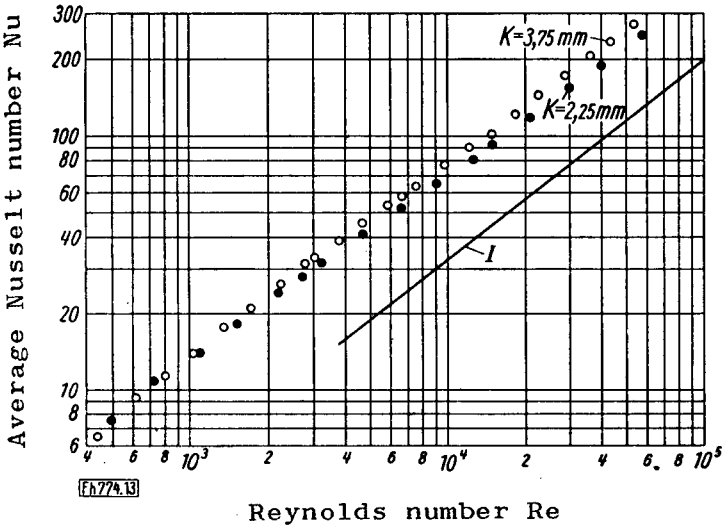

Fig. 13.--The average Nusselt number Nu as a function of the Reynolds number Re for the tube with ring-shaped turbulence inserts. K = ring height; I = comparison curve according to Equation (14) for the smooth tube without inserts.

tion of the rings from the wall amounted to about 5 and 6.5 mm, respectively.

4.21 Pressure Loss

Fig. 12 shows the measured ψ,Re curves which have a course similar to those in Figs. 3 and 4 for the discs with K = 5 mm and with the small reference ring distance. The coefficient of resistance for the small rings in Fig. 12 is below the curve for the larger rings. The change-over from the laminar to the turbulent state of flow for the small rings as well as for the discs with K = 5 mm occurs at almost the same Reynolds number.

4.22 Heat Transfer

Just as in the case of the coefficient of resistance, the course of the Nusselt number as a function of the Reynolds number for ring inserts according to Fig. 13 is very similar to the one which was found for discs with K = 5 mm ($L'/K \approx 10$) (compare Fig. 8), with the exception that the curves in Fig. 13 are somewhat lower. The surprisingly small difference in the heat transfer between the ring inserts and the disc-shaped inserts is explained later in Section 5.36 on the basis of special measurements. Fig. 11 also contains the measurement values for Nu as a function of ψ/ψ_o for ring inserts; these points are also close to the curves which are valid for the discs with K = 5 mm.

4.3 Baffleplate-shaped Turbulence Inserts

In another measuring series baffleplate-shaped inserts were utilized which, in contrast to the above-described inserts, are supposed to cause flow turbulence from the center of the tube. Fig. 14 shows a few of the baffle-plate inserts which were utilized; Table 2 contains their most important data.

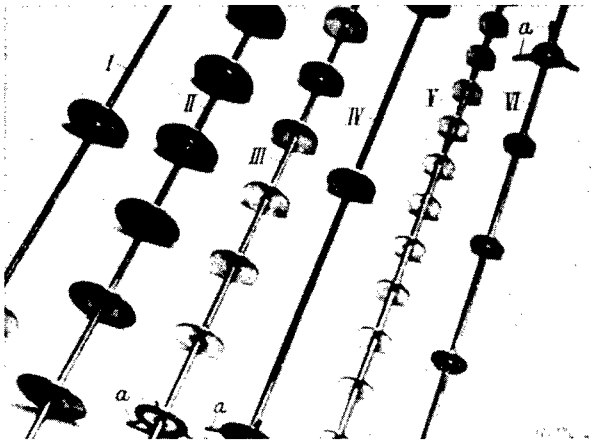

Fig. 14.--Examples of baffleplate inserts. I to VI = arrangements I, H, E, G, A and B corresponding to Table 2; a = spacer.

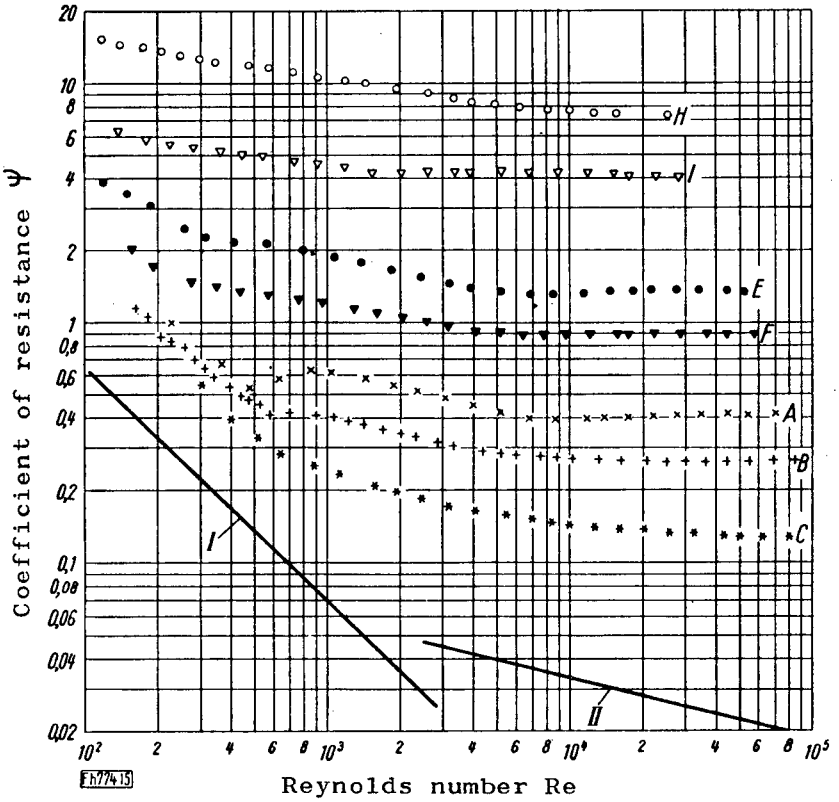

Fig. 15.--The coefficient of resistance ψ in the tube with baffleplate inserts as a function of the Reynolds number Re. I and II = comparison curve according to Equations (6) and (7) respectively for the smooth tube without inserts; the capital letters refer to the corresponding arrangements in Table 2.

Table 2

Data for Baffle Plate Inserts

External Plate Diameter d_S mm	Aperture Ratio m* -	Reference Plate Distance° L'/d_S	Denotation of the Arrangement
20	0.84	1.55	A
		3.8	B
		9.8	C
30	0.64	0.65	D
		1.63	E
		3.27	F
		5.45	G
40	0.36	1.44	H
		3.5	I
		8.15	K

°The plate distance L' is measured between the center planes of two neighboring baffleplates.

The external diameters d_S of the brass plates of 1 mm thickness were selected in such a manner that the aperture ratios m* for the ring-shaped gaps resulted in the same amounts as for the disc inserts. A brass rod pushed through the center of the plates and soldered onto them served for the introduction of the system into the experimental tube. Individual plates were provided with three spacer rods which made possible a concentric position to the tube axis.

4.31 Pressure Loss

4.311 Influence of the Reynolds Number:--Fig. 15 shows the course of the coefficient of resistance as a function of the Reynolds number (for the sake of clarity some of the curves which were measured have been omitted). Strangely enough no unequivocal statement is possible about the transition from the laminar into the turbulent flow. Only in the case of plates with d_S = 20 mm (curves A and B) is it pos-

sible to recognize transition areas ($400 \leqq Re \leqq 600$) and at the left of this there are also curve portions the course of which indicates a laminar character of the flow. Above $Re \approx 5000$, ψ remains almost independent of the Reynolds number; only curve C for d_S = 20 mm drops slightly toward the right, since the proportion of wall friction in this case is still relatively high with respect to the total resistance. The highest coefficients of resistance are about 400 times as large as in smooth tubes.

4.312 Influence of the Distance Ratio L'/d_S:--It is evident from Fig. 16 how the coefficient of resistance ψ changes with the referred plate distance L'/d_S at Re = 40,000 (L' denotes the distance of the center planes of two neighboring plates). The curves for m* = const have a similar course to those in Fig. 4 and exhibit a maximum which is found at the point $L'/d_S \approx 0.9$ for the average aperture ratio m* = 0.64. For large L'/d_S values ($L'/d_S \rightarrow \infty$) the coefficient of resistance of the smooth tube must also be attained here, while for very small L'/d_S values ($L'/d_S \rightarrow 0$) the coefficient of resistance of a ring-gap flow must be reached.

4.313 Influence of the Aperture ratio m*:--Fig. 17 shows the course of ψ as a function of m* with L'/d_S as the parameter for Re = 40,000. The values have been partly interpolated from Fig. 16. Similar to Fig. 15, the curves can be represented by an empirical equation; the following is true in the range $0.36 \leqq m^* \leqq 0.85$ and $8 \geqq L'/d_S \geqq 1.5$:

$$\psi = \frac{100}{L'/d_S} e^{-m^*[6-0.1(L'/d_S)]} \qquad (29)$$

Since ψ hardly changes with Re in the range $Re \geqq 8000$, Equation (29) is also valid for other Reynolds numbers than 40,000.

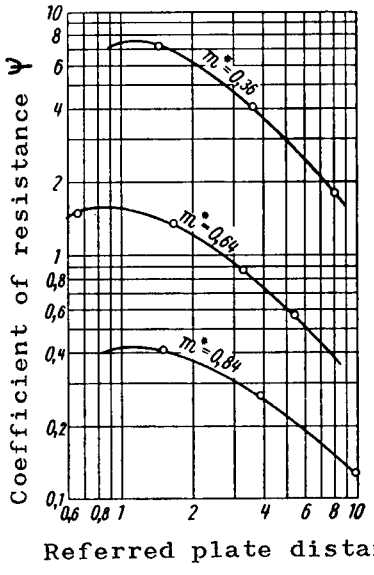

Fig. 16.--The coefficient of resistance Ψ in the tube with baffleplate inserts as a function of the referred plate distance L'/d_S for different aperture ratios m* and for a Reynolds number Re = $4 \cdot 10^4$.

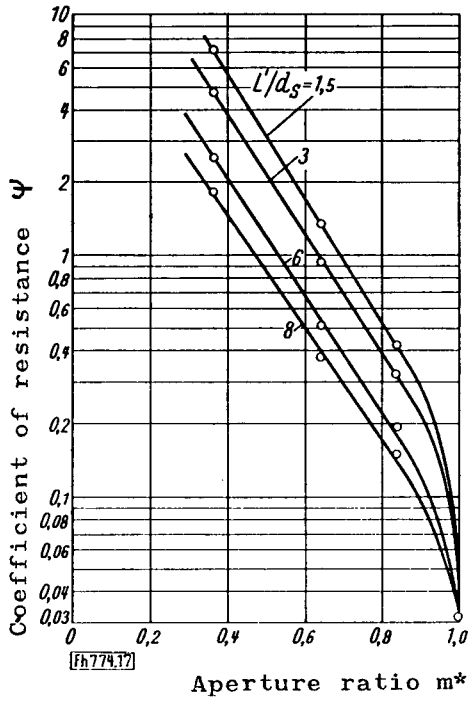

Fig. 17 .--The coefficient of resistance Ψ in the tube with baffleplate inserts as a function of the aperture ratio m* for different referred plate distances L'/d_S and a Reynolds number Re = $4 \cdot 10^4$.

The influence of the plate thickness was not investigated further. The latter might influence the pressure loss only under extreme conditions, such as, for example, with very small tube or plate diameters.

4.32 Heat Transfer

4.321 Influence of the Reynolds Number:--In the course of the average Nusselt number Nu as a function of Re in Fig. 18 it is again noticeable that in a large proportion of the turbulent range all curves run parallel to curve I for the smooth tube. The Nu values are up to 5 times as large as in the smooth tube; if the Re values are not too small, the Nu-values are considerably influenced by the aperture ratio, while the L'/d_S factor has a more extensive effect mainly with small m* values. With decreasing Re all curves approach each other more closely and at Re $\approx$ 600 they run into one curve.

4.322 Influence of the Aperture Ratio m*:--Fig. 19 shows Nu/Nu_o as a function of m* with L'/d_S for a parameter. The curves represent the average values for the range $10{,}000 \leqq Re \leqq 40{,}000$. The maximum deviation of the individual values amounts to ±3%. But if the validity range is expanded up to Re = 80,000, then individual values deviate by a maximum of 12% from the curves. The greatest deviations occur at $m^* \approx 0.5$. A maximum of Nu/Nu_o for a certain value of L'/d_S could not yet be determined on the basis of experimental results. While in the case of disc-shaped inserts 4.5 times as high Nu-values as in the smooth tube could be attained as a maximum, the upper limit of Nu/Nu_o in the baffleplate-shaped inserts might be considerably higher. The curves have a very steep course in the range $1 \geqq m^* \geqq 0.85$.

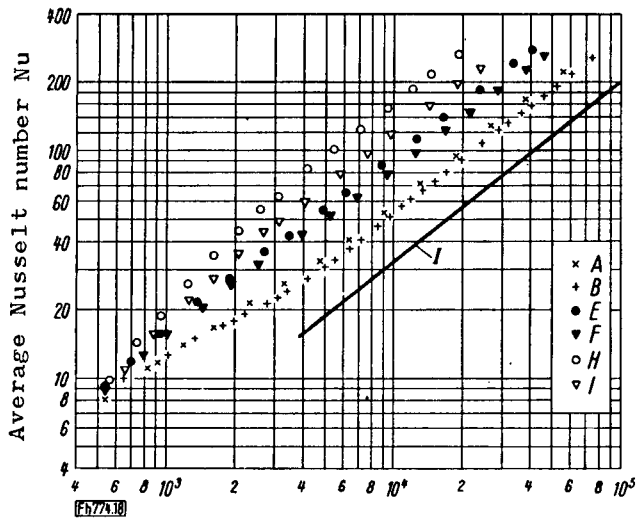

Fig. 18.--The average Nusselt number Nu as a function of the Reynolds number Re for the tube with baffleplate inserts. I = comparison curve according to Equation (14) for the smooth tube without inserts; the capital letters refer to the corresponding arrangements in Table 2.

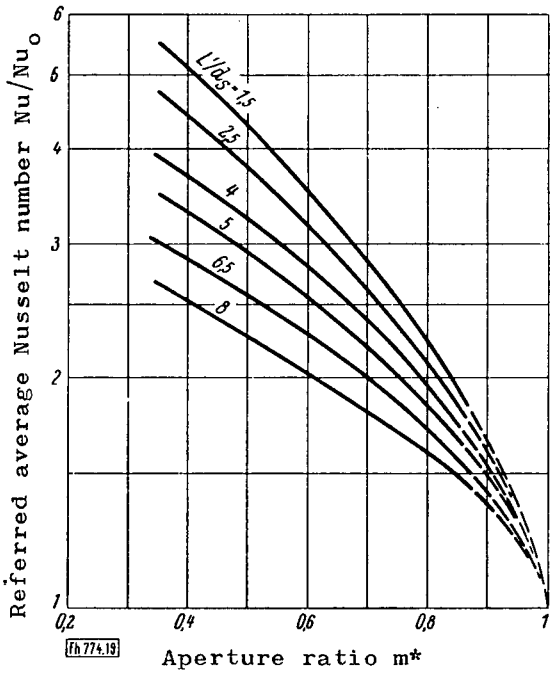

Fig. 19 .--The referred average Nusselt number Nu/Nu_o as a function of the aperture ratio m* at different referred baffleplate distances L'/d_S for the Reynolds number range $Re = 10^4$ to $4 \cdot 10^4$ for the tube with baffleplate inserts.

4.323 Relation between Heat Transfer and Resistance:--

The heat-economy value of tubes with baffleplate inserts was compared to that of smooth tubes at accelerated velocity in Fig. 20 similar to Fig. 11. The three groups of curves are valid for Re = 4000, 10,000 and 40,000. The points found for every type of plate (m* constant) at Re = const have been interconnected by curves. At Re = 40,000 only one case was found for the plates in which the Nusselt numbers had exactly the same magnitude as for a smooth tube with correspondingly increased velocity (plates with d_S = 40 mm, $L'/d_S \approx 1.5$). With decreasing Re the baffle turbulence producers behave increasingly more favorably. It is also true for baffleplates that Nu decreases somewhat with m* at equal Ψ / Ψ_o. While the curves of plates with d_S = 20 mm and 30 mm are almost parallel to the straight lines I to III for the smooth tube, the course of the curves for plates with d_S = 40 mm is steeper. Thus, larger L'/d_S values have a considerably more unfavorable effect here than in the case of smaller types of baffleplates.

4.4 Propeller-Shaped Turbulence Promoters

Baffles such as propellers cause flow turbulence in an entirely different manner than do discs, rings and plates. The additional tangential component of the rate of flow, which occurs in the center as well as near the wall of the flow in the presence of torque, decisively changes the entire character of flow in comparison to flow in a purely axial direction.

The propellers utilized for the measurements were produced from a brass plate of 50 mm diameter and 1 mm thickness. Vane-shaped sections were formed by means of six slits made from the outside which were twisted uniformly at an angle of

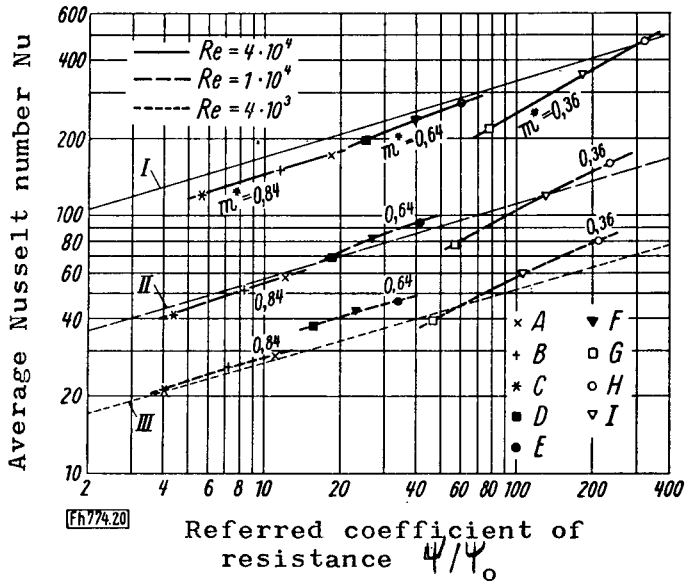

Fig. 20.--The average Nusselt number Nu as a function of the referred coefficient of resistance ψ/ψ_o for tubes with baffleplate inserts at different values of the aperture ratio m* and of the Reynolds number Re. I to III = path of Nu for the smooth tube at a velocity increase corresponding to the increase of the coefficient of resistance from ψ_o to ψ; letters A to I refer to the corresponding classifications in Table 2.

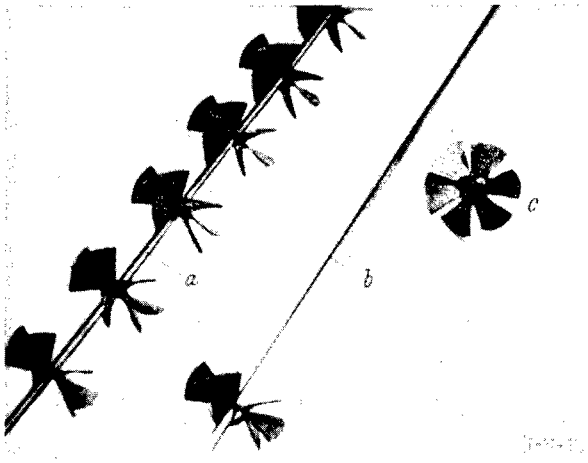

Fig. 21.--Examples of propeller-shaped inserts. a and b = arrangements ready for installation with closely and widely spaced propeller distances L', respectively; c = individual propeller.

about 45° to the central axis of symmetry. The individual propellers were mounted on a brass rod of 4 mm thickness onto which they were soldered at distances L' amounting to 49, 98, 326 or 980 mm (Fig. 21).

4.41 Pressure Loss

The resistance curves represented in Fig. 22 for propeller inserts have an entirely different character than the ψ, Re curves for disc, ring and plate inserts. Due to the swirling motion enforced by the propellers, the flow receives properties which have a continuous course of the coefficient of resistance as a consequence covering the entire range of Re, even in the case of widely spaced propellers. The curves run similar to the case of a fill of packing material; at large Re values it appears that they asymptotically approach a straight line with very little slope and at very small Re values (Re < 100), on the other hand, they come close to a straight line at 45° to the abscissa. Strangely enough, the ψ,Re curves for L' = 98 and 326 mm converge at high Re values.

4.42 Heat Transfer

Fig. 23 shows how Nu changes with Re. Above Re $\approx 3 \cdot 10^4$ the curves have a parallel course to the straight line I for the smooth tube. Below Re$\approx$600 all measuring points again fall on the same curve. In the intermediate range, especially in the case of smaller and medium-propeller distances L', the curves are somewhat higher than was to have been expected on the basis of previous results.

A few Nu values for different propeller arrangements have been plotted in Fig. 24 as a function of the referred coefficient of resistance ψ / ψ_o and were interconnected by

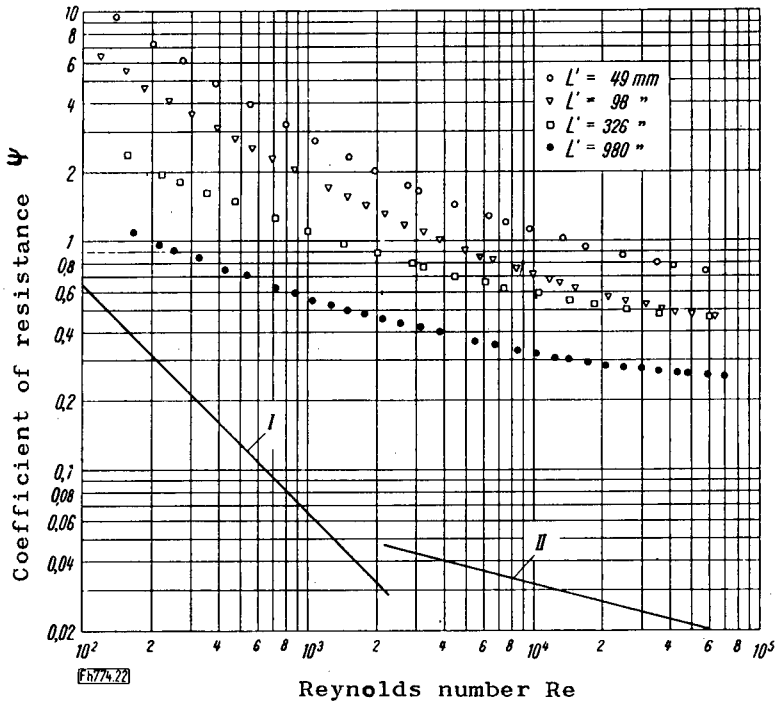

Fig. 22.--The coefficient of resistance ψ in the tube with propeller-shaped inserts as a function of the Reynolds number Re. I and II = comparison curve according to Equations (6) and (7), respectively, for the smooth tube without inserts; L' = propeller distance between the center planes of two neighboring insert units.

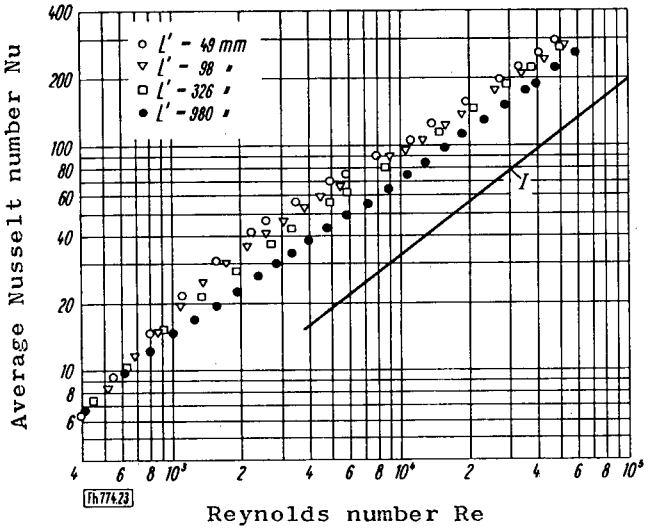

Fig. 23.--The average Nusselt number Nu as a function of the Reynolds number Re for the tube with propeller-shaped inserts. I = comparison curve according to Equation (14) for the smooth tube without inserts; L' = propeller distance.

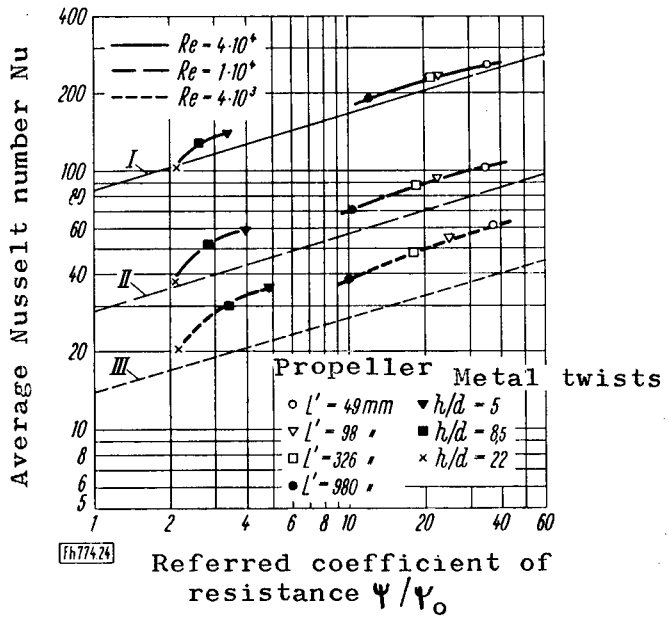

Fig. 24.--The average Nusselt number Nu as a function of the referred coefficient of resistance Ψ/Ψ_o for tubes with propeller-shaped or with spiral-shaped inserts for different Reynolds numbers Re. L' = propeller distance; h = pitch of the twists; d = tube diameter; I to III = path of Nu for the smooth tube at a velocity increase corresponding to the increase of the coefficient of resistance from Ψ_o to Ψ.

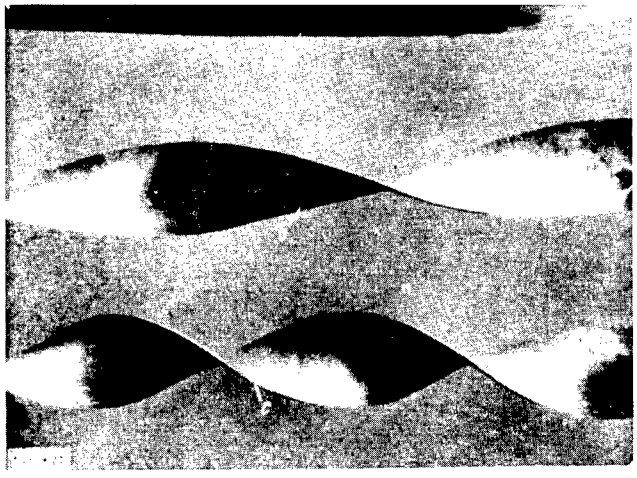

Fig. 25.--Helically twisted inserts. a to c = metal spirals with a referred pitch h/d = 22, 8.5 and 5, respectively.

curves for Re = const. These run approximately parallel to the straight lines I to III which are valid for the smooth tube. It is worthy of note that the extension of the curves which are contained in Fig. 11 for discs with K = 5 mm almost leads to the curves for propeller inserts in Fig. 24. Insofar as the disc-shaped inserts are properly dimensioned, they can thus serve for the attainment of ψ/ψ_o values and therefore also Nusselt numbers of approximately the same orders of magnitude as can be attained with propeller inserts.

4.5 Helically Twisted Metal Sheets as Turbulence Promoters

Because of the simple manner in which they can be produced, helically twisted metal strips are often proposed for turbulence inserts which are easily introduced later into a smooth tube. However, in the case of a small pitch h of the turns, the production of such strips proved to be difficult. For this reason, split cement molds were utilized inbetween which a soft aluminum strip of 1 mm thickness, 50 mm width and approximately 2 m length was pressed into the desired shape at certain intervals. Three such strips were available for the experiments (Fig. 25) having 0.9, 2.3 and 3.9 twists per meter (corresponding to a referred pitch h/d = 22, 8.5 and 5). For the helix with h/d = 5 the surface structure was no longer very good, however. This disadvantage could possibly be prevented with the aid of a special rolling arrangement; nevertheless, strips with small h/d values probably can hardly be produced without a heat treatment of the sheet metal.

4.51 Pressure Loss

The resistance curves of Fig. 26 display a certain similarity to the course of those found for propeller inserts

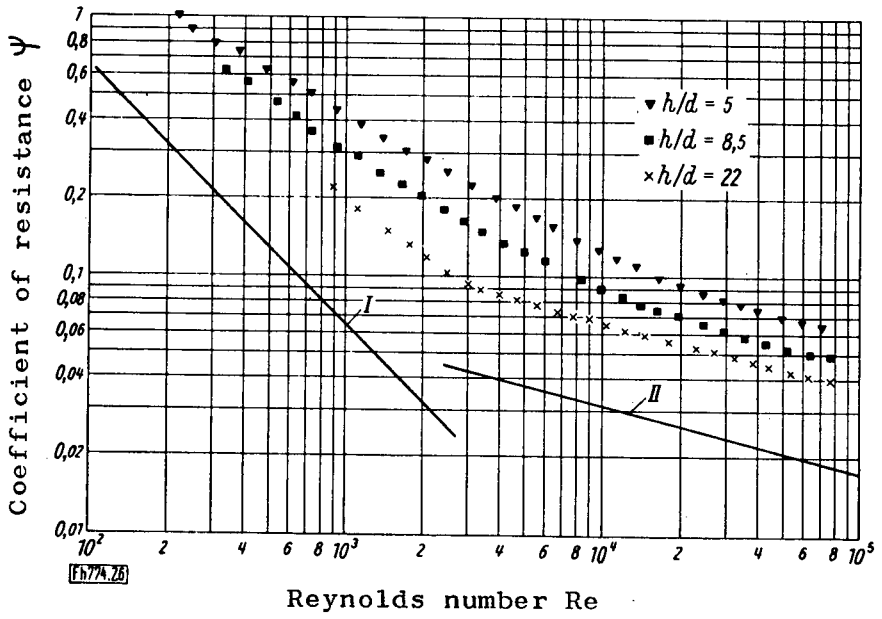

Fig. 26.--The coefficient of resistance ψ in the tube with helically twisted inserts as a function of the Reynolds number Re. I and II = comparison curve according to Equations(6) and (7) for the smooth tube without inserts; h = pitch of twists; d = tube diameter.

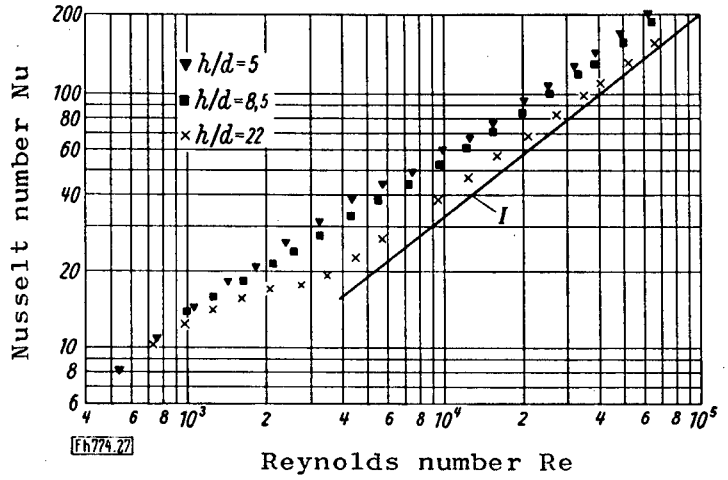

Fig. 27.--The average Nusselt number $\overline{Nu}$ as a function of the Reynolds number Re for the tube with helically twisted inserts. I = comparison curve according to Equation (14) for the smooth tube without inserts; h = pitch of the twists; d = tube diameter.

(compare Fig. 22). It can be concluded from the course of the curves in Fig. 26 that the total pressure loss rests to a large part on the wall friction of the strips. This holds true to the fullest extent in the case of infinitely large pitch. In that case the tube would be subdivided into two halves by means of an axial separating wall. The coefficients of resistance of the turbulent range for this case of a smooth transmission flow can be calculated with the aid of the hydraulic diameter. If the hydraulic diameter is selected as the reference magnitude for the measuring values, then the Ψ,Re curve for h/d = 22 is only approximately still 15% higher than the curve for the smooth tube, while the difference between the curves for h/d = 22 and II in Fig. 26 amounts to approximately 100%.

4.52 Heat Transfer

According to Fig. 27, the Nu,Re curves also run similar to those for propeller inserts (compare Fig. 23), but in Fig. 27 the Nu values are smaller. Nevertheless it is worthy of note that the Nusselt number of the smooth tube can be more than doubled by means of the twist.

Fig. 28 shows the course of the referred Nusselt number Nu/Nu_o as a function of the referred pitch h/d. Nu/Nu_o increases with decreasing Re. With decreasing pitch Nu/Nu_o tends towards a limit value which is apparently almost attained already at $h/d \approx 5$.

The relation between Nu and the referred coefficient of resistance Ψ/Ψ_o is shown in Fig. 24. With sufficiently large helical twist, the heat transfer in comparison to the smooth tube is improved to the same proportion in the range of smaller Ψ/Ψ_o values as in the case of propeller inserts in the range of larger Ψ/Ψ_o values. For the metal strip with

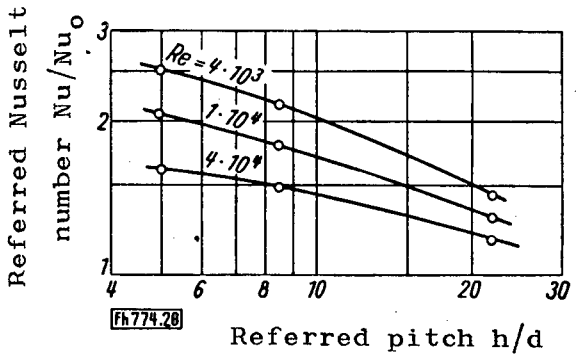

Fig. 28.--The referred Nusselt number Nu/Nu_o as a function of the referred pitch h/d at different Reynolds numbers Re for the tube with helically twisted inserts.

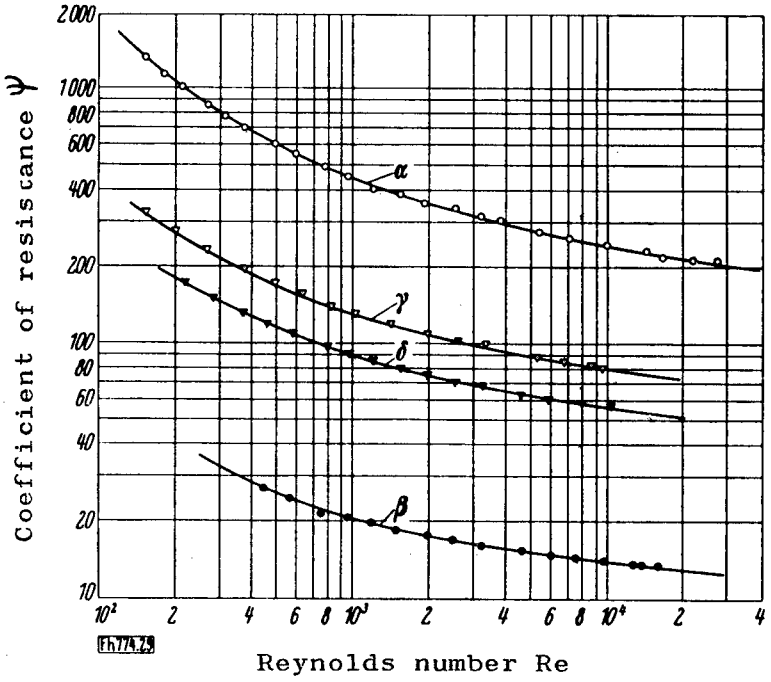

Fig. 29.--The coefficient of resistance ψ as a function of the Reynolds number Re for packed tubes. α to δ packing materials according to Table 3.

the least amount of twist the curves descend more steeply, because the relatively large wall friction resistance of the strip at best contributes only indirectly and to a small extent to the heat transfer.

4.6 Tubes with Packing Materials

As is known from earlier investigations, very large values are assumed by heat transfer and pressure loss in tubes with packing materials [21]. Therefore it seemed indicated to include a few experimental series with such tubes and to check the results which have so far been published.
Five mm and 16 mm Raschig rings as well as 10 and 12 mm stoneware balls served as packing materials, the characteristics of which are reproduced in Table 3.

Table 3

Data of the Packing Materials

Type of Packing Material	Aver. O.D. of Rings or Balls d_K mm	Aver. I. D. of Rings d_i mm	Ring Height h_r -	Refer. Tube Diam. d/d_K -	Rel. Space Vol. ε_L -	Denotation of Arrangement -
5 mm Raschig rings	5.39	2.79	5.64	9.28	0.565	α
16 mm Raschig rings	16.71	12.05	15.44	3.0	0.766	β
10 mm balls	10.4	-	-	4.81	0.578	γ
12 mm balls	12.7	-	-	3.94	0.505	δ

They were poured into the experimental tube as well as into portions of the intake and outlet sections with the greatest possible density. Screens held by low clamping rings braced the filling at the beginning and end of the filled tube sections. The screens were dimensioned in such a manner that their pressure loss remained negligibly small for every case.

For the 16 mm Raschig rings, the ratio d/d_K (with d_K as the external diameter of the rings and balls, respectively) was quite small, so that the edge effect was already considerable and resulted in a large relative space volume ξ_L (space volume through free tube volume). But this is also of great significance for the pressure loss. In the ball packings d/d_K was also relatively small.

Overpressures up to 1 atm occurred in the experimental arrangement during this series, for which the equipment had not been originally planned. In order to avoid leaks at the flange couplings, determinations of the rate of air flow in the packing material experiments were carried out in a measuring section mounted behind the experimental tube.

4.61 Pressure Loss

The Ψ,Re curves in Fig. 29 have the characteristic course for bulk materials and are almost parallel to each other. Depending on the type of packing material, Ψ is about 600 to 10,000 times as large as in the smooth tube. A comparison with other measurements, however, is hardly possible, since these experiments as a rule were based on much larger d/d_K values.

4.62 Heat Transfer

The Nu values are a little more scattered for the packed tubes than for the other turbulence inserts, Fig. 30. This is due to the fact that the difference between the tube wall temperature and the average flow temperature fell back up to 3°, so that small errors in temperature measurement already had a distinct effect. It is noteworthy that all packing materials under investigation resulted in equal Nu values within a scatter range of ±15%, although the pressure loss

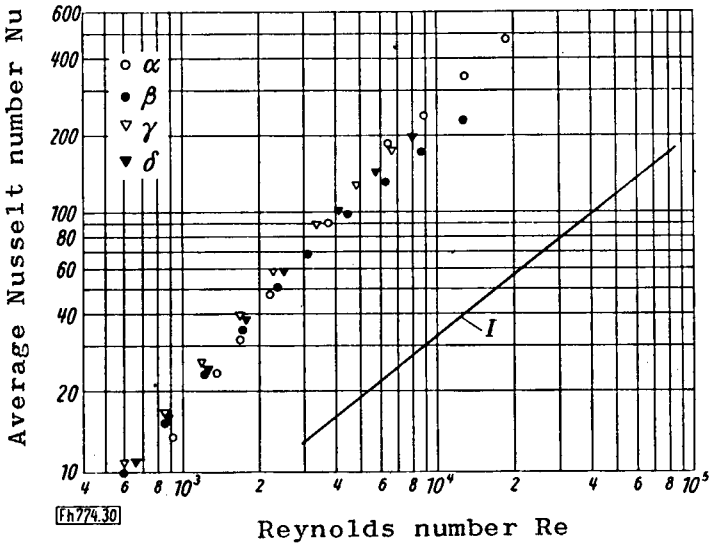

Fig. 30.--The average Nusselt number Nu as a function of the Reynolds number Re for packed tubes. I = comparison curve according to Equation (14) for the smooth tube without inserts; α to δ packing materials according to Table 3.

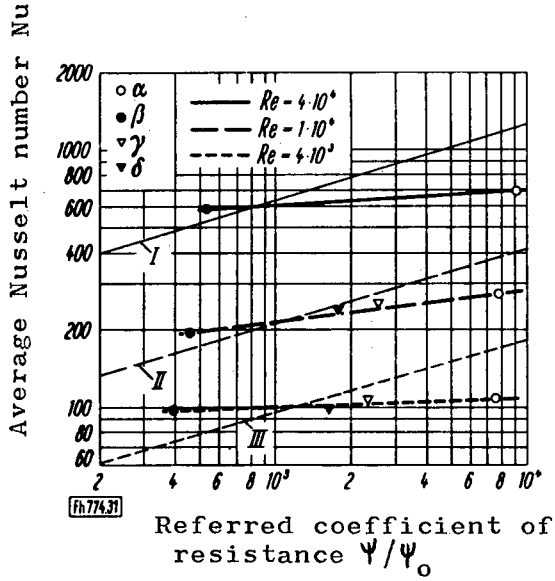

Fig.31.--The average Nusselt number Nu as a function of the referred coefficient of resistance Ψ/Ψ_0 at different Reynolds numbers Re in packed tubes. α to δ = packing materials corresponding to Table 3; I to III = path of Nu for the smooth tube with a velocity increase corresponding to the increase of the coefficient of resistance from Ψ_0 to Ψ.

assumes very differential values. At Re > 10^4 the Nusselt numbers on the average are about eight times as large as in the smooth tube.

It is evident from Fig. 31 that tubes with packing materials from the economical standpoint are rarely more advantageous than a smooth tube in which the rate of flow has been increased correspondingly. Only the tube which had been filled with 16 mm Raschig rings exhibited better heat transfer results than the smooth tube for the same Ψ/Ψ_o value. In this case also the position of the curves changes somewhat in favor of the tubes with packing materials, if Re is decreased. Since all packing materials influence the heat transfer in almost the same way, it must be that from among the different types those would be most favorable which cause the least pressure loss. However, this simple deduction is probably only valid up to a minimum order of magnitude of the packing material and pressure loss, respectively.

4.7 Flow and Temperature Field Patterns

The flow and temperature field patterns indicate the character of a flow and permit an insight into the mechanism of heat transfer. Therefore such field patterns were measured in the smooth tube as well as for a few insert arrangements.

The test cross section usually was approximately 100 mm before the tube end; therefore the results could not be falsified by secondary effects. In this case the turbulence promoters were arranged in the experimental tube in such a manner that the test plane generally was located in the center between two inserts. With respect to the height of the inserts, measurements could only be taken from the center of the tube up to a distance y from the wall, corresponding

approximately to the disc and ring heights. The test values described below usually represent the mean of two or four individual measurements which were determined on a perpendicular and horizontal plane at equal distance from the wall y.

Since the total pressure was determined with a Pitot tube, the local static pressure had to be subtracted from the test values in order to obtain the pressure head. At this point the static pressure was constant throughout the cross section and corresponded almost exactly to the pressure loss of the subsequent inserts. The latter can be calculated from the total pressure loss of the experimental tube and from the number of inserts. The accuracy of all velocity distributions was checked in such a way that the rate of air flow determined with the aid of the restrictor was compared with the rate of air flow resulting from the planimetry of the velocity distribution over the tube cross section. The agreement in general was very good.

4.71 Velocity Distributions

Fig. 32 shows the velocity distribution profiles of the smooth tube and of the tube equipped with discs of K = 5 mm for two Re-values in dimensionless representation. The relation of the wall distance y to the tube radius r was selected for the abscissa, and the relation of the local velocity w_y at wall distance y to the maximum velocity w_{max} in the tube axis was chosen for the ordinate.

For the disc arrangements the form of the velocity profiles within the measuring range remains practically independent of Re. In the smooth tube this does not hold true [3]. In comparison to the velocity distribution of the smooth tube, the two other profiles are considerably more pointed. Since

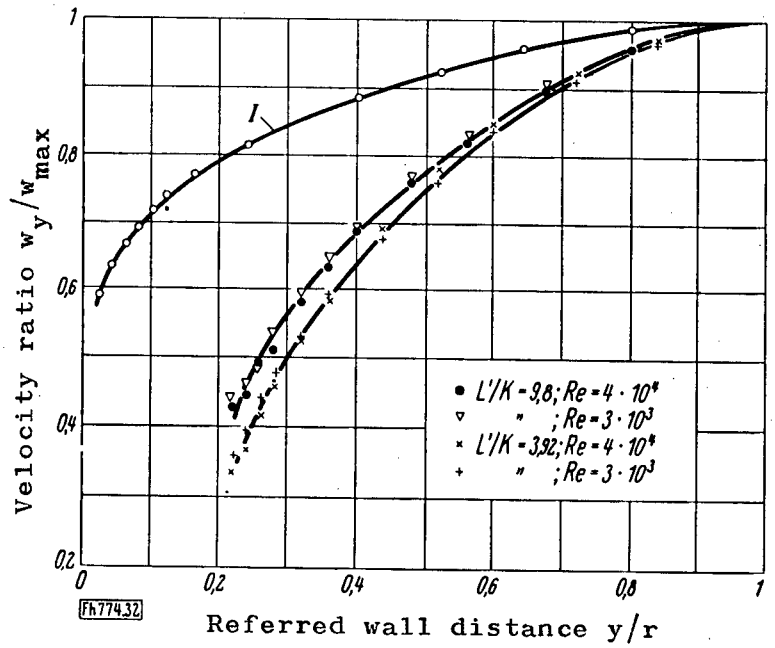

Fig. 32.--Velocity distributions for discs with K = 5 mm.

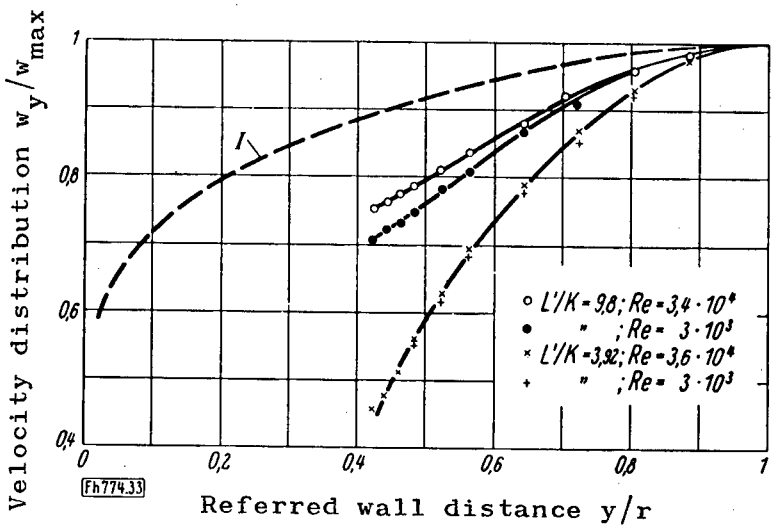

Fig. 33.--Velocity distributions for discs with K = 10 mm.

Figs. 32 and 33.--Velocity distributions in the tube with disc-shaped inserts. w_y = velocity at wall distance y; w_{max} = velocity in the center of the tube; r = tube radius; L' = ring distance; K = ring height; Re = Reynolds number; I = comparison curve for the smooth tube at Re = 4.10⁴.

this condition was also observed in the case of rough tubes in which the velocity distributions become increasingly sharper with increasing roughness, it is possible to conceive of the disc-shaped inserts as extreme roughness projections. Understandably, the most pointed profile results with the closest disc arrangement ($L'/K = 3.92$), since in this case after a certain intake section has been traversed the velocity field pattern hardly changes from disc to disc. The flow behaves similar as in a rough tube, the radius of which is equal to the internal disc radius.

Fig. 33 shows the results for disc arrangements with $K = 10$ mm $L'/K = 3.92$ and $L'/K = 9.8$. For a comparison, the curve for the smooth tube has been plotted again (Re $4 \cdot 10^4$). The discs extended from $y/r = 0$ to 0.4, so that test values are absent in this range. At $L'/K = 3.92$ the arrangement with $K = 10$ mm exhibits a considerably more pointed velocity distribution in comparison to the one with $K = 5$ mm. The relatively flat curve path of w_y/w_{max} at $L'/K = 9.8$ indicates that the velocity distribution changes considerably from disc to disc. The weight rate of flow control resulted in the greatest error of 10% for this determination.

The velocity distributions for the two ring arrangements coincide almost completely with the distribution obtained for the disc arrangement with $K = 5$ mm and $L'/K = 3.92$. Fig. 34 shows the profile for rings with $K = 3.75$ mm.

Measurements taken at various distances from the individual were intended to give information on the manner in which the velocity distribution changes behind a disc-shaped insert. For this purpose a single disc ($K = 5$ and 10 mm, respectively) was introduced into the experimental tube and supported by low piston rings which were installed in front and behind it.

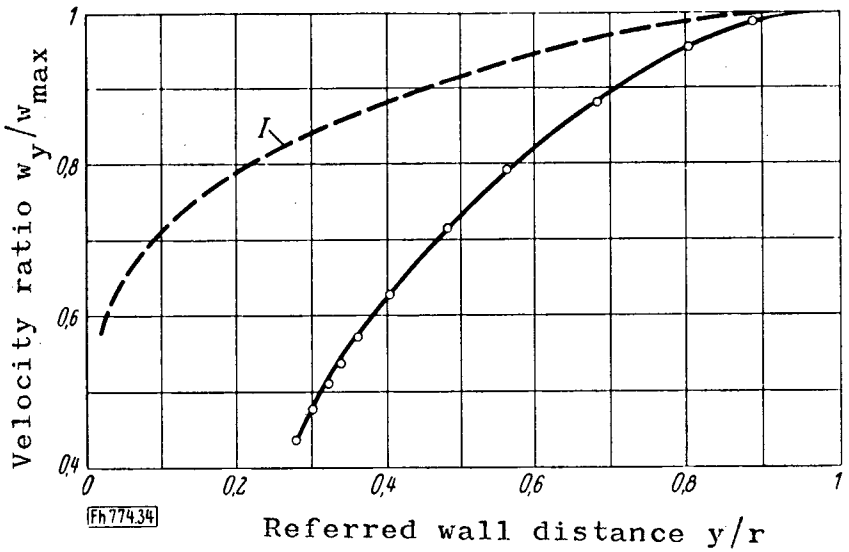

Fig. 34.--Velocity distribution in the tube with ring-inserts with a ring height of 3.75 mm and a Reynolds number $Re = 4 \cdot 10^4$. I = comparison curve for the smooth tube at $Re = 4 \cdot 10^4$; w_y, w_{max}, y and r as in Figs. 32 and 33.

By displacing these inserts, the distance between the test cross section and the individual disc could be changed. A comparison of the rate of flow determination with the cross section integration again served for an accuracy check of all velocity distributions. With diminishing distance between the insert and the Pitot tube, the accuracy of the measuring values decreases due to strong cross currents and due to the static pressure which is variable over the tube cross section. The highest error amounted to 8%.

Fig. 35 shows the velccity transformation behind the disc with K = 5 mm. In the disc cross section itself the velocity distribution will be almost rectangular. The first useable profile could only be determined at a distance of 1 = 100 mm behind the insert. At that point the flow again adheres completely to the tube wall. From here on the velocity equalizes very quickly over the entire cross section due to the extraordinarily strong, turbulent intermixture. At 1 = 500 mm the velocity in the center flow is almost constant, while a greater velocity gradient occurs at the wall. At 1 = 900 mm the profile has regressed somewhat again. After a path of corresponding length the fully developed, turbulent velocity profile is attained again (curve I).

For the disc with K = 10 mm only the measurements for $1 \geq 170$ were useable, since the flow only adhered to the wall again at this point (Fig. 36). At $1 \approx 200$ mm the velocity profile has transformed to such an extent that it almost coincides with the one determined at the same point behind the disc with K = 5 mm. In its subsequent course the velocity in the cross section first equalizes still more rapidly than behind the disc with K = 5 mm due to increased turbulent exchange processes. At $1 \approx 900$ mm, finally, the velocity profiles which

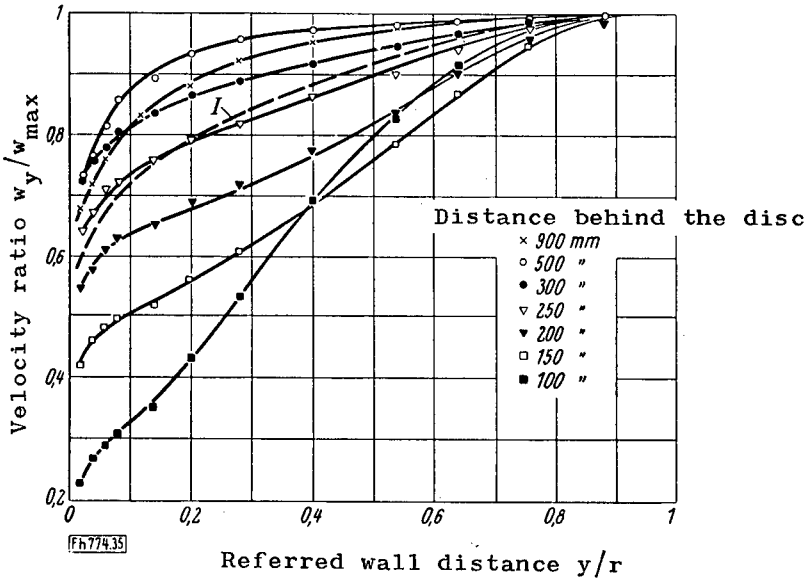

Fig. 35.--Velocity profiles behind a disc having an aperture ratio m* = 0.64 and a ring height K = 5 mm.

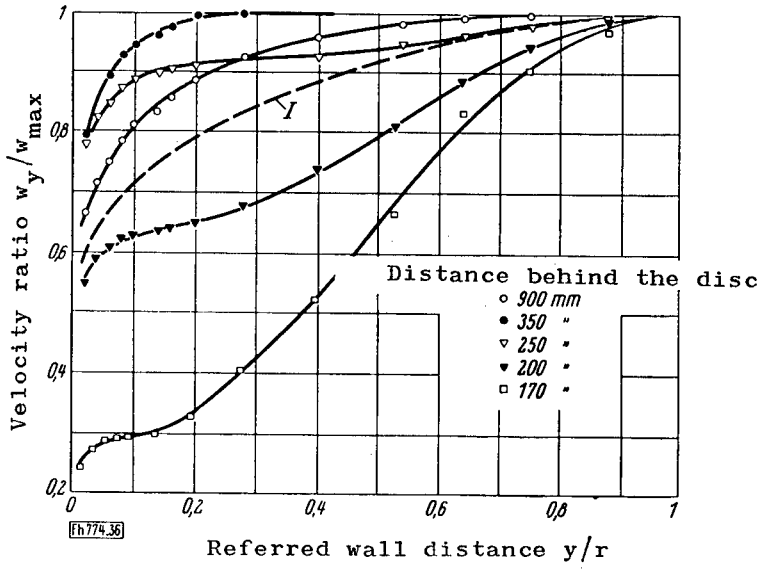

Fig. 36.--Velocity profiles behind a disc having an aperture ratio m* = 0.36 and a ring height K = 10 mm.

Figs. 35 and 36.--Transformation of the velocity profile behind an individual disc with a Reynolds number Re = $4 \cdot 10^4$. I = comparison curve for the smooth tube at Re = $4 \cdot 10^4$; w_y, w_{max}, y and r as in Figs. 32 and 33.

have already regressed somewhat coincide completely for both types of inserts.

4.72 Temperature Field Pattern

The temperature profiles corresponding to the velocity profiles of Figs. 32 and 33 are evident from Figs. 37 and 38. The referred overtemperature ϑ according to

$$\vartheta = (t_w - t)/(t_w - t_{min}) \qquad (30)$$

was plotted as the ordinate with t as the local temperature at wall distance y and t_{min} as the lowest temperature in the cross section.

The Reynolds number considerably influences the form of the temperature profiles. With increasing Re values the temperature path becomes flatter, because the heat resistance of the flow center decreases due to the increased exchange processes. For the same reasons the curves corresponding to disc arrangements with $L'/K = 9.8$ are flatter than those for $L'/K = 3.92$.

In Fig. 38 for discs with K = 10 mm, the profiles for $L'/K = 9.8$ are found above the curve I for the smooth tube, while the other two profiles for $L'/K = 3.92$ in the aperture range of the discs ($1 \geq y/r \geq 0.4$) are found below. Very large temperature gradients occur here at the wall, while from there the temperatures change only little up to $y/r \approx 0.4$. Therefore in this range the heat resistance is very small.

These relations are very well represented by Fig. 39 in which temperature profiles are reproduced which were determined at different points between a pair of discs for the arrangement with K = 10 mm and $L'/K = 3.92$. In the range $1 \geq y/r \geq 0.4$ the profiles practically do not differ. In

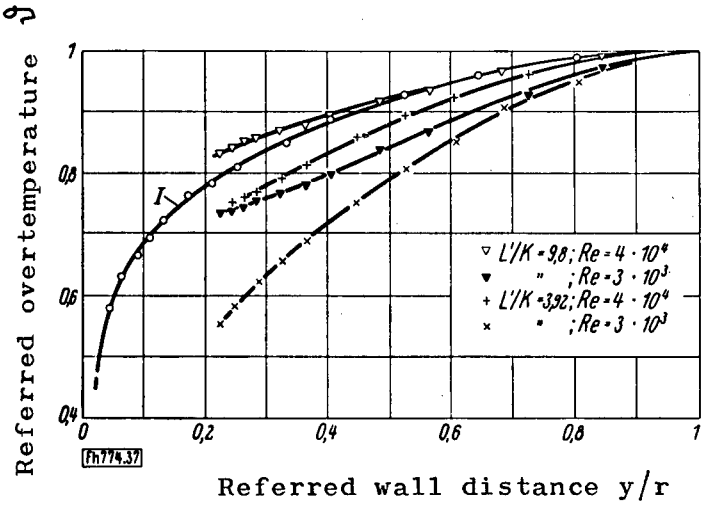

Fig. 37.--Temperature distributions for discs with K = 5 mm.

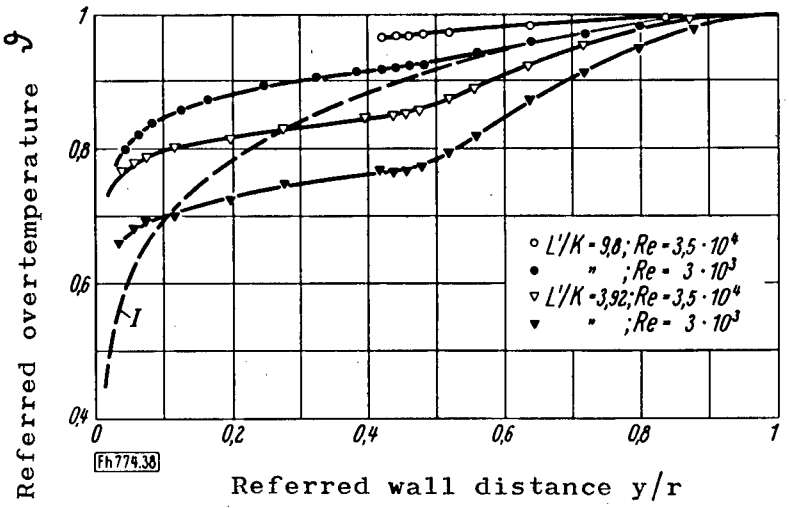

Fig. 38.--Temperature distributions for discs with K = 10 mm.

Figs. 37 and 38.--Temperature distributions in the tube with disc-shaped inserts. y = wall distance; r = tube radius; L' = ring distance; K = ring height; Re = Reynolds number; I = comparison curve for the smooth tube at Re = $4 \cdot 10^4$.

contrast, the external portions of the curves in the direction of flow become increasingly more flat. Directly before the next disc located in the downstream direction the temperatures have almost equalized in the boundary zone. At the same time, the temperature gradients at the tube wall increase more and more. From this it can be concluded that in the case of flow media with a higher Prandtl number these turbulence

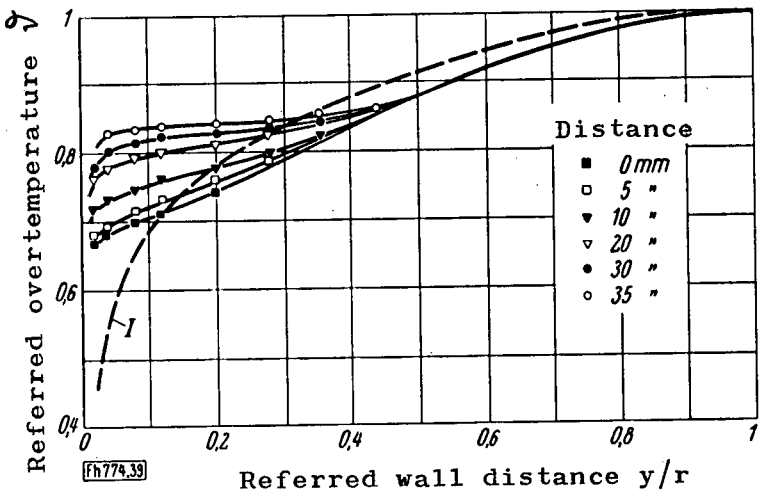

Fig. 39.--Temperature distributions at various distances behind the all-but-last disc. y, r and I as in Figs. 37 and 38.

inserts do not increase the heat transfer in the same manner as in the case of air, since in that case the heat resistance of the center of flow is already correspondingly low for a flow without inserts.

Fig. 40 and 41 show the shift of the temperature profiles at different distances l from a single disc. At a distance of more than $l \approx 300$ mm, the temperature profile transforms in a very similar manner to the corresponding velocity profile. In the range of $l \leq 300$ a comparison is not easily possible insofar as the velocity profile at $l = 0$ deviates very much

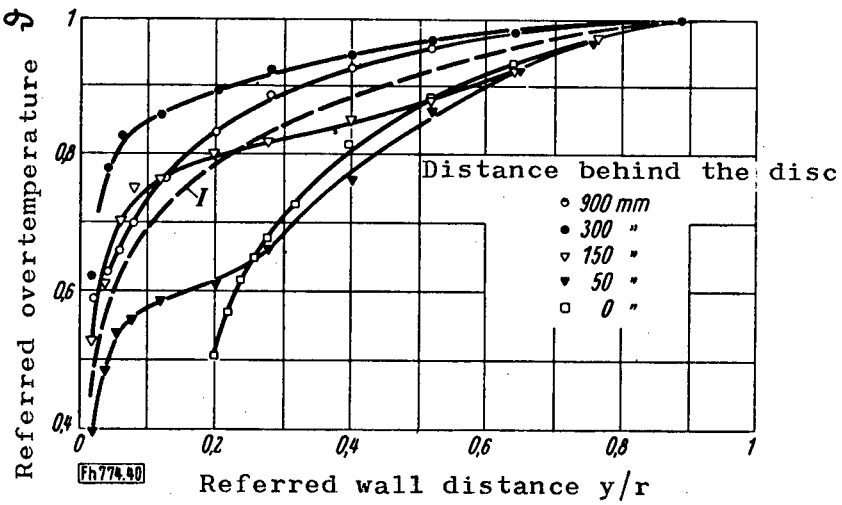

Fig. 40.--Temperature profiles behind a disc having an aperture ratio m* = 0.64 and a ring height K = 5 mm.

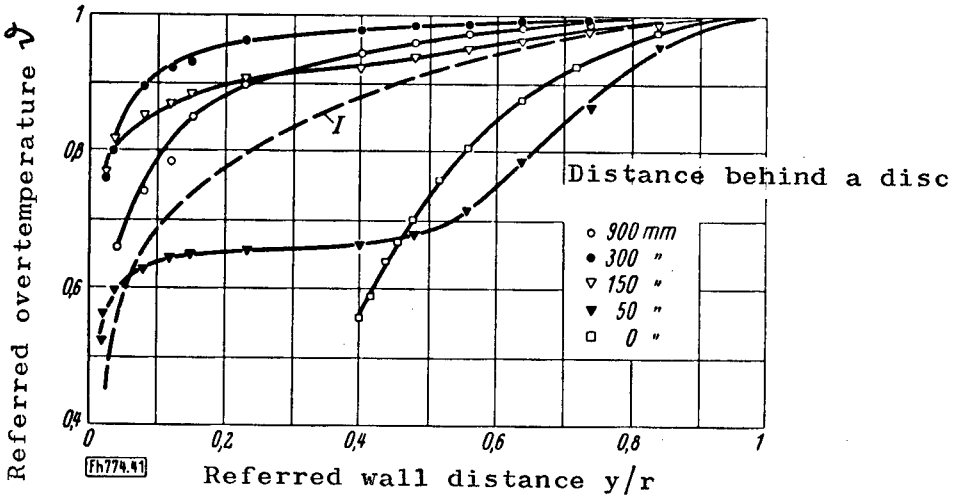

Fig. 41.--Temperature profiles behind a disc having an aperture ratio m* = 0.36 and a ring height K = 10 mm.

Figs. 40 and 41.--Transformation of the temperature profile behind an individual disc at a Reynolds number Re = $4 \cdot 10^4$. y, r and I as in Figs. 37 and 38.

from the form of the temperature profile. In a crude approximation one might assume about the same mechanism for the exchange of impulse and heat.

In the smooth tube the temperature field pattern at small Reynolds numbers is greatly influenced by free convection. Fig. 42 shows the course of ϑ over the cross section

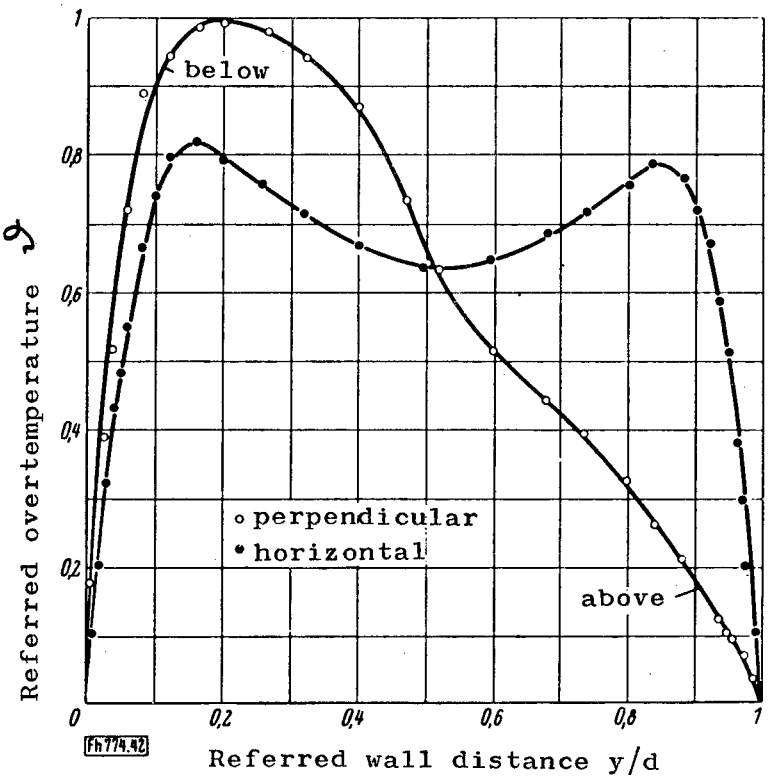

Fig. 42.--Perpendicular and horizontal temperature distribution in the smooth tube with a Reynolds number Re = $3.4 \cdot 10^3$.

of the tube in perpendicular and horizontal direction. A transverse convection flow, presumably consisting of several partial flows, is superimposed over the main flow along the tube. Therefore the temperature profile is practically symmetrical in a plane through the tube horizontal to the tube axis, but not in a plane which traverses the tube perpendicularly.

4.73 Pressure Distribution

The course of the static overpressure Δp_o against the outlying area was determined longitudinally as well as transversally to the tube axis between a pair of discs for disc arrangements with K = 10 mm; this was done between the last two inserts between which the velocity profiles had also been determined. This was to check the usefulness of the assumption on which the determination of the velocity profiles were based, i.e. that the static pressure does not change over the tube cross section.

A probe of 2 mm external diameter, containing two pressure borings of 0.2 mm diameter which faced each other transverse to the direction of flow, served as the measuring instrument. It is true that measuring errors are easily possible in the case of strongly turbulent flow; however, the measuring values are reported nevertheless, since they at least provide a good point of reference.

Figs. 43 and 44 show the path of Δp_o as a function of the distance l behind the last disc but one for various values of y/r. On the basis of these measurements, the static pressure in the tube cross section is only approximately constant in the center between two inserts. In this manner the assumption is confirmed which was the basis for the calculation of the velocity profiles for the essential static pressure. At y/r = const. the static pressure in the direction of flow does not drop linearly in contrast to the fully developed flow with pure wall friction in the tube. This behavior can be explained as follows: An overpressure prevails before the disc in contrast to the unaffected flow; behind the disc an underpressure exists due to the contraction of the flow, as can be clearly seen in the path of the individual curves. However,

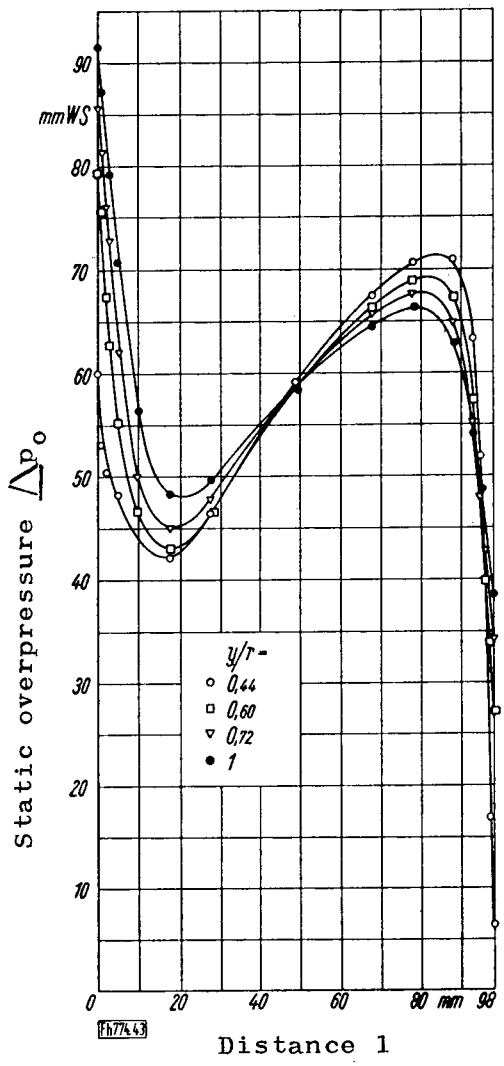

Fig. 43. Pressure distributions at a referred ring distance L'/K = 9.8.

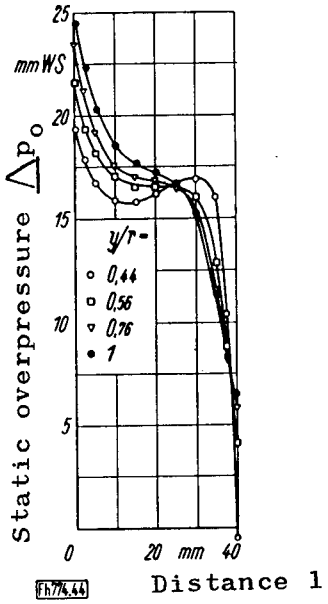

Fig. 44.--Pressure distributions at a referred ring distance L'/K = 3.92.

Figs. 43 and 44.--Course of the static overpressure Δp_o between two discs as a function of the distance 1 from the foremost disc in the direction of flow, as well as at different referred wall distances y/r. Ring height of discs K = 10 mm; aperture ratio m* = 0.36; Reynolds number Re = $3.5 \cdot 10^4$.

more accurate data are not possible since too many unexplained effects coincide.

Fig. 45 shows how the static pressure and the rate of flow w_{max} change along the tube axis in one case. Shortly behind the disc a velocity maximum occurs, while a minimum exists shortly before the disc. Admittedly the absolute value of the velocity fluctuates at the most by only about 3%. This course of the velocity can be easily interpreted. Shortly behind a disc the main flow is somewhat constricted. Therefore the velocity increases. When the main flow expands again in its subsequent path, the velocity decreases correspondingly. Shortly before the next disc the flow is constricted again; and the flow rate increases again.

5. Interpretation of Experimental Results

5.1 Mechanism of Heat Transfer

The experimental results show that the coefficient of heat transfer for turbulence inserts assumes very different values depending on the type of insert, and that it is not directly related to the pressure loss. Therefore it appeared desirable to clarify the mechanism of heat transfer in the case of turbulence promoters still more closely. For a starting point, the corresponding processes in a smooth tube shall be considered.

The processes in the boundary layer are first of all decisive for the heat transfer from the wall to a flowing medium. The greatest heat resistance of the turbulently flowing medium is found in a very thin layer close to the wall, which mainly has laminar properties. Its thickness δ depends considerably upon the wall shear stress τ_w which therefore represents an important magnitude characterizing the flow as well as the heat transfer.

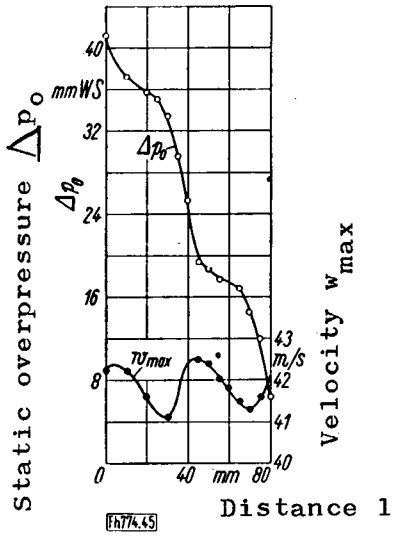

Fig. 45.--Course of the static overpressure Δp_o and the velocity w_{max} in the tube axis as a function of distance 1 between two discs in the direction of flow. Disc height K = 10 mm; aperture ratio m* = 0.36; referred ring distance L'/K = 3.92; Reynolds number Re = $3.5 \cdot 10^4$.

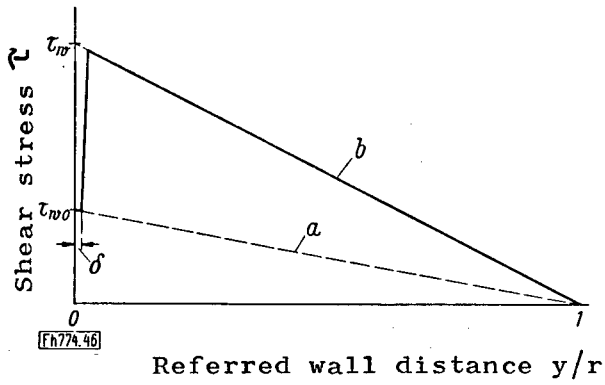

Fig. 46.--Scheme of the course of shear stress in rough tubes according to W. Nunner [1]. a = course in the smooth tube with wall shear stress τ_{wo}; b = course in the rough tube with wall shear stress τ_w.

In the case of isothermal, hydrodynamically developed flow in a smooth tube the pressure loss Δp is only produced by wall friction, while the static pressure p drops linearly along the tube. The local shear stress τ at wall distance y provoked by forces of friction also varies linearly from y = 0 to y = r (drop of τ_w to $\tau = 0$). If the equilibrium between the forces of pressure and friction are considered for a tube section of length L, then it follows:

$$1/4\,\pi\, d^2\, \Delta p = \pi\, dL\, \tau_w \tag{31}$$

or

$$\tau_w = 1/4\, \Delta p\, d/L \tag{32}$$

and after substitution of Δp by means of Equation (1), respectively,

$$\psi \triangleq 8\, \tau_w/\varrho\, w^2 \tag{33}$$

While until now flow has been considered as an aggregate, more detailed individual points shall now be examined. L. Prandtl [12, 22] subdivided flow into two areas: the layer close to the wall with an impulse exchange mainly due to molecular exchange, and the center of flow in which a turbulent exchange prevails. The following is valid for the so-called viscous wall layer:

$$\tau = \eta\, dw_y/dy \tag{34}$$

as well as:

$$\tau_w = \eta (dw_y/dy)_{y=0} \tag{35}$$

for the wall itself (y = 0). Since the wall layer is very thin, all characterizing magnitudes, and especially the shear stress, can be set as constant in this range of thickness δ.

The velocity distribution in the two domains from the wall to the tube center can be represented universally by means of two dimensionless parameters. These are the velocity ratio

$$w_y/u^+ = w_y \sqrt{\varrho/\tau_w} \tag{36}$$

with

$$u^+ = \sqrt{\tau_w/\varrho} \tag{37}$$

as the so-called rate of shear stress, as well as the dimensionless wall distance

$$y^+ = u^+ y/\nu \tag{38}$$

formed in the manner of a Reynolds number. If a value $y^+ = y_o^+$ is given to the thickness δ of the laminar wall layer, then Equation (38) provides the relation

$$\delta = y_o^+ \sqrt{\varrho/\tau_w} \tag{39}$$

according to which $\delta \sim 1/\sqrt{\tau_w}$ changes. This relation is of great importance for the subsequent considerations.

Due to the turbulent motion in the turbulent center of the flow, fluid or gas particles having a certain velocity partly reach flow paths of a slower velocity and partly those of greater velocity. For reasons of continuity, the exchanged mass in each partial domain of the flow must remain the same. This impulse exchange has the effect of an apparent viscosity of the flow medium. Therefore, similar as in Equation (34), the following is set for the center of flow:

$$\tau = A_\tau \, dw_y/dy \tag{40}$$

where A_τ is the magnitude of turbulent exchange.

If the course of velocity is examined over the tube cross section (for example, Fig. 32), a few conclusions can be drawn with the aid of Equations (35) and (40). In the center of the tube we have $dw_y/dy = 0$; in other words, the shear stress drops from τ_w at the wall to $\tau = 0$ at the tube center. Within the layer close to the wall the velocity gradient is very large and approximately constant; beginning with the turbulent center it drops very quickly up to the center of the tube. Since, however, the shear stress decreases only slowly from the value τ_w at the wall, A_τ must be considerably greater than η.

The Prandtl boundary layer theory has been further refined over the course of time. Thus, for example, E. Hofmann [23] divided the flow into three zones. The final step was taken by H. Reichardt [24-27] when he eliminated all imagined boundaries between the different zones and assumed that the turbulence fades out continuously up to the tube wall. Subsequent considerations in this article, however, are only based on the simple theory of two zones, since the calculation would otherwise become too complex.

In the smooth tube the two flow layers affect the heat transfer in such a manner that the heat in the layer close to the wall is transported only by heat conductance and in the center of flow only by turbulent heat exchange. In the wall layer the following is valid, with T_y for the absolute temperature at wall distance y, with respect to the heat flow density q transverse to the direction of flow:

$$q = \lambda \, dT_y/dy \qquad (41)$$

and for the heat flow density q_w at the wall

$$q_w = \lambda (dT_y/dy)_{y=0} \tag{42}$$

Since q remains practically constant in the wall layer and $q = q_w$ is valid, we therefore have according to the simple Prandtl theory $q_w \sim 1/\delta$ and according to Equation (39), approximately $q_w \sim \sqrt{\tau_w}$.

The relation resembling Equation (40) results for the heat flow density in the turbulent center

$$q = c_p A_q dT/dy \tag{43}$$

with A_q as the magnitude of turbulent heat exchange. The exact relationship between the turbulent impulse and heat exchange is so far unknown. It seems reasonable, however, to consider the relation A_τ/A_q over the tube cross section as constant, although strictly speaking this does not hold true. In the case of an equivalence of the impulse and heat exchange mechanisms, we would have $A_\tau/A_q = 1$, which had first been assumed as valid by O. Reynolds and later by L. Prandtl, E. Hofmann and W. Nunner in their theoretical considerations. It follows from the temperature profile (e.g. Fig. 37) as well as from Equations (42) and (43), similar to the comparison of A_τ and n, that $c_p A_q$ must be considerably greater than the molecular heat conductivity coefficient λ. According to E. Hofmann [23] the heat resistance of the zone near the wall (including the laminar-turbulent transition zone) with air flow amounts to about 70% of the total heat resistance. This portion still increases more with increasing Pr. Thus the greatest portion of the total heat resistance is located in the viscous wall layer as far as substances with not too small a Prandtl number are concerned. However, since the wall shear

stress τ_w represents a measure for the thickness δ of this layer, τ_w is an important effective magnitude for all theoretical heat transfer equations. Admittedly it occurs rarely directly, but indirectly it enters into all of these equations via the coefficient of resistance ψ, since ψ and τ_w are interrelated by Equation (33). This is also true for Equation (16) by W. Nunner, which gives a good insight into the practical possibilities.

W. Nunner started with the same fundamental assumptions as W. Prandtl, but he used a shear stress course for the rough tube which differed from that of the smooth tube and which is explained as follows. At the tube wall itself the flow behaves similar as in a smooth tube at equal Reynolds number, i.e. due to wall friction shear stress τ_{wo} occurs directly at the wall just as in a flow which has not been disturbed by roughnesses. However, this pure wall friction only represents a part of the total tube resistance. At some distance from the wall--approximately at the boundary of the viscous wall layer--the roughnesses begin to affect the flow by increasing the tube resistance by a certain amount due to separation phenomena. Consequently the shear stress increases very steeply at the boundary of the viscous wall layer to attain a value which practically corresponds to the value τ_w calculated according to Equation (32). From there to the tube center the shear stress then again drops to zero (Fig. 46). On the basis of this shear stress course, τ_w and τ_{wo} enter Equation (16) in the form of very important magnitudes which become identical for the smooth tube; for from Equation (33) the following results

$$\tau_w = 1/8 \psi \varrho w^2, \quad \tau_{wo} = 1/8 \psi_o \varrho w^2 \qquad (44)$$

with index 0 for the smooth and without index 0 for the rough tube. Thus, in Equation (16) $\Psi/\Psi_o = \tau_w/\tau_{wo}$ is valid. In the final form of Equation (16) the shear stress does not appear any longer only because it can be better expressed by easily measurable magnitudes. As can be seen From Equation (16), the effect of roughnesses in a flow is similar in manner to an increased Prandtl number.

The differences in $Pr = \nu/a$ essentially originate from different viscosities of the substances. If Pr increases by a certain amount due to an increase in viscosity, then (the dimensions of the tube remaining the same) the velocity must be increased by the same amount if $Re = w\,d/\nu$ is to remain the same. With an equal Re, the thickness δ of the wall layer remains unchanged; but the turbulent exchange increases due to the greater velocity. Consequently, the heat resistance of the turbulent center drops, while the heat resistance of the viscous wall layer remains the same. The turbulent exchange of the center flow is also increased by roughnesses, but the wall layer is practically not influenced at all.

As was to be expected, the heat transfer could not be satisfactorily reproduced by Equation (16)neither in the case of large disc inserts or with the remaining turbulence promoters. L. Prandtl already pointed out that his heat transfer equation was only valid when the pressure loss develops only by friction at the tube wall [28]. The result for Equation (16) is analogously that it is only applicable with the existence of the relationship between shear stress and pressure loss as given by Equations (32) and (33), respectively. This relationship is made possible in the case of a fully developed velocity profile of the flow, a linear pressure drop along the tube, and a constant pressure over the tube

cross section. If, however, the flow is disturbed only from time to time by individual wall projections or other interference bodies (i.e. by turbulence inserts of any type), then these assumptions no longer hold true due to the high form resistance of the inserts. Now no known relationship exist any longer between the shear stress at the edge of the turbulent center--which shall now be designated by τ_k--and the pressure loss. Furthermore, the wall shear stress no longer has the value τ_{wo}, but the unknown value τ_w. The shear stresses τ_w and τ_k probably depend on the type and arrangement of the turbulence producers in an unclear manner and would hardly be constant along the tube.

From the comparison of the velocity and temperature profiles with disc-shaped turbulence inserts it was concluded that the heat resistance of the turbulence center decreases considerably upon interference with the flow due to turbulence inserts. Therefore, a still greater part of the total heat resistance must be located in the layer near the wall in the case of tubes with turbulence inserts than in the case of the smooth tube. Since τ_w represents a measure for δ and thus also for q_w, a theoretically logical relationship will also exist between the heat transfer coefficient and the wall shear stress for the case of turbulent flow. With this, the the difference in magnitude of the heat transfer coefficient depending on the type of insert could also be better interpreted. An encouraging factor for such an investigation was the finding that Nu varied with Re for all experimental arrangements in the same manner as in the smooth tube; for it can be expected on the basis of this that the average wall shear stress in tubes with inserts also depends on Re in an equal fashion as in the smooth tube. This also pro-

vides a possibility of control for the measured wall shear stresses. For these reasons τ_w was measured in tubes with turbulence inserts.

5.2 Fundamentals of the Measuring Instrument for Wall Shear Stress

The principle of measuring to determine the wall shear stress according to H. Ludwieg [29] rests on the fact that a local heat transfer coefficient is determined (α_ϑ) which according to theory is in uniform relation to the wall shear stress τ_w. For the measurements which are to be undertaken during isothermal flow a small instrument is utilized which is installed in the tube wall and which gives off heat to the flow layer near the wall. It follows from the difference between the surface temperature t_D of the heated spot of the wall and the undisturbed flow temperature t_L, the heating output Q_H and the heating area F of the measuring element that:

$$\alpha_\vartheta = \frac{Q_H}{F_E(t_D - t_L)} \tag{45}$$

From the heat transfer coefficient α_ϑ and the width s of the heated spot along the direction of flow, a local Nusselt number $Nu_\vartheta = \alpha_\vartheta \, s/\lambda$ of the measuring instrument results for which the relation

$$Nu_\vartheta \sim \tau_w^{1/3} \tag{46}$$

holds true according to theoretical considerations [29]. All of the secondary effects which are neglected in the theory can be eliminated by calibrating the instrument during fully developed flow in the tube. In order to be able to utilize the relation $Nu_\vartheta = f(\tau_w)$--determined by calibration--for flows with very large pressure gradients in the direction of

flow (such as for example in the case of turbulence promoters), care has to be taken that the heat boundary layer originating from the measuring point projects as little as possible from the viscous wall layer. For this purpose a construction type of the instrument according to M. Herbeck [30] is to be considered mainly, the heat source of which is as narrow as possible in the direction of flow.

Figs. 47 and 48 show the measuring instrument which was utilized. A platinum-iridium band a (compare Fig. 48) of 0.007 mm thickness, 0.1 mm width and 10 mm length serves for a heating element, which is mounted with its length transverse to the direction of flow. The band is cemented onto a bakelite support b by means of a very thin layer of lacquer. The two bakelite bodies b and d represent a part of the internal tube wall with their surfaces. Careful operation of the instrument and the tube wall makes possible an undisturbed flow towards the measuring point.

The heating element is connected to the electrical circuit over two copper electrodes c which are sunk into the bakelite body d and which are in contact with the heating element a by means of pressure exertion. Thus the heating element serves not only as the source of heat but also as a resistance thermometer. The element forms a partial resistance of a Wheatstone bridge circuit which consists of precision resistances, a mirror galvanometer for a zero indicator and a storage-battery cell for the source of power. The total current flowing through the bridge circuit can be regulated with the aid of a slide rheostat and can be read off from an ammeter with a measuring accuracy of 0.2% of the full deflection.

The experimental tube was provided with turbulence promoters in the same manner as in the pressure loss and heat

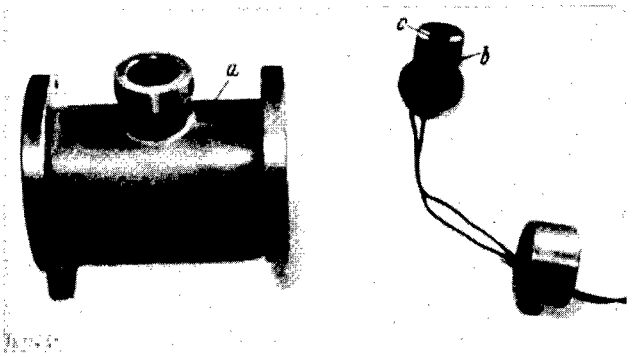

Fig. 47.--View of the measuring instrument for shear stress. a = tube spacer with nipple for the introduction of the measuring instrument; b = shear stress measuring instrument; c = surface of the measuring instrument forming a part of the tube wall with the heating element.

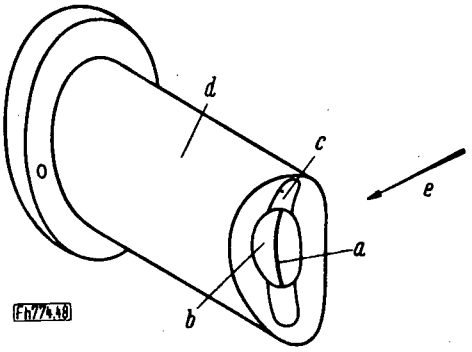

Fig. 48.--Sketch of the shear stress measuring instrument. a = heating element; b = bakelite base; c = electrode; d = bakelite body; e = direction of flow.

transfer determinations. The heating element had an overtemperature of 25° in comparison to the unheated air (t_L = 20°C) in all experiments and its electrical resistance was checked before every experimental series in the unheated state. This overtemperature corresponded to an increase of the resistance of about 5% as could be found with the aid of the temperature coefficient of the platinum-iridium alloy. Before the measurement the variable bridge resistance was adjusted in such a manner that the heating area exhibited this resistance at the compensated bridge. Since the heating element cooled off more or less depending on the rate of air flow prevailing near the wall, the bridge current had to be varied until the bridge had again been compensated.

Fig. 49 shows the standardization curve of the measuring instrument as recorded in the smooth tube and as checked

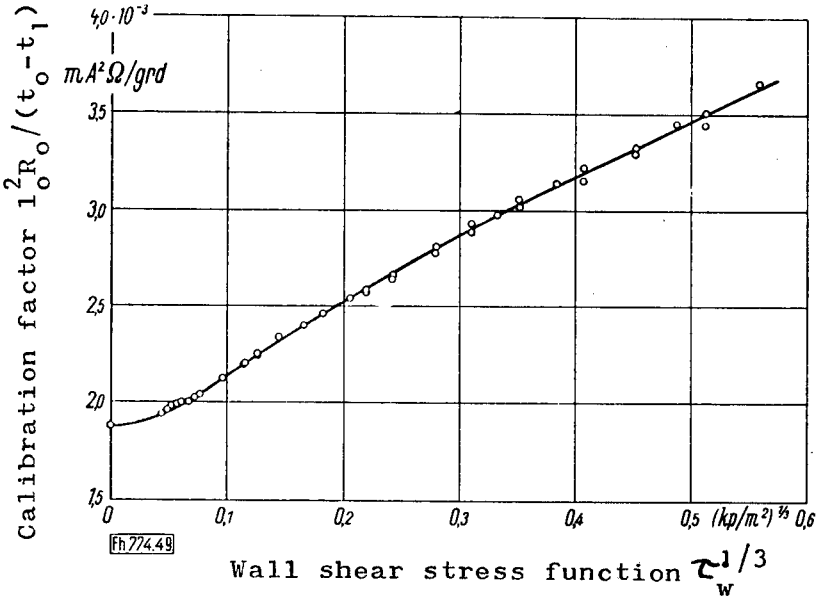

Fig. 49.--Calibration curve for the wall shear stress measurement. τ_w = wall shear stress; I_D = current intensity of the heating wire; R_D = wire resistance; t_D-t_L = 25° overtemperature of the wire compared to the air in the experimental tube.

several times between the experimental series, which makes possible a reading of the wall shear stress τ_w as a function of the local Nusselt number Nu_ϑ of the heating element over the entire determinable range of Reynolds numbers. For the abscissa the 1/3-exponent of the wall shear stress is plotted which was calculated according to Equation (32) from a pressure loss measurement undertaken simultaneously with the electrical measurements. The magnitude $I_D^2 R_D/(t_D - t_L)$ plotted on the ordinate represents the Nusselt number of the heating element up to a constant; I_D here designates the current intensity flowing through the wire and R_D denotes the wire resistance. The wire temperature always amounted exactly to 45°C. The standardization curve permits the great influence of the free convection for $\tau_w^{1/3} = 0$ (weight rate of flow equals zero), which has an unfavorable effect on the accuracy of very small τ_w-values with low weight rates of flow under certain circumstances.

The standardization curve according to Fig. 49 was used for a base for a determination of τ_w in the experiments with turbulence promoters. The local course of the shear stress between a pair of turbulence producers was determined by a displacement of the entire group of inserts at constant weight rate of flow (identical to constant Re) and every time with three different Reynolds numbers (Re = $4 \cdot 10^3$, 10^4 and $4 \cdot 10^4$).

5.3 Results of the Wall Shear Stress Measurement

5.31 Baffle plate Inserts

5.311 Course of the Wall Shear Stress Along the Tube:--

Baffleplate inserts were investigated first, since they permit the expectation of the best measuring values due to the rela-

tively distinct state of flow. For an example the course of the shear stress as a function of the plate distance 1 in the direction of flow is shown in Figs. 50 to 52 for various experimental series.

All of the curves exhibit a few peculiarities independent of the type of plate and the arrangement. Directly behind the plate τ_w rises very rapidly to its maximum value and afterwards drops again just as rapidly. Shortly before the next plate τ_w starts to increase again. At larger referred distances L'/d_s a zone with almost constant shear stress forms after the maximum and the subsequent minimum.

This course of the shear stress permits the following interpretation of the behavior of flow. The flow rate is rather high at 1 = 0, since the plates partly close off the cross section. Behind the plates the flow is further constricted up to a point which presumably coincides with the shear stress maximum. Subsequently the flow expands into the space between two inserts with concurrent great retardation, i.e. τ_w decreases. The renewed constriction of the flow before the next plate is always indicated by the steep increase of the shear stress.

Since τ_w is a measure for the heat flow density q_w through the wall, the local heat flow must vary periodically along the tube just as τ_w. In subsequent considerations, average values over the entire tube length L shall be set as a base for the influential magnitudes. Thus, an average wall shear stress τ_{wm} was also determined in all cases by a planimetry of the corresponding curves.

5.312 Dependence of the Average Wall Shear Stress on the Reynolds Number:--In all experiments described in the following the same experimental tube and the same flow medium (at

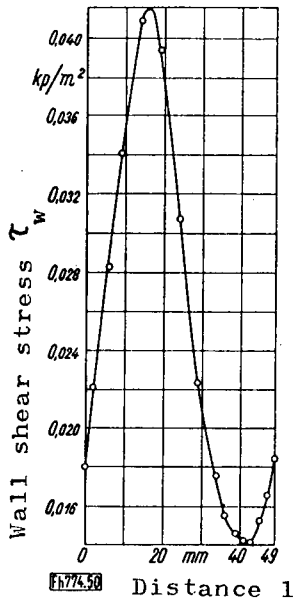

Fig. 50.—Course for a baffleplate diameter d_S = 30 mm, a referred plate distance L'/d_S = 1.6 and a Reynolds number Re = 10^4.

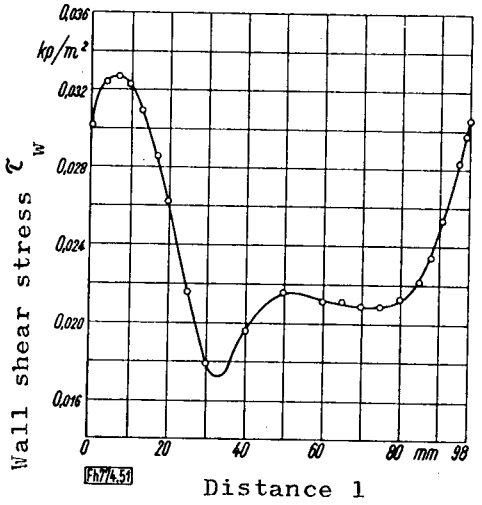

Fig. 51.--Course for a baffleplate diameter d_S = 30 mm, a referred plate distance L'/d_S = 3.2 and a Reynolds number Re = 10^4.

Fig. 52.—Course for a baffleplate diameter d_S = 20 mm, a referred plate distance L'/d_S = 9.8 and for different Reynolds numbers Re.

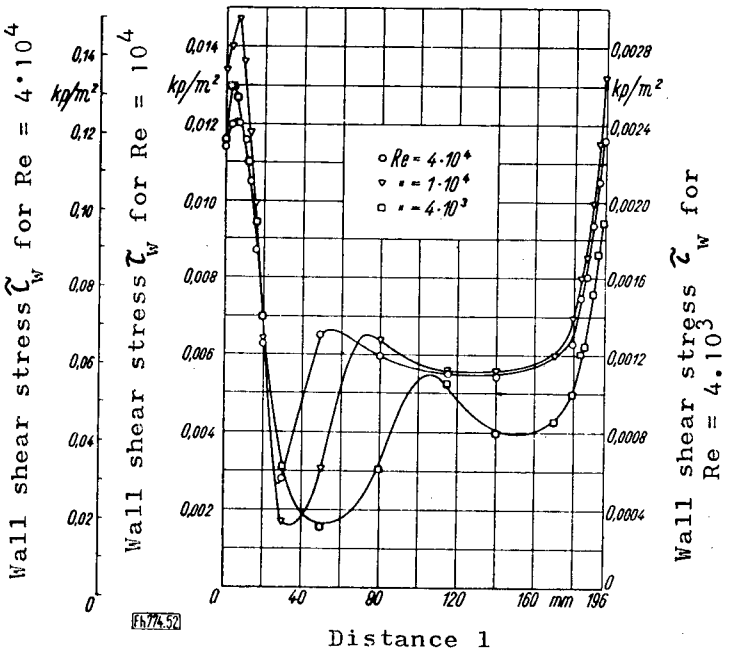

Figs. 50 to 52.--Course of the wall shear stress τ_w as a function of the distance 1 from a baffleplate in the direction of flow for baffleplate inserts.

the same temperature) were always used, so that the Reynolds number Re only depended on the average rate of flow w. Thus the following is valid for the smooth tube according to Equations (7) and (44):

$$\tau_w = \left(\frac{0.316}{8} \frac{\nu\eta}{d^2}\right) Re^{1.75} \qquad (47)$$

with a constant parenthetical expression.

Since the average Nusselt number in all turbulence promoters varies with the Reynolds number in the same manner as in the smooth tube, it was reasoned that the average wall shear stress τ_{wm} in tubes with turbulence promoters must depend on Re just as in the smooth tube. Thus the following is also valid:

$$\tau_{wm} \sim Re^{1.75} \qquad (48)$$

Fig. 53 shows the course of τ_{wm} as a function of Re. The lines drawn through the test points have the slope of 1.75 and thus confirm Equation (48) very well.

5.313 Dependence of the Heat Transfer on the Average Wall Shear Stress:--Under the given basic conditions (tube dimensions always remaining the same and practically constant magnitude of substance), the following results according to Equation (14) for the smooth tube traversed by flow:

$$Nu = C_1 Re^{0.786} \qquad (49)$$

with C_1 for a constant. An unusual path can now be followed and the Reynolds number (really the velocity) in Equation (49) can be substituted by the shear stress τ_w according to Equation (47). Then the following results for the smooth tube

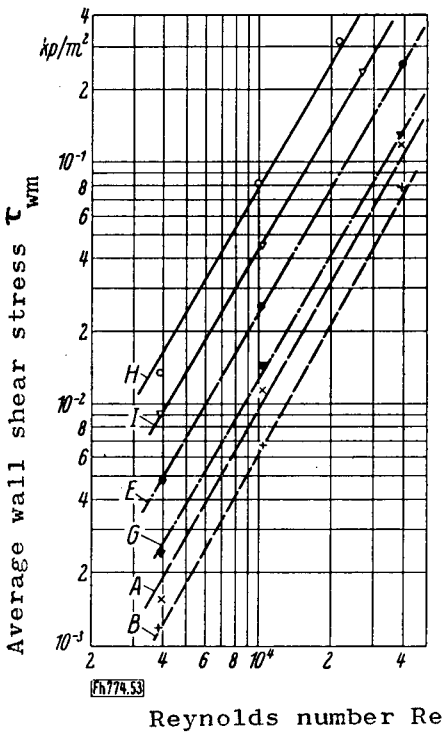

Fig. 53.--The average wall shear stress τ_{wm} as a function of the Reynolds number Re for baffleplate inserts. The capital letters refer to the corresponding classifications in Table 2.

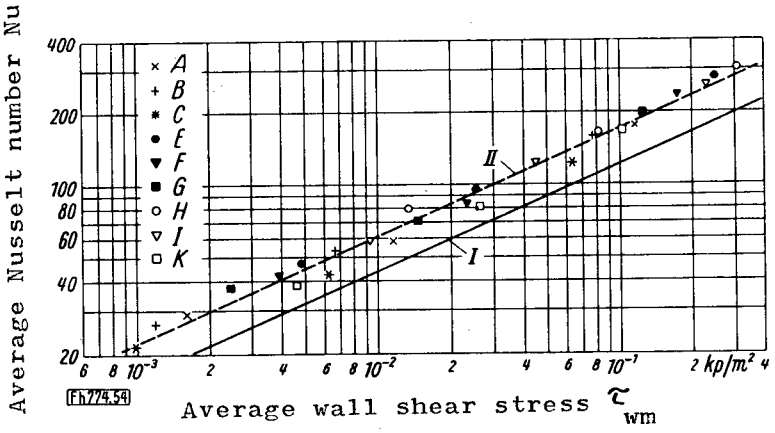

Fig. 54.--The average Nusselt number Nu as a function of the average wall shear stress τ_{wm} for baffleplate inserts. The capital letters refer to the corresponding classifications in Table 2; I = comparison curve for the smooth tube; II = equalization curve through the test points for the baffleplate inserts.

with C_2 for a new constant:

$$Nu = C_2 \tau_w^{0.45} \tag{50}$$

and, similar as before, for tubes with turbulence inserts:

$$Nu = C_3 \tau_{wm}^{0.45} \tag{51}$$

Here C_3 is another constant. It could be considered as somewhat annoying that dimensionless factors are in a relationship with the wall shear stress in Equations (47) to (51) (i.e. the constants are not dimensionless). However, these equations are not generally valid, but only under the assumption of constant substance magnitudes and constant tube dimensions.

Equation (50) is represented by straight line I for the smooth tube in Fig. 54; constant C_2 resulted from the measuring values. In addition, Fig. 54 contains all test points for the plate inserts; they are grouped around the straight line II within a small range of scatter and with a slope of 0.45. Thus Equation (51) is confirmed. In other words if Nu is related to τ_{wm}, the differences, which occurred in Nu for a certain Reynolds number depending on the type and arrangement of the inserts and which previously had been hardly explainable, disappear. It is surprising that the type and arrangement of the plate inserts have no noteable influence on Nu for τ_{wm} = const even under very different conditions. It is clear that curve I for the smooth tube must be attained again in the case of very large plate distances ($L'/d_S \rightarrow \infty$) and also with an increasing aperture ratio ($m^* \rightarrow 1$). It is true that this tendency can be recognized from the plotted measuring values for τ_{wm} = const; but the Nu values differ only little from each other. Therefore it would be useless to cause the flow to be too turbulent by means of inserts, for example by

a considerable increase of the plate diameters; for the effect of the intensity of turbulence is only small in comparison to the influence of the wall shear stress, i.e. a favorable influence on the flow in direct proximity of the wall.

The generally higher position of curve II in Fig. 54 in comparison to curve I can be understood for the following reasons. The heat resistance of the central flow, which amounts to about 30% of the total heat resistance in smooth tubes traversed by air flow according to E. Hofmann [23], is very much decreased by the plates acting as turbulence producers. An intensive intermixing of the air caused by continuous re-formation of the velocity profile and strong separation phenomena is superimposed on the turbulent exchange motion which was present originally. Since the impulse and heat exchanges are related to each other, the heat exchange is increased with an increased impulse exchange.

5.314 Relation Between the Total Pressure Loss and the Wall Friction Pressure Loss:--The pressure loss of a flow can be imagined to be composed of the form resistance of the inserts and the wall friction resistance which influences the wall shear stress. If a coefficient of resistance ψ_r including only the pressure loss caused by wall friction is defined for a flow with turbulence promoters according to Equation (33), then we have

$$\psi_r = 8 \tau_{wm} / \rho w^2 \qquad (52)$$

This resistance coefficient ψ_r depends on L'/d_s and m^* in a manner similar to the resistance coefficient ψ. Unfortunately no simple empirical equation can be given for these relations from the measuring values which were obtained.

Table 4, in which all measuring values for pressure loss and shear stress are compiled once more, contains a column for Ψ_r/Ψ. Since the proportion of wall friction resistance in the total pressure loss increases with increasing values of L'/d_s and m*, Ψ_r/Ψ increases correspondingly. The Ψ_r/Ψ values are found within a range of about 6 to 30%.

5.32 Disc Inserts

In comparison to the baffleplate inserts, somewhat more unfavorable circumstances exist for the disc inserts with respect to a wall shear stress determination, insofar as blind pockets of the flow occur near the wall, although the flow in the case of discs is perspicuous in the center of the tube. From the relation of the Nusselt number to the Reynolds number (compare Figs. 8 and 9) it can be concluded here too, however, that on the average the flow in the zone near the wall obeys laws similar to flow in a smooth tube. Presumably the wall shear stress in the case of small disc distances is only produced by turbulences which develop between each disc pair from the wall up to an approximate disc height K. In the case of large disc distances, blind pockets appear near the disc which are filled with circulating turbulences; outside of these zones the main flow adheres to the tube wall. The turbulences which are suppressed by internal friction and wall friction are continuously supplied with new energy from the main flow. Only occasionally do they circulate in a stationary manner, but the main stream periodically carries them away. This can cause small erroneous readings in the measuring instruments since the latter are not able to keep up with very short-term fluctuations.

Table 4

Compilation of the Shear Stress Measuring Values for the Tube with Baffleplate Inserts

Plate Diam. d_S mm	Aperture Ratio m*	Ref. Plate Dist. L'/d_S	Reynolds Number Re	Aver. Wall Shear Stress τ_{wm} kp/m²	Frict. Resist. Coeff. ψ_r	Total Resist. Coeff. ψ	Ratio ψ_r/ψ %
40	0,36	1,44	$2{,}18 \cdot 10^4$ $9{,}9 \cdot 10^3$ $3{,}97 \cdot 10^3$	0,306 0,0814 0,01346	0,458 0,591 0,606	7,3 7,55 8,3	6,28 7,83 7,3
		3,5	$2{,}72 \cdot 10^4$ $1{,}04 \cdot 10^4$ $3{,}97 \cdot 10^3$	0,229 0,0443 0,00914	0,221 0,293 0,413	4,0 4,15 4,18	5,52 7,06 9,88
		8,15	$2{,}7 \cdot 10^4$ $1{,}08 \cdot 10^4$ $3{,}96 \cdot 10^3$	0,102 0,0260 0,0045	0,0995 0,159 0,204	1,77 1,8 1,82	5,62 8,82 11,2
30	0,64	0,65	$4{,}01 \cdot 10^4$ $1{,}02 \cdot 10^4$ $3{,}91 \cdot 10^3$	0,224 0,0176 0,0027	0,0994 0,120 0,126	1,52 1,30 1,20	6,54 9,22 10,5
		1,63	$3{,}99 \cdot 10^4$ $1{,}03 \cdot 10^4$ $4{,}02 \cdot 10^3$	0,249 0,02532 0,004785	0,111 0,169 0,211	1,35 1,32 1,37	8.22 12,8 15,4
		3,27	$3{,}97 \cdot 10^4$ $1{,}04 \cdot 10^4$ $3{,}94 \cdot 10^3$	0,1743 0,0235 0,00381	0,079 0,156 0,175	0,89 0,88 0,91	8,88 17,75 19,23
		5,54	$3{,}97 \cdot 10^4$ $1{,}05 \cdot 10^4$ $3{,}97 \cdot 10^3$	0,1247 0,01452 0,00239	0,0564 0,0946 0,108	0,57 0,58 0,62	9,9 16,3 17,4
20	0,84	1,55	$3{,}94 \cdot 10^4$ $1{,}05 \cdot 10^4$ $3{,}94 \cdot 10^3$	0,115 0,0115 0,00157	0,0528 0,075 0,072	0,41 0,39 0,44	12,87 19,25 16,38
		3,8	$3{,}99 \cdot 10^4$ $1{,}05 \cdot 10^4$ $3{,}9 \cdot 10^3$	0,0769 0,00665 0,001184	0,0344 0,0433 0,0555	0,258 0,265 0,29	13,35 16,35 19,14
		9,8	$3{,}88 \cdot 10^4$ $1{,}02 \cdot 10^4$ $3{,}96 \cdot 10^3$	0,06335 0,00617 0,000958	0,030 0,0424 0,0436	0,127 0,140 0,162	23,6 30,3 26,9

5.321 Course of the Wall Shear Stress Along the Tube:-- Figs. 55 and 56 show the course of τ_w as a function of the distance 1 behind a disc for discs with K = 5 mm in the case of two different L'/K values. The Reynolds number exerts no significant influence on the path of the curves. The reproduction of other τ_w,1 curves for disc inserts was dispensed with since they offered no further peculiarities in comparison to Figs. 55 and 56.

If the discs adhere unobjectionably to the tube wall, then τ_w has to disappear directly before and after them. While the course of the wall shear stress always indicates this tendency, it does not attain a value of zero directly at the inserts but exhibits another steep rise. This might be explained by the fact that the discs do not adhere tightly to the wall and that due to the large pressure differences before and after the inserts, small partial flows pass between the wall and the disc with great velocity. Still, this rise has no great influence on the average value τ_{wm} of the wall shear stress. Aside from this side-effect, τ_w rises steeply to a maximum behind a disc which possibly occurs at a point where the contraction of the main flow is also greatest. Subsequently τ_w first drops a little in order to remain almost constant over a longer or shorter section depending on the disc distance L' and finally disappears almost completely only shortly before the next disc.

5.322 Dependence of the Average Wall Shear Stress on the Reynolds Number:--Fig. 57 shows the course of the average shear stress τ_{wm} in the tube with disc-shaped inserts as a function of the Reynolds number. This slope in these curves also amounted to 1.75 so that it could be assumed that the

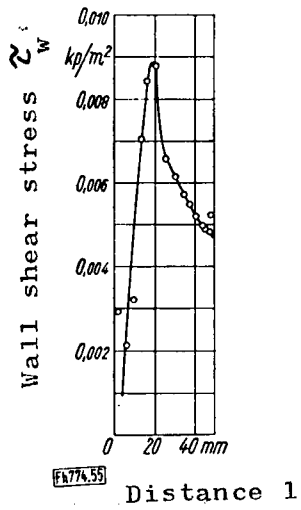

Fig. 55.--Course with a disc height K = 5 mm, an aperture ratio m* = 0.64, a referred ring distance L'/K = 9.8, and a Reynolds number Re = 10^4.

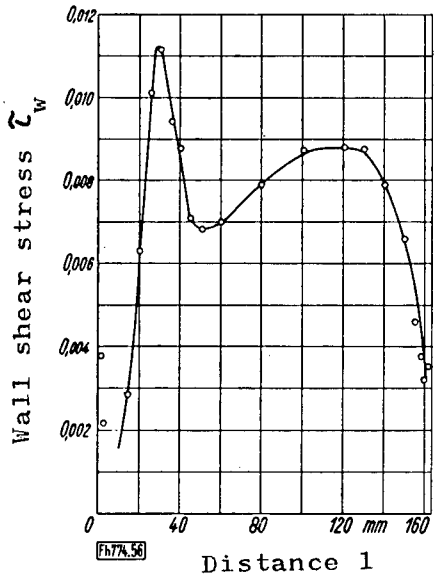

Fig. 56.--Course with a disc height K = 5 mm, an aperture ratio m* = 0.64, a referred ring distance L'/K = 32.7 and a Reynolds number Re = 10^4.

Figs. 55 and 56.--Course of the wall shear stress τ_w as a function of the distance l from a disc in the direction of flow for disc-shaped inserts.

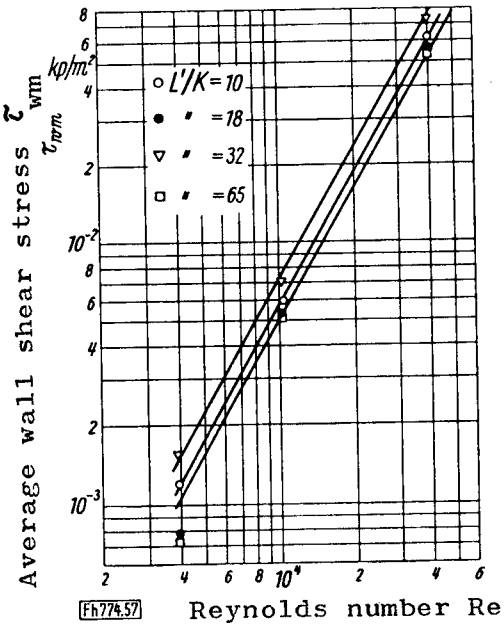

Fig. 57.--The average wall shear stress τ_{wm} as a function of the Reynolds number Re for disc-shaped inserts with an aperture ratio m* = 0.64 having different referred ring distances L'/K and a disc height K = 5 mm.

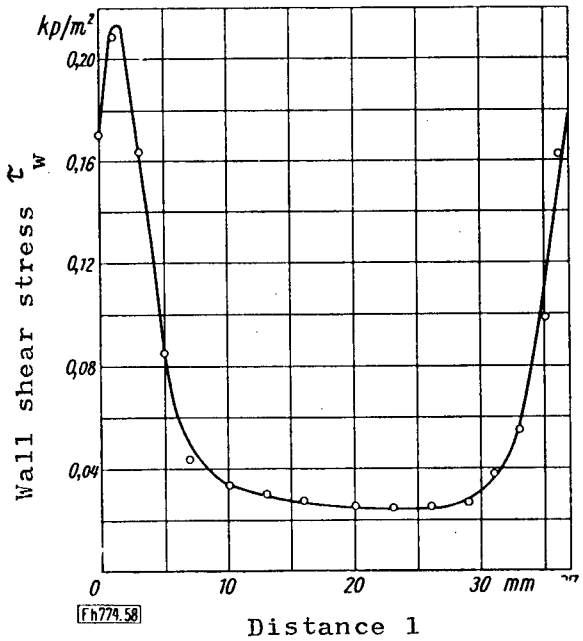

Fig. 58.--Course of the wall shear stress τ_w as a function of the distance l from a ring in the direction of flow for ring-shaped inserts with a ring height K = 3.75 mm and a referred ring distance L'/K ≈10 for a Reynolds number Re = 10^4.

measurements are not essentially inhibited by unstationary processes.

In tubes with disc inserts at K = 5 mm, τ_{wm} at equal Re is approximately equal to the wall shear stress τ_w in the smooth tube. This was the most important assumption which W. Nunner made in the derivation of the theoretical heat transfer equation for rough tubes; thus it is being confirmed with this new determination. Especially it can be assumed that this assumption is also valid for still smaller wall projections. However for the discs with K = 10 mm and 12.5 mm it can no longer be satisfied.

Table 5 once more shows all of the important measuring results for resistance for the tube with disc inserts. The relationship between Nu and τ_{wm} for these and all other inserts will be generally discussed later in Section 5.36.

5.33 Ring Inserts

The shear stress τ_w has been plotted in Fig. 58 as a function of the distance l for a concentric ring type (ring height K = 3.75 mm). Directly below the rings τ_w attains generally rather high values and between them it drops to low values. Due to the pressure difference before and after the rings, a part of the air flows through the gap between the tube wall and the ring at high velocity and thus causes the high shear stress near the rings. Presumably these partial flows are diverted from the wall towards the center of the tube due to the underpressure, in such a manner that the velocity, and thus τ_w, near the wall becomes small over a large zone between a pair of rings.

Evidently it is a coincidence that these ring inserts ($L'/K \approx 10$) and the discs with K = 5 mm with a small referred

Table 5

Compilation of the Shear Stress Measuring Values for the Tube with Disc-Shaped Inserts

Disc Height K mm	Aperture Ratio m*	Ref. Ring Dist. L'/K	Reynolds Number Re	Aver. Wall Shear Stress τ_{wm} kp/m^2	Frict. Resist. Coeff. ψ_r	Total Resist. Coeff. ψ	Ratio ψ_r/ψ
12,5	0,25	26,2	$3{,}25 \cdot 10^4$ $1{,}05 \cdot 10^4$ $3{,}93 \cdot 10^3$	0,0925 0,01545 0,00214	0,0623 0,10 0,0995	3,8 3,8 3,65	1,64 2,63 2,72
10	0,36	9,8	$3{,}39 \cdot 10^4$ $1{,}03 \cdot 10^4$ $3{,}97 \cdot 10^3$	0,108 0,0127 0,00176	0,0668 0,0853 0,0795	4,06 3,83 3,58	1,65 2,22 4,5
		32,7	$3{,}9 \cdot 10^4$ $1{,}02 \cdot 10^4$ $3{,}97 \cdot 10^3$	0,1128 0,00968 0,001145	0,0528 0,0662 0,0517	1,72 1,61 1,51	3,07 4,12 3,42
5	0,64	9,8	$4{,}02 \cdot 10^4$ $1{,}04 \cdot 10^4$ $3{,}95 \cdot 10^3$	0,0557 0,00534 0,000799	0,0246 0,0354 0,0365	0,64 0,60 0,625	3,85 5,9 5,84
		18,0	$3{,}93 \cdot 10^4$ $1{,}04 \cdot 10^4$ $3{,}93 \cdot 10^3$	0,0619 0,00596 0,001207	0,0285 0,0392 0,0555	0,51 — 0,455	5,59 — 12,2
		32,7	$3{,}9 \cdot 10^4$ $1{,}03 \cdot 10^4$ $3{,}88 \cdot 10^3$	0,0716 0,00707 0,001591	0,0335 0,0478 0,0753	0,355 — 0,31	9,43 — 24,3
		65,0	$3{,}9 \cdot 10^4$ $1{,}02 \cdot 10^4$ $3{,}96 \cdot 10^3$	0,0521 0,0051 0,000722	0,0244 0,0351 0,0328	0,215 0,200 0,195	11,3 17,5 16,8

distance ($L'/K \approx 10$) result in the same average wall shear stress τ_{wm}. Both inserts projected almost equally far into the tube; but the discs adhered tightly to the wall, while the rings were separated from the wall by a gap of 2.75 mm width. Table 6 shows data of the shear stress and resistance for both ring inserts.

Table 6

Compilation of the Shear Stress Measuring Values for the Tube with Ring-Shaped Inserts

Ring Height K mm	Referred Ring Distance L'/K	Reynolds Number Re	Aver. Wall Shear Stress τ_{wm} kp/m^2	Frict. Coeff. ψ_r	Total Frict. Coeff. ψ	Ratio ψ_r/ψ %
3.75	≈ 10	$3.91 \cdot 10^4$	0.0720	0.0336	0.58	5.8
		$1.03 \cdot 10^4$	0.00606	0.0411	0.542	7.6
		$3.99 \cdot 10^3$	0.00110	0.0492	0.555	8.92
2.25	≈ 10	$3.95 \cdot 10^4$	0.0435	0.0198	0.335	5.9
		$1.02 \cdot 10^4$	0.00359	0.0245	0.320	7.66
		$3.95 \cdot 10^3$	0.000618	0.0282	0.35	8.05

5.34 Propeller Inserts

In the propeller-shaped inserts τ_w remains almost independent of distance 1. Near the inserts the values scatter badly. The Nu, τ_{wm} curves for the propeller distances L' = 50, 327 and 980 mm are generally 70% above the Nu, τ_w curve for the smooth tube.

Due to the twist caused by the inserts, the flow approaches the surface of the measuring instrument for shear stress at an angle rather than parallel to it. This angle varies somewhat with 1, but otherwise has the order of magnitude of the angle of incidence of the propeller vanes. According to H. Ludwieg [29] the shear stress instrument indicates lower values in the case of oblique flow than in the case of parallel flow. In the experiments described here the sensitivity of the heating element towards the direction of flow

was especially high due to its dimensioning. For this reason a reproduction of the wall shear stress determinations is omitted.

5.35 Ball Packings

In packing the experimental tube with balls care was taken that the latter did not touch the heating wire but that they were nevertheless deposited normally near the measuring instrument. Due to the oblique flow approach of the heating element and other coincidences based onthe nature of the filling, measuring errors can occur easily. Therefore several test points were repeated for a control after the tube had been entirely refilled with balls. The results fitted well into the other measuring values. The measuring range extended from Re $\approx$ 1000 to $\approx$10,000.

The wall shear stress increases more steeply than with a power of 1.75 in the case of increasing Re. This is not especially astonishing since the path of the Nu,Re curve in this area is also steeper than in the smooth tube according to Fig. 30.

5.36 Relation between Heat Transfer and Average Wall Shear Stress

Fig. 59 shows the course of Nu as a function of τ_{wm} for the following inserts: discs with K = 5 mm as well as $L'/K \approx 10$ and ≈ 18 (this arrangement was prepared later only for the shear stress measurements); discs with K = 10 mm and $L'/K \approx 10$; two ring inserts ($L'/K \approx 10$),and a packing with 12 mm stone balls. The average Nusselt number of all of these inserts can be represented by a single curve with the aid of τ_{wm}, which again confirms Equation (51) and around which there is relatively little scattering of test points.

For purposes of a clearer view, other measuring values have not been entered into Fig. 59 (for example, for disc

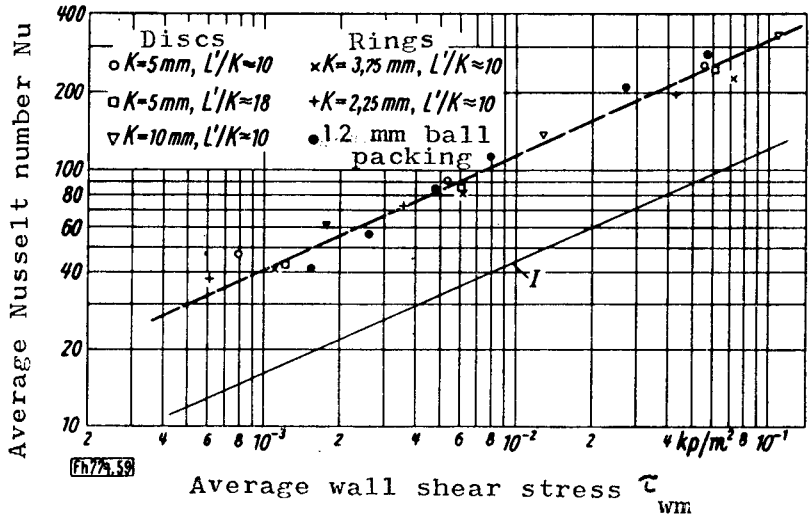

Fig. 59.--The average Nusselt number Nu as a function of the average wall shear stress τ_{wm} for disc- and ring-shaped inserts as well as for a ball packing. K = disc and ring height, respectively; L' = ring distance.

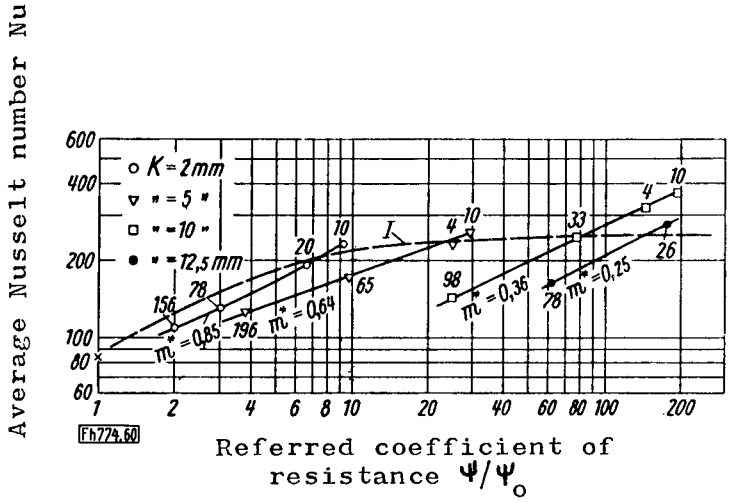

Fig. 60.--The average Nusselt number Nu as a function of the referred coefficient of resistance ψ/ψ_o for disc-shaped inserts at a Reynolds number $Re \approx 4 \cdot 10^4$. I = theoretical course for rough tubes according to Equation (16); K = disc height; m* = aperture ratio; the numbers written near the test points denote rounded-off values of the referred ring distances according to Table 1.

arrangements with K = 5 mm and 10 mm at higher L'/K values). These values are found between curve I and the equalization curve through the test points. This can be explained by the fact that curve I for the smooth tube must be reached with increasing L'/K ($L'/K \rightarrow \infty$) and $m^* \rightarrow 1$. The measuring values for propeller inserts are also found between the two lines. In the following only the results cited in Fig. 59 will be taken into account since they are best suited for the subsequent considerations.

It is very informative that the Nusselt numbers even in the case of small ring-shaped inserts (K = 2.25 mm, L'/K 10) for τ_{wm} = const. are of the same order of magnitude as in packing materials.It might have been assumed, actually, that the packing materials are better able to cause the flow to be turbulent than the rings. Since this is not true, it is apparent that at an equal τ_{wm} even a moderate turbulence production already increases the heat transfer to a value which presumably can no longer be surpassed by any type of turbulence producer. The equalization curve entered into Fig. 59 might represent this upper limit. In the following it will now be investigated why the Nusselt number is able to assume almost three times the values of a smooth tube for a certain wall shear stress in the case of turbulence promoters.

In rough tubes (at Re and Pre = const.) for large ψ/ψ_o values, i.e. for a certain shear stress ratio τ_w/τ_{wo}, Nu asymptotically approaches a final value according to Equation (16) which is almost three times the Nusselt number at $\psi/\psi_o = 1$ (Fig. 60). If τ_w (and thus ψ/ψ_o also) continues to increase, then the heat transfer finally can no longer improve since the greatest part of the heat resistance is then in the viscous wall layer. A similar situation is true for the turbulence

promoters for which Fig. 59 is valid. Instead of an equal Reynolds number, an equal wall shear stress τ_{wm} is assumed here again for comparison purposes. In these turbulence producers, too, the heat transfer evidently cannot be more than tripled compared to the smooth tube even by the strongest turbulence production which corresponds to a high shear stress τ_k at the start of the turbulent center flow. If the fundamental assumption for Equation (16) could be retained, then the heat transfer could also be calculated with Equation (16) for turbulence inserts if in addition to the average wall shear stress τ_{wm} a reasonably averaged shear stress τ_{km} along the tube would be known which occurs outside of the turbulent center and which would thus represent a measure for the turbulence in the center.

Finally, Fig. 54 for the plate inserts is referred to for a comparison. For plate inserts at τ_{wm} = const. average Nusselt numbers result which are 45% higher than in the smooth tube, while this increase amounts to about 150% for other turbulence promoters (compare Fig. 59). At first it is surprising the Nu values attained in the case of large plates with small distances L' and for a certain τ_{wm} are not as high as in the case of small disc and/or ring inserts. The reason can be found in the fact that the turbulence produced by the baffleplates cannot advance so close to the wall since this is where the main flow is present. On the other hand, the disc and ring inserts mainly influence the zone near the wall.

5.37 Effect of the Prandtl Number

In contrast to flow in a smooth tube, turbulence inserts increase the turbulent exchange, while the molecular exchange

remains approximately equal. Consequently the heat transfer is increased in a similar manner as in a fully developed tube flow by an increase of the Prandtl number. For a comparison of these two analogous influences, the wall shear stress shall also be established here as an important flow magnitude, which, however, can only be done in a good approximation. For tubes with inserts a Prandtl number can be determined from Nu at a certain τ_{wm} value which has the same effect on the heat transfer in flow through smooth tubes as in the case of the presence of inserts. Accordingly, at a certain τ_{wm}, the turbulence promoters cited in Fig. 59 influence the heat transfer approximately similar as a Prandtl number of six times the value, propeller inserts approximately three times and baffleplate inserts approximately two times as great a Prandtl number.

If a flow medium of Pr ≈ 0.72 is turbulently circulated in a tube with inserts, then the increase of the heat transfer can be approximately calculated on the basis of the given data and the cited experimental values of Section 4. Accordingly, the ratio $(Nu/Nu_o)_{Pr=0.72}$ for air with Pr = 0.72 is determined first, for instance from Fig. 10, for the corresponding inserts. Before this ratio is transposed to another flow medium, it must be corrected in case Nu still varies with Pr at Re = const. The empirical heat transfer equations are almost exclusively valid for certain ranges of Pr and therefore cannot be utilized over large ranges of Pr in these considerations. A representation of E. Hofmann [23] gives a rather good description how Nu depends on Pr at Re = const. If B_1 and B_2 designate values which supply the ratio with which the Nusselt number increases when the Prandtl number at Re = const. is increased for once from 0.72 to b·0.72 and

another time when the true Prandtl number Pr is increased to b Pr (with b as an arbitrary factor), then we have

$$(Nu/Nu_o)_{Pr} = \frac{B_2}{B_1} (Nu/Nu_o)_{Pr=0.72} \qquad (53)$$

The quotient B_2/B_1 in the range $0.1 < Pr < 10$ is approximately equal to one and assumes considerably smaller values with very large Pr values. For $Pr < 0.5$ the conditions are not as well comprehended by Equation (53), since the influence of τ_w decreases with decreasing Pr. However, since flow media with small Prandtl numbers still exhibit a high heat resistance within the center flow, turbulence inserts of every type would have to have the most favorable effect for these cases.

6. Separating the Concepts of Turbulence Inserts and Roughnesses

Reference has already been made to the fact that frequently no clear differentiation is made in literature between turbulence inserts and roughnesses, because this is connected with certain difficulties. Knowledge on the flow and heat transfer processes in rough tubes has been greatly expanded by the investigations of W. Nunnert [1] so that it seems more readily possible to delineate a differentiation between roughnesses and turbulence promoters on the basis of the interrelationships for rough tubes. For example, if the heat transfer in tubes which are traversed by an air flow and in which wall projections point into the flow takes place in a manner satisfying the theoretical heat transfer equation for rough tubes (Equation [16]), then evidently roughnesses are involved; otherwise, the obstructions shall be denoted as turbulence inserts. Using this definition as a base, it shall be determined whether the disc-shaped inserts under investigation shall be considered to be roughnesses or turbulence promoters.

Fig. 60 shows the Nu values of all disc arrangements for $Re = 4 \cdot 10^4$ as a function of the referred resistance coefficient Ψ / Ψ_o. Test points for the same type of disc are interconnected by curves; the numbers at the test points indicate the L'/K values. The broken curve I corresponds to Equation (16).

According to Fig. 60, the measuring values for discs with $m^* \geq 0.64$ and $L'/K \approx 4$ to ≈ 20 are well comprehended by Equation (16); these insert arrangements thus can be considered roughnesses. On the other hand, in the case of large L'/K values the test points deviate considerably from the theoretical curve for rough tubes, and they do so more for small aperture ratios than for large ones. Disc arrangements with $m^* < 0.64$ also no longer act as roughnesses, just as it resulted from wall shear stress measurements. For it was found that τ_{wm} for disc arrangements with $m^* = 0.36$ and 0.25 was not nearly as large any more when Equation (16) was used for a base. The point of intersection of the curves which are valid for these aperture ratios with the theoretical curve I in Fig. 60 therefore has no close relation to the theory which has been developed.

It can easily be explained why Equation (16) is no longer valid for the case of small disc heights but large disc distances ($m^* = 0.64$ and 0.85; $L'/K > 20$). For this purpose the true flow processes have to be compared with those which are the basis for the derivation of Equation (16) for rough tubes. The main assumption for Equation (16) was a constant shear stress progressing along the tube as a function of the tube cross section according to Fig. 46. However, for large disc distances such a course of the shear stress does not definitely adjust itself. It is true that the wall shear stress τ_w remains approximately constant over a fairly long section along

the tube, and the average wall shear stress τ_{wm} is approximately equal to τ_{wo}; but the maximum shear stress τ_k in the roughness and turbulence zone, respectively, no longer takes place according to Equation (44). Rather, near the disc a high shear stress occurs which, however, fades out soon with an increase of 1. Finally, with sufficiently large disc distances, the shear stress from a certain point on changes again as in a smooth tube, i.e. τ drops linearly from the wall ($\tau = \tau_w$) up to the tube center ($\tau = 0$). Thus, no average value can be substituted in Equation (16) for the differential ratio τ_w/τ_{wo} which is identical with the expression Ψ/Ψ_o. For it follows from the structuring of Equation (16) that Nusselt numbers calculated with an average value of τ_w and/or τ_w/τ_{wo} would be too large.

In summary it can be stated that only those disc-shaped inserts act just as wall roughnesses, the aperture ratio of which is $m^* \geq 0.64$ and the referred distance of which is $L'/K \leq 20$. While the limit value of m^* which separates the area of roughnesses from that of turbulence inserts can shift in the case of other wall projections, the limit value of L'/K probably would remain equal. More or less high wall projections which point into the flow can be considered to be roughnesses. Baffleplates, propeller-shaped inserts, helical metal strips and packing materials accordingly represent turbulence inserts. The concentric ring inserts assume a special position, since they act quite similar to pure wall projections in spite of the fact that they do not adhere to the tube wall.

In conclusion reference should be made to the fact that it is difficult to attempt to differentiate roughnesses and turbulence inserts with the aid of the velocity distribution theory. The velocity distribution in rough tubes can be

represented by means of an exponential equation as well as by means of a logarithmic formulation [4]. W. Nunner [1] and H. Möbius [19] have determined numerous velocity distributions in tubes with disc-shaped inserts and for the most part have represented them satisfactorily by means of such theoretical interrelations. However, some of these inserts (especially those with large L'/K values) must be considered turbulence inserts due to their effect on heat transfer. This inaccuracy is based on the fact that the velocity profile was usually measured in the center between two inserts and therefore has only limited significance. However, in the center of the tube and near the tube wall, the exponential equations or the logarithmic formulations for velocity distribution are no longer exactly valid, even in the case of genuine wall roughnesses. Therefore it cannot be accurately decided on the basis of a measured velocity profile--even if it remains generally constant along the tube--whether the wall projections under consideration involve roughnesses or turbulence inserts. The velocity profiles determined by the author for disc arrangements with $K = 5$ mm and 10 mm ($m^* = 0.64$ and 0.36 and $L'/K \approx 10$) no longer follow the cited theories by any means.

7. Comparison with Earlier Experimental Results

The influence of turbulence promoters on heat transfer already has been investigated several times. However, the results can only be evaluated insofar as the pressure loss is also known in addition to the heat transfer. In the following the most important earlier studies are to be referred to for the sake of comparison.

7.1 Experimental Results with Air Currents

A. P. Colburn and W. J. King [31] permitted air to flow through a steel tube of 66 mm internal diameter and 900 mm length which was cooled externally by means of water in a countercurrent. The air which had been preheated in an electric furnace streamed into the experimental tube at 100 to 300°C. Data on the length of the intake section are not available. A picture of the experimental arrangement leads to the conclusion, however, that the intake section was too short for a complete development of the turbulent velocity profile. This is probably the main reason for the fact that the pressure loss and the coefficient of heat transfer were about 30% higher in the smooth tube than was to have been expected (Figs. 61 and 62). The experimental range extended from about Re = 3000 to 9000 (with Re according to Equation 26).

No accurate data are available on the dimensions of the turbulence promoters which were utilized. The data cited in the following are estimated values derived from a photograph of the turbulence inserts[7]: Inserts No. 1 and No. 3 were helically twisted metal strips of 66 mm width with $h/d \approx 7$ and $h/d \approx 6$, respectively; insert No. 9 was a propeller similar in type to that described in the above experiments with $L'/d \approx 1$.

The fact that the experimental conditions deviate somewhat must be taken into account in a comparison of the Nu,Re curves for these inserts Nos. 1, 3 and 9 with the new results. Generally it is found that the Nu and ψ-measuring values of A. P. Colburn and W. J. King both for the smooth tube as well as for the inserts are about 20 to 30% higher throughout than

---

7) The number of inserts agrees with that which was cited in the original study [31].

Experiments according to A. P. Colburn [31]

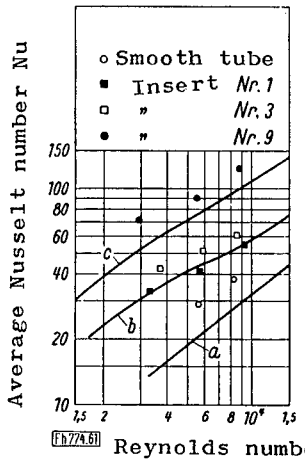

Fig. 61.--Comparison of the Nusselt numbers.

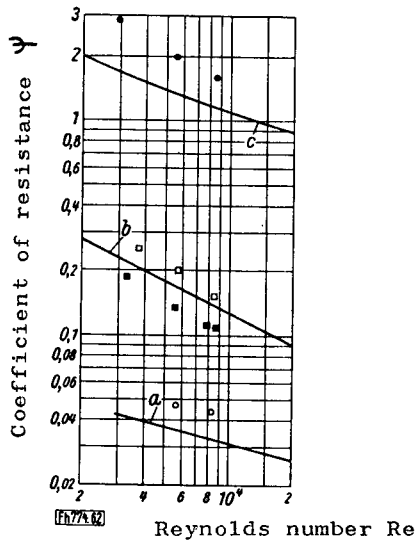

Fig. 62 .--Comparison of the coefficients of resistance.

Figs. 61 and 62.--Comparison of the average Nusselt numbers Nu and the coefficients of resistance Ψ for propeller and helically twisted inserts with the experimental results of A. P. Colburn and W. J. King [31]. a to c = the author's own experiments for the smooth tube, a metal twist of h/d = 5 (h = pitch, d = tube diameter) and for propeller inserts of L'/d = 1 (L' = distance between propellers); Inserts Nos. 1 and 3 correspond to a metal twist of h/d = 7 and 6, respectively, and insert No. 9 corresponds to propellers with L'/d = 1.

the new determinations. Basically, however, the path of the curves for the compared inserts within the small Re-range investigated by A. P. Colburn and W. J. King agrees quite well with the comparison curves.

J. Evans and R. J. Sarjant [32] conducted investigations with an experimental arrangement similar to the one described just above (internal diameter of experimental tube--76 mm, length--2.44 m, intake section--10 d). Among others, helically twisted metal strips of 63.5 mm width d_B and 2.13 m length also served as turbulence promoters. Thus the strips were less underdimensioned in comparison to the experimental tube and were shorter than the heated section of the tube. Eight different metal spirals were investigated having reference pitches h/d_B of about 6 to 20. The experimental range extended from Re $\approx$ 3000 to $\approx$ 10,000.

On the basis of the data of J. Evans and R. J. Sarjant, the experimental results for the smooth tube agree satisfactorily with the known theoretical relationships. Since determinations were carried out at high gas temperatures, the heat current transmitted by metal spirals by radiation is considered separately by J. Evans and R. J. Sarjant as these could also provide pure convection values. No accurate data are available on prevailing temperatures (up to 480°C), so that it was not possible to determine the material magnitudes as necessary for a dimensionless representation. However, J. Evans and R. J. Sarjant cite the magnification factors for the coefficient of heat transfer and the pressure loss compared to the values for the smooth tube as a function of the pitch of the metal spirals. Presumably the magnification factors represent average values over the entire Re-range.

If approximately equal reference temperatures are assumed in the smooth tube and in tubes with inserts, then the data of J. Evans and R. J. Sarjant can be compared with the new experimental results (Fig. 63). While the Ψ/Ψ_o, h/d_B curve from these authors agrees to some extent with the corresponding curves from the new measurements, the Nu/Nu_o values from the earlier determinations are lower. The deviations presumably can be explained by the fact that J. Evans and R. J. Sarjant utilized metal spirals which were more narrow and shorter in relation to the dimensions of the experimental tube than in the case of the new measurements.

R. Schumacher [21] classified numerous experimental results which were obtained with packed tubes traversed by a gas flow and demonstrated that the Nusselt numbers, quite independent of the size and type of packing material, are found in a range which is delimited by the curves a and b as drawn in Fig. 64. The internal diameter of the packed tube (not perchance the particle diameter) is to be substituted as the reference magnitude in Re and Nu in this one-sided representation. The new measuring values for packed tubes confirm these data by R. Schumacher very well.

The limiting curves a and b each exhibit two breaks, the position of which admittedly can be easily changed, since the true Nu,Re curves do not have breaks, but rather have a more or less curved path. R. Schumacher assumes that the heat transfer determinations in packed tubes which are traversed by a gas flow can also be transposed to other flow media. However, this is probably permissible only under certain restrictions for reasons which have already been mentioned.

In the determinations of H. Rietschel [33] a pipe line of large cross section was provided with a steam-heated space

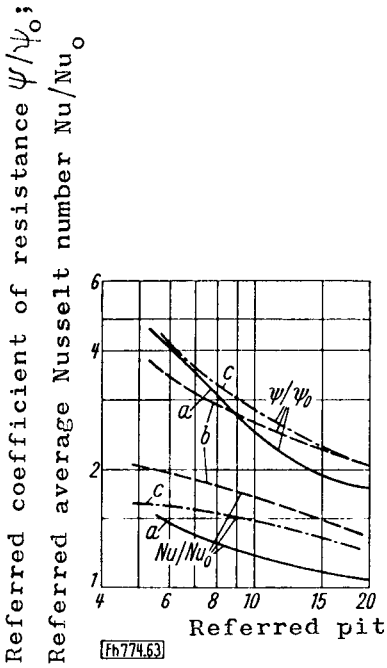

a = course corresponding to [32];

b and c = course corresponding to the new determinations for a Reynolds number Re = 10^4 and $4 \cdot 10^4$, respectively.

Fig. 63.--Comparison of the referred coefficients of resistance Ψ/Ψ_o and the referred average Nusselt numbers Nu/Nu_o with the experimental results of J. Evans and R. J. Sarjant [32] for helically twisted inserts.

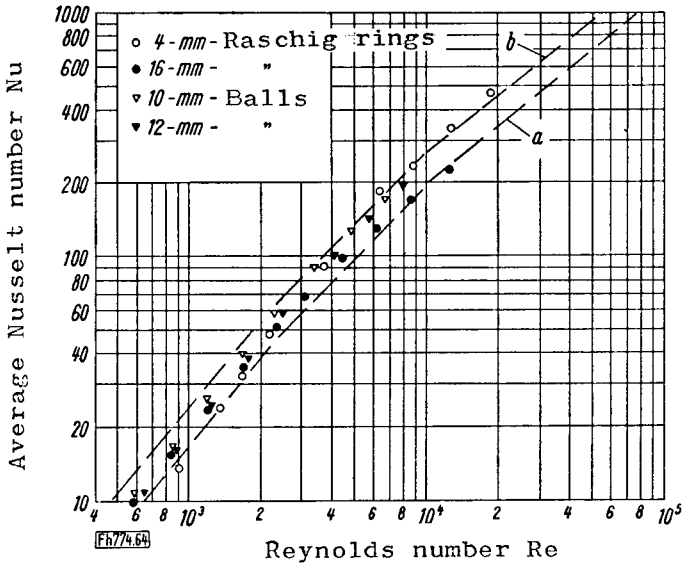

Fig. 64.--Comparison with data of R. Schumacher [21] on the course of the average Nusselt number Nu as a function of the Reynolds number Re for packed tubes. a and b = lower and upper limit curve, respectively, corresponding to [21].

heater of equal diameter which was shielded from the bordering tube parts by an insulating screen. The heater contained five tubes which were located parallel to the axis of the pipeline and which were welded into the pipe floor, and which were traversed by a flow of cold air. The tubes had a diameter of 70 mm and a length of 1 m. Different turbulence promoters were located in front of the tubes, the shapes of which are illustrated in Figs. 65 a to f. The turbulence producers were arranged in such a manner that their cylindrical part fitted smoothly to the tube wall.

The Nu values calculated from the reported experimental values for the smooth tube agree very well with the known theoretical relationships, if the intake effects of the hydrodynamically and thermally undeveloped flow are taken into consideration. However, the values, which have not been represented in a dimensionless manner, have been partly extrapolated to excessively small velocities. A comparison of the measured pressure losses with the new experimental values was not possible, because uncontrollable intake losses due to contraction, separations and transformations of the velocity profile, as well as outlet losses due to pressure drop occurred in H. Rietschel's determination.

G. Grass [34,35] discussed heat transfer in a tube of 40 mm diameter which was traversed by air flow and externally heated by steam. The air arrived in the experimental tube directly from the surroundings; the tube could be provided with different intake arrangements and/or disc-shaped inserts. There was no intake section. The steam jacket of the experimental tube exhibited many little chambers along the tube axis from each of which the condensate drained individually. Thus, the heat flow transmitted to a certain section of the tube could be determined.

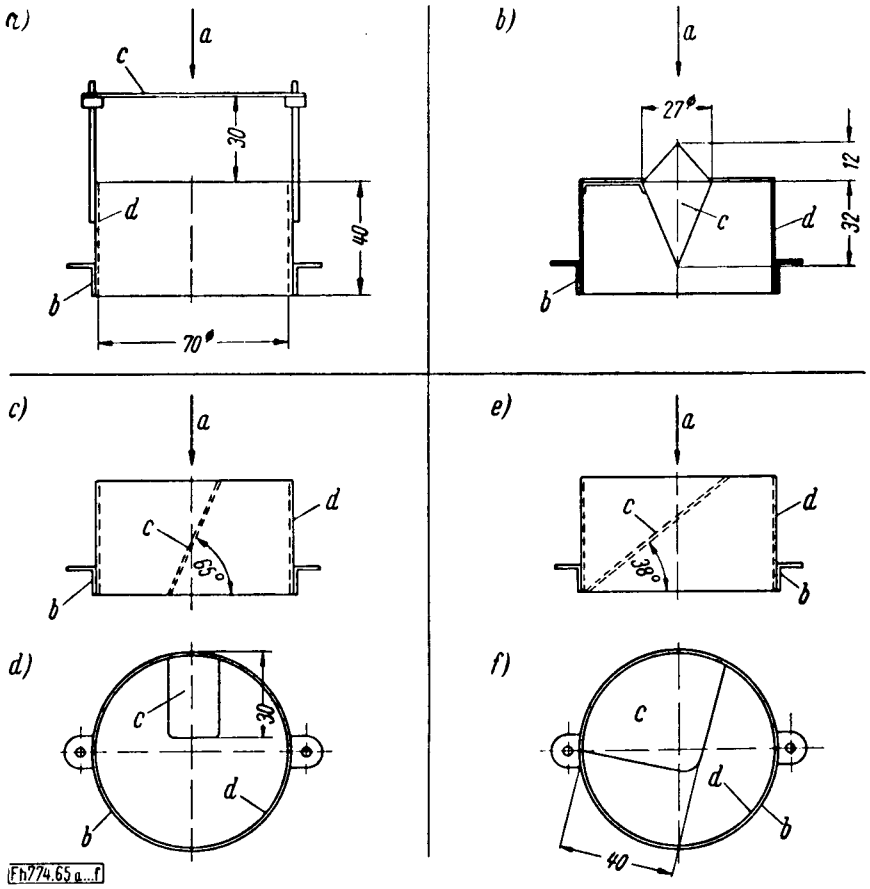

Figs. 65 a to f.--Turbulence producers according to H. Rietschel [33]. a = direction of flow; b = tube; c = turbulence producer; d = cylindrical part of the turbulence producer; a) = baffleplate; b) cylindrical double cone; c) metal sheet as turbulence producer obliquely inclined at 65°; d) top view onto c); e) metal sheet as turbulence producer obliquely inclined at 38°; f) top view onto e).

First G. Grass investigated the effect of the type of intake on the course of the heat transfer coefficient along the tube [34]. Further determinations [35] were to clarify the extent to which inserted discs increase the heat transfer in the tube. In this case the tube diameter amounted to 67 mm. The discs had an aperture ratio $m^* = 0.35$ and 0.8, respectively, and were rounded off. Unfortunately data are lacking on their width and on the manner in which they were mounted to the tube wall. The first section of the experimental tube of 12 d length remained always free from inserts; then there were two or three discs, respectively, at distances of 4 to 12 d. This corresponds to L'/K values of about 76 to 230 at $m^* = 0.8$, and of about 20 to 60 at $m^* = 0.35$, respectively.

G. Grass compared the heat transfer coefficients determined for the disc inserts to those which are valid at the same Reynolds number for a smooth tube with hydrodynamically and thermally developed flow. Here G. Grass found the heat transfer coefficient with discs to increase twice as much as was found in the new experiments. Probably this great difference is due to the fact that the tube intake as well as the discs themselves in the experimental arrangement of G. Grass caused additional intake effects. According to G. Grass, the most favorable disc distance L' is at approximately 8 d. Disc distances < 6 d he considers uneconomical. This is in contrast to the experimental results of W. Nunner [1] and to the new experimental results. The data of G. Grass are not sufficient for a comparison of the pressure loss.

7.2 Experimental Results with a Water Flow

Z. Nagaoka and A. Watanabe [36] allowed water to flow through a tube of 27 mm diameter and 1.7 m length which was externally heated with oil in direct current. The inlet sec-

tion had a length of 37 d. Only the experimental results which are valid for propeller inserts shall be discussed here. Other findings by Z. Nagaoka and A. Watanabe for wire inserts have already been treated in greater detail by W. Nunner [1]. The propeller-shaped inserts were well structured from the flow-technological point of view. The core of 8 mm diameter which was structured as a hub contained twisted foils and snake-like, coiled fins. Table 7 provides a short summary.

Table 7

Propeller-shaped Inserts According to Z. Nagaoka and A. Watanabe [36]

Number of Inserts	Number of Foils	Remarks	Approximate Angle of Discharge to the Tube Axis
3	4	Single twist	63°
4	1		63°
5	3		75°
6	3		75°
7	1	Double twist	75°

At the beginning of the experimental tube there was only one propeller-shaped insert. The referred propeller distance corresponded to about $L'/d = 63$ and thus was more than three times as large as the widest propeller spacing according to Section 4.4.

In the measuring range of $Re \approx 4 \cdot 10^3$ to $2 \cdot 10^4$ which was investigated the values for the smooth tube agree completely with the known theoretical relationships (Figs. 66 and 67). The results for the propeller-shaped inserts can be very well represented by curves which are only slightly less inclined in their path than curve a for the smooth tube. All ψ and Nu values are lower than for the most widely spaced propeller

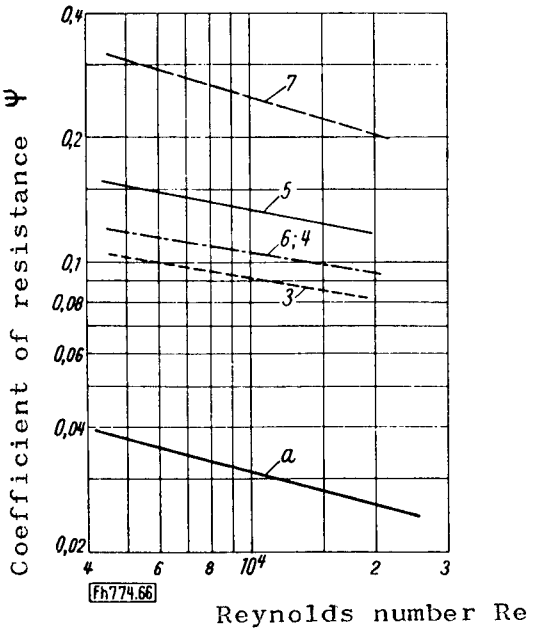

Fig. 66.--Result of the pressure loss measurements.

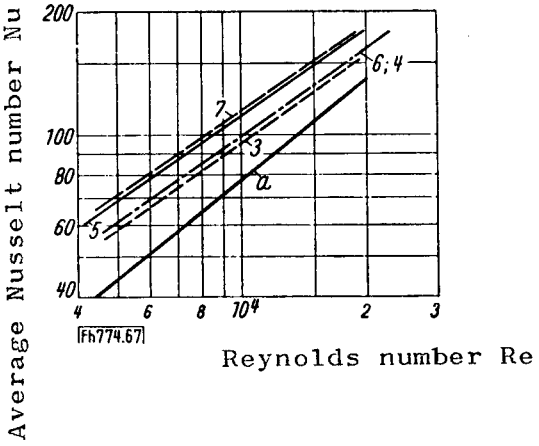

Fig. 67.--Result of the heat transfer measurements.

Figs. 66 and 67.--The coefficient of resistance ψ and the average Nusselt number Nu as functions of the Reynolds number Re for propeller-shaped inserts corresponding to measurements by Z. Nagaoka and A. Watanabe [36]. a = course for the smooth tube; the digits at the remaining curves refer to the number of the inserts corresponding to Table 7.

arrangement according to Section 4.4. A detailed comparison of results according to Figs. 66 and 67 with the new determinations is not possible, since the shape of the propeller inserts and the Prandtl number of the flow media utilized in the two cases are too different from each other. The experimental values of Z. Nagaoka and A. Watanabe are considered more closely later in Section 8.2.

8. Economy of Turbulence Inserts

The design of a heat transmitter usually includes the problem with respect to a given material flow of supplying or removing a certain flow of heat in the most economical manner. Thus the most favorable relation must be found between the type and size, and thus the cost, of the heat transmitter on one hand, and the procurement and operating costs of the blower installation, which serves for the transport of the flow medium, on the other hand. For tubes as transport areas through which flow passes longitudinally, the heat transfer in the tubes can be increased by means of the installation of turbulence promoters. However, with these the pressure loss increases simultaneously as well as the transport efficiency of the blower. Consequently, various construction types of a heat transmitter must be investigated with respect to their economical properties, in order to find the optimum design for the particular given conditions. Two methods in which the variable costs for the heat transfer areas can be taken into consideration unobjectionably, seem particularly suited for such an evaluation on the basis of general points of view.

8.1 Evaluation Method According to O. Walger

O. Walger [2,37] referred to the fact that as yet equal

Reynolds numbers do not represent a useable basis for a critical comparison of heat transmitters, since differing geometrical forms of the transmission planes under certain circumstances lead to different Reynolds numbers under equal conditions of operation. In contrast, he assumes the equivalence of the material flow, of the heat flow and of the pressure drop for the heat transmitters which are to be evaluated. Undisturbed longitudinal flow through a smooth tube serves as the basis of comparison for flow through tubes with inserts. According to O. Walger, a Reynolds number Re' is determined for the tubes with inserts from the measuring values; this Re' results in equal operating conditions (i.e. equal transmitted heat flow at equal pressure loss) in flow through a smooth tube as the tube with inserts at a Reynolds number Re. The ratio L/L_o of the total expense of tube length for the tube with inserts of length L and for the smooth tube of length L_o approximately represents the cost relation of the two heat transmitters and is inversely proportional to the ratio of the Nusselt numbers which correspond to the Reynolds numbers Re and Re'.

H. Glaser [38] already formulated an evaluation procedure previous to O. Walger which was based on almost the same fundamental assumptions, but which appears in an entirely different form externally. In the following the method of H. Glaser which basically does not differ from that of O. Walger will be described in greater detail and applied to the experimental results.

8.2 Evaluation Procedure According to H. Glaser

The economy of turbulence promoters can also be judged in comparison to smooth tubes without special restrictions

if, according to H. Glaser [38], the heating area requirement is determined as a function of an efficiency coefficient $\xi = Q/N$, where Q is the transported flow of heat and N the blower and/or pump output necessary for the transport of the flow medium. An efficiency coefficient $\xi_1 = \xi/\Delta t$ is appropriately utilized, i.e. the flow of heat referred to the transport efficiency and to a temperature interval of 1° between the wall and the flow medium. Thus, an equal efficiency coefficient means an equal output expenditure for the transport of a certain heat flow to a given material flow. With this it can be easily determined which type of heating area will be the smallest necessary for a chosen or fixed efficiency coefficient. At an equal tube diameter for all cases, the required tube length L or the particular required heating area H is directly equal in proportion. Then only the different costs per unit of heating area must still be taken into consideration. However, the turbulence inserts which have been investigated do not increase essentially the total costs of a heat transmitter.

It should still be noted that in the cases under consideration here the same efficiency coefficients are provided with different rates of flow and thus different Reynolds numbers. Consequently, a relationship exists between the required heating area H and the required free flow cross section referred to the mass weight rate of flow $f' = f/G$ (where f is the free flow cross section and G the mass weight rate of flow). With increasing ξ_1, the particular Reynolds number of the corresponding heat transmitter decreases.

Fig. 68 shows the required heating area H as a function of ξ_1 for the smooth tube and for tubes with those disc inserts which had been found to be especially favorable among the

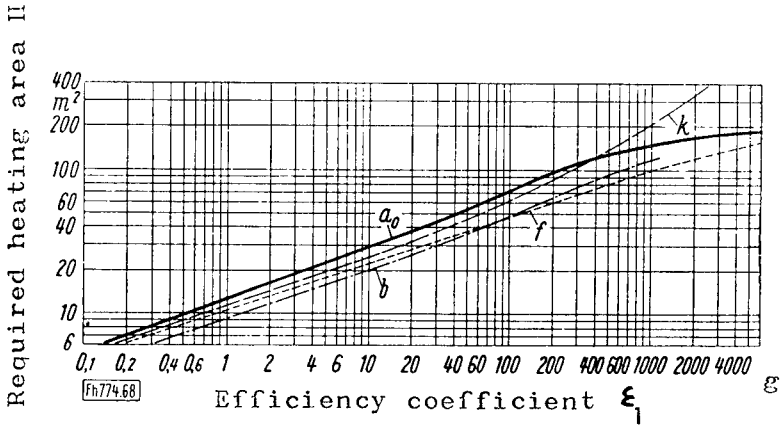

grd = degree

Figure 68

The required heating area H as a function of the efficiency coefficient ε_1 for the experimental tube containing disc-shaped inserts. a_o = smooth tube; b, f and k refer to the classifications with the same designations corresponding to Table 1.

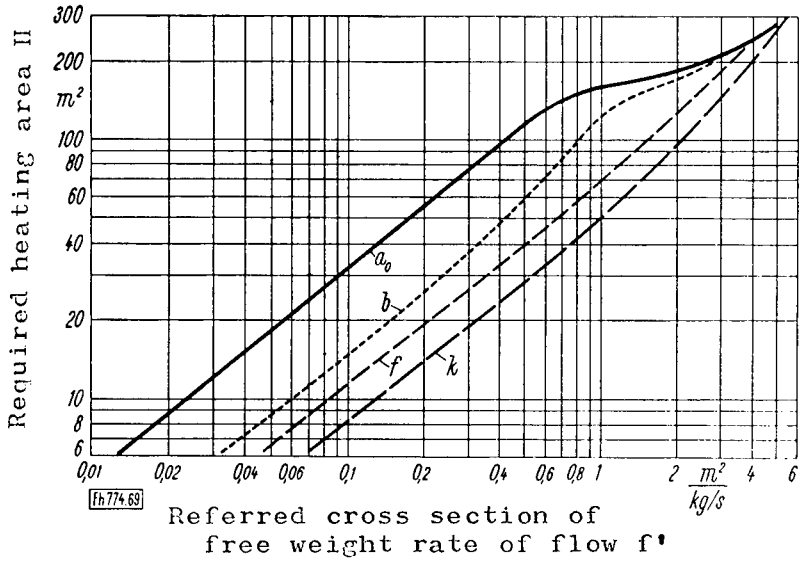

Fig. 69.--Required heating area H as a function of the referred cross section of the free weight rate of flow f' for the experimental tube containing disc-shaped inserts. a_o = smooth tube; b, f and k refer to the equally designated classifications corresponding to Table 1.

disc inserts under investigation. It can be recognized that over a wide range the heating area requirement is far lower for the tubes provided with discs than for the smooth tube. The smaller the height K of the discs, the more favorable is their effect if the efficiency coefficients are not too large. At ξ_1 = 1 degree^{-1}, the heating area requirement for discs with K = 2 mm only amounts to 70% of that for the smooth tube, while it amounts to about 85% for higher K values. With increasing ξ_1 the advantage offered by discs with K = 10 mm decreases visibly at first and finally becomes a disadvantage. For tubes provided with discs of K = 5 mm the greatest heating area savings are obtained (about 50%) at $\xi_1 \approx 300$ degree^{-1}. Partly these inserts have an especially favorable effect in the change-over zone of the flow ($\xi_1 \approx 200$ to ≈ 2000 degree^{-1}), since turbulence inserts further delay the fade-out of turbulence. At very high ξ_1 values (correspondingly small Re values), the smooth tube becomes more favorable again for every case, since the turbulence inserts at small Reynolds numbers increase only the pressure loss but not the heat transfer.

In the case of a constant efficiency coefficient ξ_1, the rate of flow w in tubes with turbulence promoters must be lower than in the smooth tube, since the pressure loss increases too much otherwise. Therefore it is a requirement for the referred free flow cross section f' to be larger in tubes with turbulence promoters than in a smooth tube. Fig. 69 shows the course of H as a function of f' for the same arrangements as in Fig. 68. The desired relationship between ξ_1 and f' results from Figs. 68 and 69. As can be expected, the required value of f' is smallest for the smooth tube. In the other tubes it increases with increasing disc height K.

Fig. 70 shows the H, ξ_1 curves for the smooth tube and for tubes with an especially favorable arrangement of baffleplates, propellers and metal spirals as well as packing materials. In narrow plate arrangements and plate diameters of 30 and 40 mm (curves d and e), the heating area requirements decreases to about 75% at small ξ_1 values in comparison to the smooth tube. With increasing ξ_1 (i.e. with decreasing rate of flow), the advantage of the plate inserts is lost more and more; at $\xi_1 \approx 100$ degree^{-1} and $\xi_1 \approx 700$ degree^{-1}, the curves for the 40 mm and 30 mm plates, respectively, run past the curve for the smooth tube.

For an equal heating area requirement, L' = 980 mm for tubes with a propeller insert and $h/d \approx 5$ for tubes with a twisted metal insert (coinciding curves f and g in Fig. 70). While at small ξ_1 values this curve almost coincides with curve d for the 40 mm discs, a heating area requirement which is 40% lower than in the smooth tube results over a large range at higher ξ_1 values in the case of propellers and twists.

Tubes which are filled with 5 mm Raschig rings (curve b) exhibit a considerably more unfavorable behavior at all ξ_1 values than the smooth tube. In contrast, the tube with the 16 mm Raschig rings (curve c) has almost the same low heating area requirement at low ξ_1 values as the one provided with propellers, but with increasing ξ_1 it rapidly becomes more uneconomical.

Fig. 71 shows the relation between H and f' for the same arrangements. On the basis of Figs. 70 and 71 it follows here too that at a certain efficiency coefficient, the smallest referred free cross section f' applies to the smooth tube (greatest rate of flow); the highest f'value is required for the packed tubes.

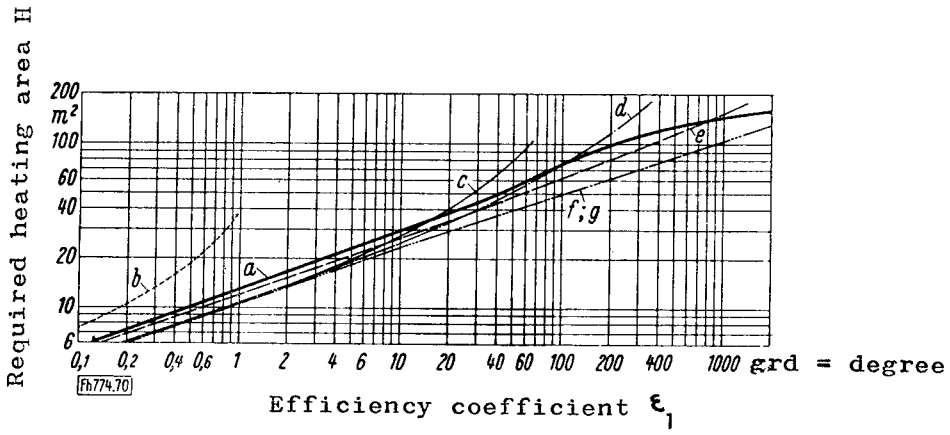

Fig. 70.--Required heating area H as a function of the efficiency coefficient ξ_1 for the experimental tube containing different types of turbulence inserts. a = smooth tube; b and c = Raschig ring packing with 5 mm and 16 mm rings, respectively; d and e = baffleplate inserts consisting of plates of 40 mm diameter with a referred distance L'/d = 1.44 and plates of 30 mm diameter with L'/d = 1.55, respectively; f = propeller inserts with L'/d = 19.6; g = metal twists with a referred pitch h/d = 5.

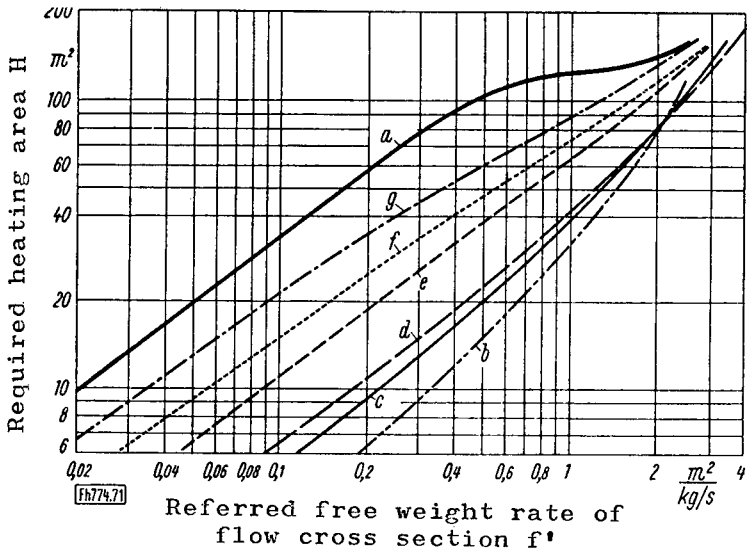

Fig. 71.--The required heating area H as a function of the free weight rate of flow cross section f' for the experimental tube containing different types of turbulence inserts. Denotations as in Fig. 70.

The results shall be briefly summarized once more. The discs, propellers and metal twists proved to be especially favorable types of inserts. Discs with a large aperture ratio ($m^* \approx 0.85$) are most advantageous in the case of high Reynolds numbers. Within a certain range of ε_1 values corresponding to the change-over zone in the smooth tube, the discs with K = 5 mm ($m^* \approx 0.65$) are still somewhat more favorable than the discs with K = 2 mm ($m^* \approx 0.85$). With respect to propeller inserts, the arrangement with the greatest propeller distance (L' = 980 mm) exhibits no disadvantages whatsoever in comparison to arrangements with a smaller spacing L'. Propeller inserts at small ε_1 values (high Re values) are not as advantageous as discs with small m*. The twisted metal strip (h = 5 d) exhibits a similarly favorable effect as in the case of propeller inserts. On the other hand, the baffleplate turbulence promoters at no time attain the good values of discs. Significant economic advantages in comparison to the smooth tube are only attained by the 40 mm plates with $L'/d_S \approx 1.5$ within a certain range. Those packing materials which produce a large pressure loss (e.g. the 5 mm Raschig rings) are considerably less economical than others which cause smaller pressure losses (e.g. 16 mm Raschig rings). With respect to tubes with packing materials reference should be made especially to the fact that the same magnitude of heating area does not correspond to equal costs for the heat transmitter, since the costs of the packing materials must be taken into account. Consequently the evaluation again changes somewhat in favor of the smooth tube. The same is true for all of the other inserts.

Figs. 68 to 71 are only valid for a tube diameter d = 50 mm. At greater d values the shift of the H, ε_1 curves

is almost equidistant in the direction of higher H values, so that only the relationships for one tube diameter have to be examined. However, if free convection still plays an additional role, then the results cannot be simply transposed to tubes with different diameters.

Fig. 72 shows the H, ε_1 values according to the experiments of A. P. Colburn and W. J. King [31] which are only compared to each other, since A. P. Colburn and W. J. King obtained higher resistance coefficients and heat transfer coefficients for the smooth tube than would be expected on the basis of known theoretical interrelations. The curve which has been drawn in is valid for the smooth tube. Inserts No. 9 (propeller) and No. 8 (inner tube with metal strips in coiled arrangement) show the most favorable results. Depending on the value of ε_1, their heating area requirement is about 25 to 55% less than for the smooth tube.All of the other inserts also exhibit an advantage at higher ε_1 values over the smooth tube. However, the measuring values cannot be simply extrapolated for other efficiency coefficients (i.e. other Reynolds numbers); for in the case of propeller inserts and metal twists, for example, ψ and Nu over increasing ranges no longer vary with Re according to a simple exponential relation (compare Figs. 22 and 23 as well as 26 and 27).

Curves a to c in Fig. 73 were calculated from the experimental results of J. Evans and R. J. Sarjant [32]. Curve b for the metal twists with h/d_B = 5.6 to 9.6 practically coincide* and are about 30% lower than curve a for the smooth tube. In comparison, the twist with the lowest number

*Translator's note: This sentence is incorrectly stated in German; either an omission or a typographical error is involved.

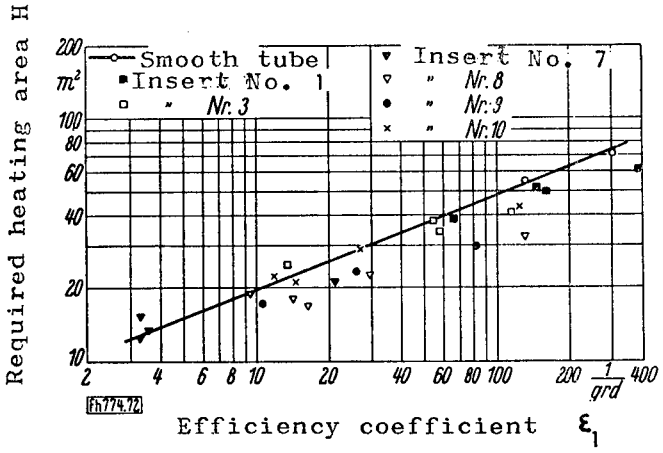

Fig. 72.--The required heating area H as a function of the efficiency coefficient ε_1 corresponding to experimental results of A. P. Colburn and W. J. King [31]. Smooth tube as well as inserts Nos. 1, 3 and 9 as in Figs. 61 and 62; inserts Nos. 7 and 8 = coiled metal strips mounted on a core tube having a referred pitch $h/d \approx 0.65$ for a core tube diameter of 22 mm and $h/d \approx 1$ for a core tube diameter of 11 mm, respectively; insert No. 10 = cone-shaped wire spirals mounted on a rod with the smallest diameter of twist equal to the rod diameter and the largest diameter of twist equal to the tube diameter d (height of a wire cone approximately 2 d).

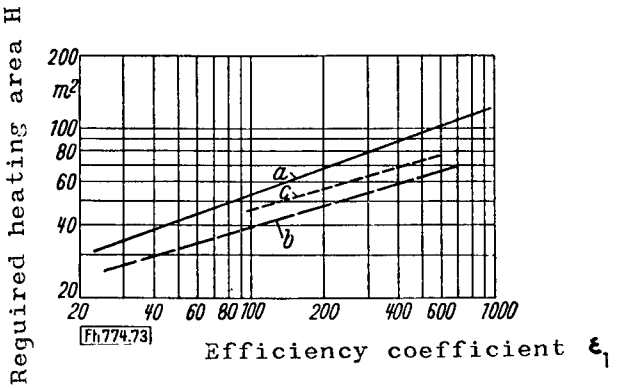

Fig. 73.--The required heating area H as a function of the efficiency coefficient ε_1 corresponding to measuring results of J. Evans and R. J. Sarjant [32]. a = smooth tube; b = metal twists with referred pitches h/d_B = 5.6, 7.2 and 9.6 (h = pitch, d_B = width of the metal strip); c = metal twists with h/d_B = 11.1.

of twists (curve c) is somewhat less favorable. These results agree only very approximately with the new experimental values, as was to be expected on the basis of the comparison according to Fig. 63.

Fig. 74 is based on the experimental results of H. Rietschel [33]. Curve a is clearly based on the hydrodynamically developed flow; curve b is valid for the experimental tube of 1 m length including the intake and outlet disturbances. In comparison to curve b, the heat transfer is increased more or less economically with all turbulence promoters, but curve f for the insert corresponding to Fig. 65e is in still more favorable position than curve a. The operating conditions on which curve b in Fig. 74 is based occur very frequently in practice. While intake and outlet losses admittedly can increase the total pressure loss considerably, this is not true for the heat transfer to the same extent. This is demonstrated by the difference between curves a and b. These disadvantages with respect to a fully developed turbulent tube flow can be eliminated and even converted to economic advantages by means of the installation of suitable turbulence promoters.

The results of Z. Nagaoka and A. Watanabe [36] have been applied in Fig. 75. Accordingly, the propeller inserts in the range under investigation are almost generally less economical than the smooth tube. Certainly this is mainly due to the fact that propellers with large angles of incidence and small numbers of vanes do not represent a favorable type of insert. Presumably the excessively large referred propeller distance of $L'/d \approx 63$ probably has an unfavorable effect because the swirling motion fades out earlier and thus influences the heat transfer only in a certain zone behind the propeller.

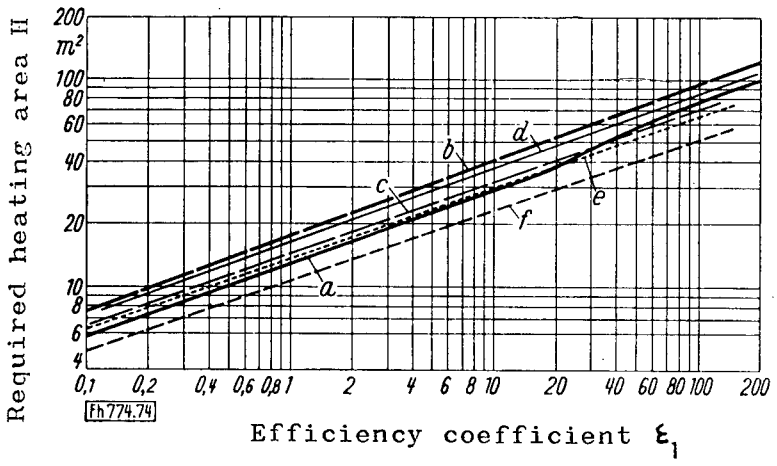

Fig. 74.--The required heating area H as a function of the efficiency coefficient ε_1 corresponding to measuring results of H. Rietschel [33]. a and b = smooth tube (hydrodynamically developed flow with intake and outlet effects, respectively); c to f = corresponding to inserts according to Figs. 65 a, b, c and e, respectively.

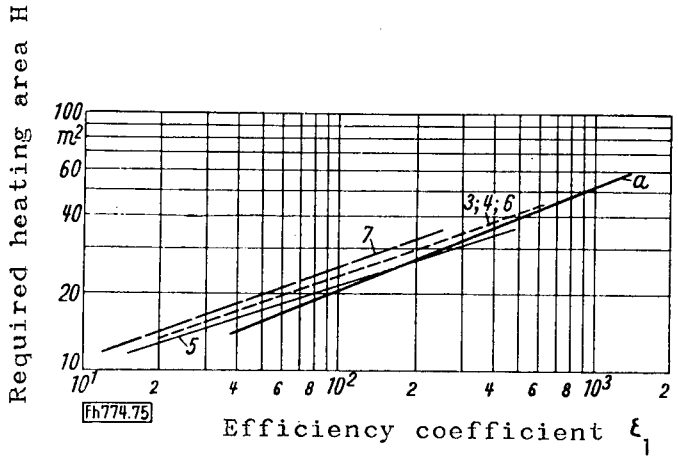

Fig. 75.--The required heating area H as a function of the efficiency coefficient ε_1 corresponding to measuring results of Z. Nagaoka and A. Watanabe [36]. Explanations as in Figs. 66 and 67.

For reasons discussed in Section 5, the effect of the turbulence promoters is not as good in the case of flow media with a high Prandtl number than at low Pr-values. Therefore, the results obtained for water with a Prandtl number ten times that of air cannot be directly transferred to an air flow.

8.3 Influence of Dirt Deposits on Heat Transfer

Fouling of the heat transfer tubes occurs frequently in practice. The dirt layer almost always has a low coefficient of thermal conductivity, decreases the cross section of flow and thus increases the average flow rate at the same weight rate of flow. The heat resistance of the dirt layer and the increased flow rate (i.e. an increased heat transfer coefficient) thus have a bad effect on the heat transmission. R. Gregorig [39] demonstrated the circumstances under which a dirt layer does not yet have unfavorable consequences. Due to the surface roughnesses of the dirt layer which increase the heat transfer coefficient still more, the results of an examination undertaken for smooth surfaces still shift somewhat.

In the case of turbulence promoters, such simple conclusions cannot be drawn. Dirt collects easily at the walls of tubes with disc-shaped inserts. But the average rate of flow increases hardly or not at all due to such layers. If, on the other hand, baffleplate or propeller inserts are utilized for turbulence promoters, then similar effects as in the smooth tube presumably result due to a dirt deposit.

9. Summary

In a smooth tube into which different passive turbulence-producing arrangements had been introduced (discs, rings, baffleplates, propellers, helically twisted metal strips, and packing materials) the pressure loss and the heat transfer

were determined in the range of Reynolds numbers Re $\approx$ 500 to 80,000 both without as well as with the inserts. The known theoretical interrelationships for pressure loss and heat transfer in a smooth tube were quite valid for the experimental tube. With respect to tubes with inserts, both the Nusselt number as well as the coefficient of resistance, which are always greater for a certain Reynolds number than in the smooth tube, depend on the type and arrangement of the inserts in an unclear manner.

In the discs under investigation having aperture ratios $m^* \approx 0.25$ to 0.85, maximum values of the pressure loss and the heat transfer occurred for a certain aperture ratio m^* in the range $4000 \leq Re \leq 80{,}000$ at disc distance $L' \approx 10\ K$ (where K is the disc height). In the case of baffleplate inserts under the same conditions ($0.36 \leq m^* \leq 0.84$), a maximum for the pressure loss could only be determined at a plate distance $L' \approx 0.9\ d_S$ (where d_S is the plate diameter).

With respect to propeller inserts, a decrease of the pressure loss and the heat transfer resulted with increasing distance L'; a simple relation to distance L', however, could not be recognized. With metal twists, the pressure loss and the heat transfer were lower with increasing pitch h. If a pitch h smaller than about five tube diameters d is selected, then the heat transfer presumably no longer increases significantly in comparison to the value at h/d = 5.

The highest values of pressure loss and heat transfer occurred in the tubes filled with packing materials (heat transfer in the turbulent range at constant Reynolds number approximately seven to eight times as high; pressure loss depending on the type of packing 600 to 10,000 times as high as in the smooth tube).

Measurements of the velocity and temperature distributions as well as of the wall shear stress in the smooth tube and in the tube with inserts resulted in valuable insight into the mechanism of heat transfer in the presence of turbulence producers. Here it was found that the wall shear stress produced by the wall friction of the flow medium decisively characterizes the heat transfer. With the aid of the average wall shear stress it was possible to represent the heat transfer for all baffleplate inserts as well as for several other turbulence producers by means of a curve. The intensity of turbulence mainly influences the heat transfer in that it causes the wall shear stress to increase. Furthermore, it could be concluded from these determinations that turbulence producers do not increase the heat transfer as much in the case of flow media with high Prandtl numbers as with those having a lower Prandtl number.

A consideration of economy factors gives information on how the correct selection and arrangement of turbulence inserts can result in economic advantages over the smooth tube.

10. Literature

[1] Nunner, W.: Pressure Loss and Heat Transfer in Rough Tubes. VDI-Forsch.Heft 455. Düsseldorf, 1956.

[2] Walger, O.: The Value of Turbulence Inserts for the Increase of Heat Transfer. Allg. Wärmetechn. 3, No. 8-9 (1952), 163-67.

[3] Nikuradse, J.: Theoretical Interrelationships of Turbulent Flow in Smooth Tubes. VDI-Forsch. Heft 356. Berlin 1932.

[4] Nikuradse, J.: Flow Theories for Rough Tubes. VDI-Forsch. Heft 361. Berlin 1933.

[5] Boussinesq, J.: On the Manner in which Velocities in a Cylindrical Tube of Circular Section with a Flared Inlet Are Distributed from this Inlet up to the Areas Where a Uniform Profile Has Established Itself. Compt. Rend. 113 (1891) 9-15; also by the same author: Calculation of the Least Length Necessary for a Circular Tube, Which Is Flared at the Inlet, so that a Generally Uniform Profile Can Establish Itself in It, and of the Weight Rate of Flow Which Is Necessary to Evoke This Profile. Compt. Rend. 113 (1891), 49-51.

[6] Blasius, H.: The Similarity Principle for Friction Processes in Fluids. Forsch.-Arb. Ing.-Wes. No. 131. Berlin 1913.

[7] Prandtl, L.: Recent Results in Turbulence Research. Z. VDI 77 (1933), No. 5, 105-14.

[8] Hermann, R. and Th. Burbach: Flow Resistance and Heat Transfer in Tubes. Leipzig 1930.

[9] Nusselt, W.: Heat Transfer Coefficient as a Function of the Tube Length. Z. VDI 54 (1910), No. 28, 1154-58.

[10] Hausen, H.: Representation of the Heat Transfer in Tubes By Means of Generalized Exponential Relations. Z. VDI Beih. Verfahrenstechnik Folge 1943, No. 4, pp. 92-98.

[11] Nusselt, W.: Heat Transfer in Pipe Lines. Forsch.-Arb. Ing.-Wes. No. 89. Berlin 1909.

[12] Prandtl, L.: A Relation Between Heat Exchange and Flow Resistance of a Liquid. Phys. Z. 11 (1910), No. 23, 1072-78.

[13] Hofmann, E.: Heat Transfer During Flow in a Tube. Z. ges. Kaelteind. 44 (1937), No. 6, 99-107.

[14] Latzko, H.: Heat Transfer in a Turbulent Fluid or Gas Flow. Z. angew. Math. Mech. 1 (1921), No. 4, 268-90.

[15] Elser, K.: Heat Transfer in the Thermal Starting Section for Hydrodynamically Developed Influx in the Tube. Schweiz. Arch. angew. Wiss. u. Techn. 15 (1949), 359-64.

[16] Berry, V. J.: Non-uniform Heat Transfer to Fluids Flowing in Conduits. Appl. Sci. Res. A 4 (1954), 61-75.

[17] "Foundry." Vol. I, 28th ed. Berlin 1955.

[18] Schiller, L.: Flow in Tubes. In: Wien, W. and F. Harms: Handbook of Experimental Physics. Vol. IV, Part 4. Leipzig 1932, pp. 1-207.

[19] Möbius, H.: Experimental Investigation of the Resistance and the Velocity Distribution in Tubes with Uniformly Arranged Roughnesses during Turbulent Flow. Phys. Z. 41 (1940), No. 8, 202-25.

[20] Hübner, E.: On Pressure Loss in Tubes with Inserts. Forsch. Ing.-Wes. 19 (1953), No. 1, 1-16.

[21] Schumacher, R.: Heat Transfer to Gases in Packed and Contact Tubes. Erdöl u. Kohle 2 (1949), 189-93.

[22] Prandtl, L.: Remarks on Heat Transfer in a Tube. Phys. Z. 29 (1928), No. 14, 487-89.

[23] Hofmann, E.: On the General Heat Transfer Principle of Turbulent Flow in a Tube and the Meaning of Characteristic Numbers. Forsch. Ing.-Wes. 20 (1954), No. 3, 81-93.

[24] Reichardt, H.: Heat Transfer in Turbulent Friction Layers. Z. angew. Math. Mech. 20 (1940), No. 6, 297-328.

[25] Reichardt, H.: The Influence of Flow Near the Wall on Turbulent Heat Transfer. Mitt. Max-Planck-Institut f. Stroemungsforschung No. 3. Goettingen, 1950.

[26] Reichardt, H.: Complete Representation of the Turbulent Velocity Distribution in Smooth Conduits. Z. angew. Math. Mech. 31 (1951), No. 7, 208-19.

[27] Reichardt, H.: The Fundamentals of Turbulent Heat Transfer. Arch. ges. Waermetechn. 2 (1951), No. 6-7, 129-42.

[28] Prandtl, L.: The Influence of Wall Roughness on Heat Transfer to Water. Forsch. Ing-Wes. 5 (1934), No. 1, 5.

[29] Ludwieg, H.: A Measuring Instrument for Wall Shear Stress of Turbulent Friction Layers. Ing.-Arch. 17 (1949), No. 3, 207-18.

[30] Herbeck, M.: Heat Exchange Between a Heated Filament and a Convection Flow. Z. angew. Math. Mech. 33 (1953), No. 10-11, 362-82.

[31] Colburn, A. P.: Heat Transfer and Pressure Drop in Empty, Baffled and Packed Tubes. Industr. Engng. Chem. 23 (1931), No. 8, 910-23.

[32] Evans, J. and R. J. Sarjant: Heat Transfer and Turbulence in Gases Flowing Inside Tubes. J. Inst. Fuel 24 (1951), 216-27.

[33] Rietschel, H.: Investigation of Heat Emission, Amount of Pressure Loss and Surface Temperature in Heaters with the Use of High Air Velocities. Mitt. Prüfungsanst. f. Heizungs- u. Lüftungseinrichtungen, No. 3 (1910).

[34] Grass, G.: Heat Transfer to Turbulently Flowing Gases in the Tube Intake. Allg. Waermetechn. 7 (1956), No. 3, 58-64.

[35] Grass, G.: Increasing the Heat Transfer in the Tube by Installation of Discs. Allg. Waermetechn. 7 (1956), No. 4, 73-75.

[36] Nagaoka, Z. and A. Watanabe: Maximum Rate of Heat Transfer with Minimum Loss of Energy. Proc. Intern. Congr. Refrig., 7th Congr. Hague/Amsterdam, 1936, 3 (1937), No. 16, 221-45.

[37] Walger, O.: Fundamentals for an Economical Design of Heat Transmitters. Chemie-Ing.-Techn. 24 (1952), No. 3, 142-45.

[38] Glaser, H.: Evaluation of Heat Exchange Systems with the Aid of an Efficiency Coefficient. Angew. Chemie 20 (1948), No. 5-6, 129-33.

[39] Gregorig, R.: Is a Dirt Layer Always Unfavorable in Convective Heat Transfer? Brennstoff-Waerme-Kraft (BWK) 7 (1955), No. 12, 565.